

# Unravelling the relative contributions of climate change and ground disturbance to subsurface temperature perturbations: Case studies from Tyneside, UK



Rob Westaway<sup>a,b,\*</sup>, Paul L. Younger<sup>a</sup>

<sup>a</sup> School of Engineering, University of Glasgow, James Watt (South) Building, Glasgow G12 8QQ, UK

<sup>b</sup> Newcastle Institute for Research on Sustainability, Newcastle University, Devonshire Building, Newcastle upon Tyne NE1 7RU, UK

## ARTICLE INFO

### Article history:

Received 18 December 2015

Received in revised form 17 May 2016

Accepted 17 June 2016

Available online 10 August 2016

### Keywords:

Subsurface urban heat islands

Subsurface heat pollution

Newcastle upon Tyne

Gateshead

North of England coalfield

## ABSTRACT

When assessing subsurface urban heat islands (UHIs) it is important to distinguish between localized effects of land-use change and the impacts of global climate change. However, few investigations have successfully unraveled the two influences. We have investigated borehole temperature records from the urban centres of Gateshead and Newcastle upon Tyne in northeast England, to ascertain the effects on subsurface temperatures of climate change and changes in ground conditions due to historic coal mining and more recent urban development. The latter effects are shown to be substantial, albeit with significant variations on a very local scale. Significant subsurface UHIs are indeed evident in both urban centres, estimated as 2.0 °C in Newcastle and 4.5 °C in Gateshead, the former value being comparable to the 1.9 °C atmospheric UHI previously measured for the Tyneside conurbation as a whole. We interpret these substantial subsurface UHIs as a consequence of the region's long history of urban and industrial development and associated surface energy use, possibly supplemented in Gateshead by the thermal effect of trains braking in an adjacent shallow railway tunnel. We also show that a large proportion of the expected conductive heat flux from the Earth's interior beneath both Gateshead and Newcastle becomes entrained by groundwater flow and transported elsewhere, through former mineworkings in which the rocks have become 'permeabilised' during the region's long history of coal mining. Discharge of groundwater at a nearby minewater pumping station, Kibblesworth, has a heat flux that we estimate as ~7.5 MW; it thus 'captures' the equivalent of roughly two thirds of the geothermal heat flux through a >100 km<sup>2</sup> surrounding region. Modelling of the associated groundwater flow regime provides first-order estimates of the hydraulic transport properties of 'permeabilised' Carboniferous Coal Measures rocks, comprising permeability  $\sim 3 \times 10^{-11}$  m<sup>2</sup> or  $\sim 30$  darcies, hydraulic conductivity  $\sim 2 \times 10^{-4}$  m s<sup>-1</sup>, and transmissivity  $\sim 2 \times 10^{-3}$  m<sup>2</sup> s<sup>-1</sup> or  $\sim 200$  m<sup>2</sup> day<sup>-1</sup>; these are very high values, comparable to what one might expect for karstified Carboniferous limestone. Furthermore, the large-magnitude subsurface UHIs create significant downward components of conductive heat flow in the shallow subsurface, which are supplemented by downward heat transport by groundwater movement towards the flow network through the former mineworkings. The warm water in these workings has thus been heated, in part, by heat drawn from the shallow subsurface, as well as by heat flowing from the Earth's interior. Similar conductive heat flow and groundwater flow responses are expected in other urban former coalfield regions of Britain; knowledge of the processes involved may facilitate their use as heat stores and may also contribute to UHI mitigation.

© 2016 Elsevier Ltd. All rights reserved.

\* Corresponding author at: School of Engineering, University of Glasgow, James Watt (South) Building, Glasgow G12 8QQ, UK.  
E-mail address: [robert.westaway@glasgow.ac.uk](mailto:robert.westaway@glasgow.ac.uk) (R. Westaway).

## 1. Introduction

*So farewell to you, Monty, I knaa your roads well -  
Your wark had been good, and your wark has been hell.  
Ne mair to yor dory old heap will aa come,  
For your coal is all finished, and your life it is done.*

‘Farewell to the Monty’  
John Pandrich (Johnny Hande), 1959

It has long been recognized that water in flooded mineworkings forms a potentially valuable heat source (e.g., Leoni, 1985; Harrison et al., 1989; Banks et al., 2003; Heitfeld et al., 2006; Watzlaf and Ackman, 2006; Michel, 2009a,b; Hall et al., 2011; Ramos and Falcone, 2013; Coldewey et al., 2014), and indeed represents a subset of the more general concept of aquifer thermal energy storage (ATES). However, although this basic concept is well-established, site- and application-specific uncertainties remain, these being bound up with more general uncertainties regarding flows of thermal energy in the Earth's shallow subsurface. In particular, the limited information currently available on hydraulic transport properties of Carboniferous age Coal Measures rocks in Britain, which have been ‘permeabilised’ (cf. Younger et al., 2015) by coal mining, impacts on one's ability to make quantitative assessments (e.g., Gillespie et al., 2013). The present study will use data from the former coalfield region of northeast England to assess the extent of human perturbations to the thermal state of the subsurface as result of coal mining and other processes, as a step towards the wider goal of increasing general understanding of subsurface thermal energy flows. Following van der Kamp and Bachu (1989), we shall undertake first-order analyses using analytical modelling, leaving more elaborate numerical modelling as an objective for the future, beyond the scope of the present study.

The closure of the Caroline Pit of Montagu Main Colliery (known locally as ‘the Monty’) in November 1959 marked the last coal mining beneath the urban area of the city of Newcastle upon Tyne in northeast England, ending almost eight centuries of local tradition. This city, at the centre of the northeast England coalfield (Fig. 1), was one of the principal powerhouses of the global Industrial Revolution in the 19th century, local coal providing the fuel for shipbuilding and other heavy engineering industries, in turn necessitating the invention, by local engineers, of the railway as a means of transport. While the hydrogeology of this abandoned coalfield has been studied extensively (e.g., Younger, 1993, 1995, 1997, 1998, 2004, 2006; Younger and Harbourne, 1995; Younger et al., 2015), very little attention has yet been given to the effects of the legacy of mining on the subsurface thermal state, resulting for example from downward conduction of heat from surface energy use or disruption of the geothermal heat flux by groundwater flow through flooded former mine workings. The present study will set out to quantify these effects, within the wider context of urban subsurface heating effects in general (cf. Menberg et al., 2013a,b), and building on the findings of the hydrogeological investigations cited above.

Many studies have established that geothermal measurements can record temperature changes in the shallow subsurface that are indicative of recent climate change, demonstrating global warming in rural areas that have experienced no local perturbations to the thermal state of the Earth's crust (e.g., Chisholm and Chapman, 1992; Huang and Pollack, 1997; Pollack et al., 1998; Huang et al., 2000; Davis et al., 2010). Anthropogenic perturbation to the thermal state of the shallow subsurface beneath urban areas, the creation of a subsurface Urban Heat Island (UHI), has also been recognized, for example beneath Osaka, Japan (Taniguchi and Uemura, 2005), Albuquerque, New Mexico, in the S.W. USA (Reiter, 2006), Winnipeg, Canada (Ferguson and Woodbury, 2007), cities in Germany (Menberg et al., 2013a,b), and most recently beneath Cardiff in south Wales (Patton et al., 2015a,b). Many other

workers have investigated UHIs in the atmosphere, directly above ground level. Attempts to model these effects in the UK have hitherto almost exclusively considered the largest city, London (e.g., Bohnenstengel et al., 2011, 2014); furthermore, although the technique used for this modelling (described by Porson et al., 2010a,b) incorporates transfer of heat between the atmosphere and the ground, it only considers the effect of diurnal variations in air temperature, not interaction between any subsurface UHI and the atmosphere.

Some authors (e.g., Huang et al., 2000; Beltrami et al., 2002; Hopcroft et al., 2007) have attempted to reconstruct changes to ground surface temperature (GST), either globally or regionally, from geothermal data; such analyses provide significant inputs into understanding how human activity is affecting the global energy balance (e.g., IPCC, 2013). Both Huang et al. (2000) and Beltrami et al. (2002) utilized a dataset comprising 616 borehole temperature records with worldwide distribution, of which 26 originate from the British Isles (England, 17; Scotland, 4; the Irish Republic, 4; and Northern Ireland, 1). This database (albeit now expanded to 953 borehole records: records 517–520 from the Irish Republic and 730–751 from the UK) is now available online (NOAA, 2013), but the modelling results for the individual boreholes (available from the same source) suggest wide variations in behaviour, including instances of cooling during the 20th century when one would expect warming consistent with the meteorological evidence (Fig. 2); these difficulties have indeed been noted previously (e.g., Westaway et al., 2015). Hopcroft et al. (2007) reassessed five borehole records from this dataset using a more advanced Bayesian inversion technique, from three sites near the south coast of England (Dorset and Devon), and two inland in central-southern England. Their analysis suggested roughly constant rates of GST rise over ~500 years, amounting to ~1.5–2 °C, at the south coast sites, whereas the inland sites indicated near-constant temperatures until ~300 years ago followed by modest temperature rises of ~≤0.5 °C. Given that the modelled geothermal data were collected in 1978–1983, and therefore do not record the subsequent atmospheric warming, the latter pattern is in close agreement with meteorological data from central England (Fig. 2), although the former pattern would require much more surface warming than is apparent from the meteorological data. This comparison thus raises the possibility that different parts of Britain have experienced significantly different GST variations, a possibility that is evidently worth pursuing through additional analyses of geothermal datasets; however, to be effective, such analyses will have to distinguish global contributions to GST change from local UHI effects, including effects of changes to land use.

Table 1 compares the time-averaged magnitude of the atmospheric UHI with the population of UK conurbations. The Spearman rank correlation coefficient between these variables is relatively low, only 0.35, suggesting that although population does affect atmospheric UHI, other factors also contribute. This is in total contrast with the findings of others (e.g., Oke, 1973; Sakakibara and Matsui, 2005) who have argued that atmospheric UHI magnitude and population are well correlated. Moreover, the UK conurbation where the largest-magnitude atmospheric UHI, 1.9 °C (Table 1), has been reported, Tyneside, the subject of the present study, has a relatively small population. Furthermore, preliminary investigation within Gateshead, on Tyneside (Fig. 3), by Banks et al. (2009a), established that the local subsurface UHI is ~5 °C, much larger than this atmospheric UHI. Banks et al. (2009a) suggested that this subsurface UHI reflects the local history of urban development and associated energy use; Westaway et al. (2015) tentatively raised the possibility that a large subsurface UHI such as this, itself a result of the local industrial history, might be influencing the magnitude

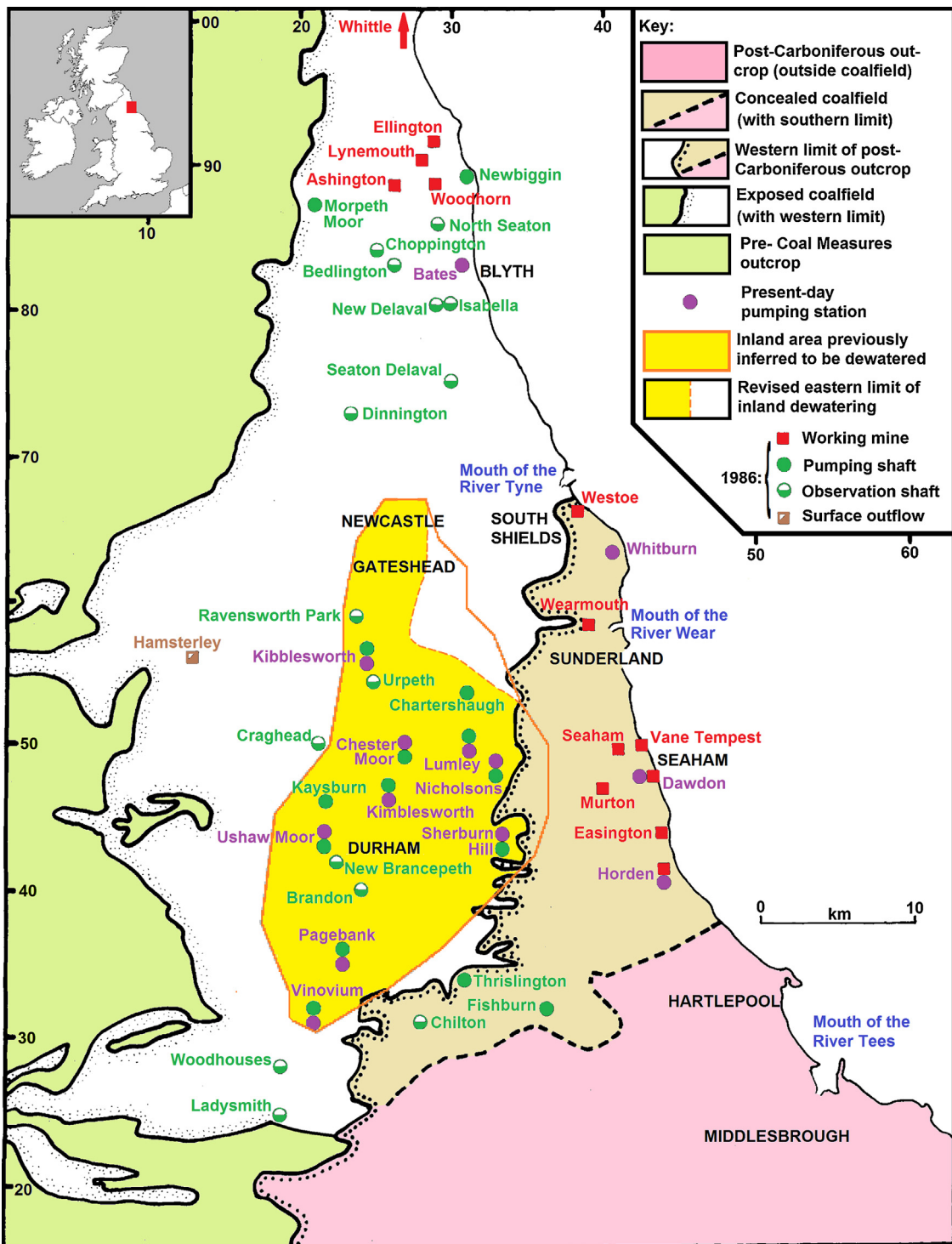


**Fig. 1.** Map of the northeast England coalfield, updated from Fig. 1 of Harrison et al. (1989), which depicted the facilities that were operational in 1986. The geometry of dewatering in the inland, exposed, part of the coalfield is from Younger (2006), as modified in the present study. Sources of information regarding other present-day facilities are documented in the main text or online supplement. The Whitburn pumping station illustrated is at the planning stage. See text for discussion.

of the local atmospheric UHI in a manner that is not considered in current modelling studies of atmospheric UHIs.

Conversely, the typical atmospheric UHI in Newcastle during the 1990s was estimated by Hughes (2006) as  $\sim 0.9^{\circ}\text{C}$ , less than half the value obtained by Kershaw et al. (2010) in Table 1. Hughes (2006) compared temperature observations at a site within the city (the former Newcastle Weather Centre, at British National Grid [BNG] reference NZ 258 648; Fig. 3) with one outside it (at Newcastle Air-

port; NZ 202 710). This 'city centre' weather station was in fact located  $\sim 1\text{ km}$  east of the city centre (Fig. 3) and so probably did not record the maximum effect. The atmospheric UHI is anyway expected to be larger now than in the 1990s due to the greater energy consumption of modern buildings (e.g., through use of air-conditioning; Costantini and Martini, 2010). On the other hand, the subsurface UHI might itself have increased on the intervening timescale and might indeed thus have fed back into increasing the

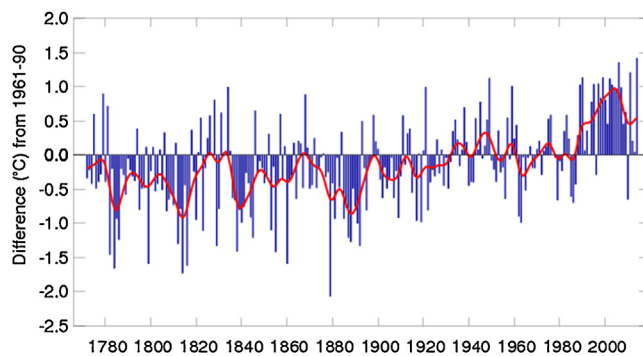


**Fig. 2.** Variation in air temperature near ground level for the years 1772–2014 in ‘central England’, from Met Office (2015) (cf. Manley, 1953, 1974; Parker et al., 1992; Parker and Horton, 2005). ‘Central England’ in this context denotes a roughly triangular region of England bounded by Lancashire, London and Bristol. Annual mean temperatures and a ten-year running mean are depicted.

atmospheric UHI; it is therefore of interest to try to establish the history of this subsurface UHI.

Aims of this study include re-examination of the Banks et al. (2009a) dataset regarding the subsurface UHI beneath Gateshead (Fig. 4) and investigation of the subsurface UHI revealed by the more recent Science Central borehole in neighbouring Newcastle (Younger, 2013; Fig. 5). The perturbed temperature profiles in both localities will be modelled to investigate their histories of development in relation to local urbanization and industrialization, the thermal history revealed by the Rowlands Gill borehole, outside this urban area (Fig. 3), will also be modelled for comparison; the wider implications of these investigations will then be discussed.

We note that Stewart (2011) has criticized much of the literature on UHIs for failure to document background information adequately, and recommended detailed examination of specific localities (as in the present account) rather than more cursory looks at inventories of data (as, for example, Huang et al., 2000; Beltrami et al., 2002; Hopcroft et al., 2007; have provided for subsurface heating effects). Like that by Westaway et al. (2015), the present study has indeed necessitated extensive use of local archives, including those held by the British Geological Survey (BGS), the UK National Archives in Kew, London, the North of England Institute of Mining & Mechanical Engineers (NEIMME) in Newcastle, the

Durham Mining Museum (DMM) in Spennymoor, County Durham, the Special Collections section of the Robinson Library of Newcastle University, and the archives of the City of Newcastle upon Tyne, Gateshead Metropolitan Borough, and County Durham (of which Gateshead was a part until 1974). These investigations have drawn together material that would be relatively inaccessible to others, and so are reported here in some detail and illustrated using historical map and air photograph imagery (see the online supplement). Other related data are readily accessible and are, therefore, not duplicated here; thus, modern detailed local topographic maps are available from the Ordnance Survey ‘Digimap’ website, online geological maps being provided by the BGS Geology DiGmap facility. Relevant details of the site histories, including our reasoning to disambiguate the various nineteenth century-mine records, so the correct stratigraphic details can be applied to each site, and associated precise co-ordinates, are provided in the online supplement.

## 2. Theoretical considerations

As we shall model both conductive and convective heat flow in the subsurface, a brief summary of relevant theory is necessary. Conductive effects of GST changes will be modelled as solutions to the one-dimensional diffusion equation for heat flow,

$$\frac{\partial T}{\partial t} = \kappa \frac{\partial^2 T}{\partial z^2} \quad (1)$$

where  $z$  is depth,  $t$  is time,  $T$  is temperature and  $\kappa$  is the thermal diffusivity of the rock mass. Since this differential equation is linear, individual solutions to it can be superposed to build up an overall solution representing the combination of effects being considered, for example from multiple time steps representing the palaeoclimate history. Consideration of more complex effects, such as the possibility of horizontal components of heat flow caused by refraction of heat by lateral variations in rock properties (cf. England et al., 1980), is beyond the scope of this study.

The subsurface effect of seasonal variations in GST can be modelled by assuming that these variations are sinusoidal with amplitude  $\Delta T_s$  about a mean value  $T_0$ , indefinitely repeating the same pattern each year. Textbooks illustrate the solution proce-

**Table 1**  
Comparison of UHI magnitudes with population for UK conurbations.

Conurbation	Urban Heat Island		Population	Rank
	$\Delta T$ (°C)	City		
Tyneside	1.9	Newcastle upon Tyne	774,891	8
South Hampshire	1.8	Portsmouth	855,569	7
Greater London	1.6	Central London	9,787,426	1
Liverpool	1.4	Liverpool	804,122	6
Glasgow	1.3	Glasgow	1,168,270	5
Edinburgh	1.3	Edinburgh	482,005	14
Sheffield	1.0	Sheffield	685,368	10
Greater Manchester	0.9	Manchester	2,553,379	2
Bristol	0.9	Bristol	617,280	11
Cardiff	0.8	Cardiff	447,287	17
West Yorkshire	0.7	Leeds-Bradford	1,777,934	4
Nottingham	0.7	Nottingham	729,977	9
Bournemouth	0.7	Bournemouth/Poole	466,266	16
West Midlands	0.6	Birmingham	2,440,986	3
Belfast	0.4	Belfast	579,554	12
Leicester	0.1	Leicester	508,916	13
Brighton and Hove	ND	Brighton and Hove	474,485	15

The 17 UK conurbations (or ‘built-up areas’) with populations of >400,000 are listed here in order of the magnitude of the annual mean atmospheric UHI,  $\Delta T$ , as reported by Kershaw et al. (2010), the cities within which each UHI measurement was made being listed. ND denotes that no UHI effect was determined by these authors. The conurbations are also ranked by population, using data from the 2011 UK census (compiled by [http://en.wikipedia.org/wiki/List\\_of\\_urban\\_areas\\_in\\_the\\_United\\_Kingdom](http://en.wikipedia.org/wiki/List_of_urban_areas_in_the_United_Kingdom)), the localities that count within each grouping being as defined in the analysis of these census data. See text for discussion.

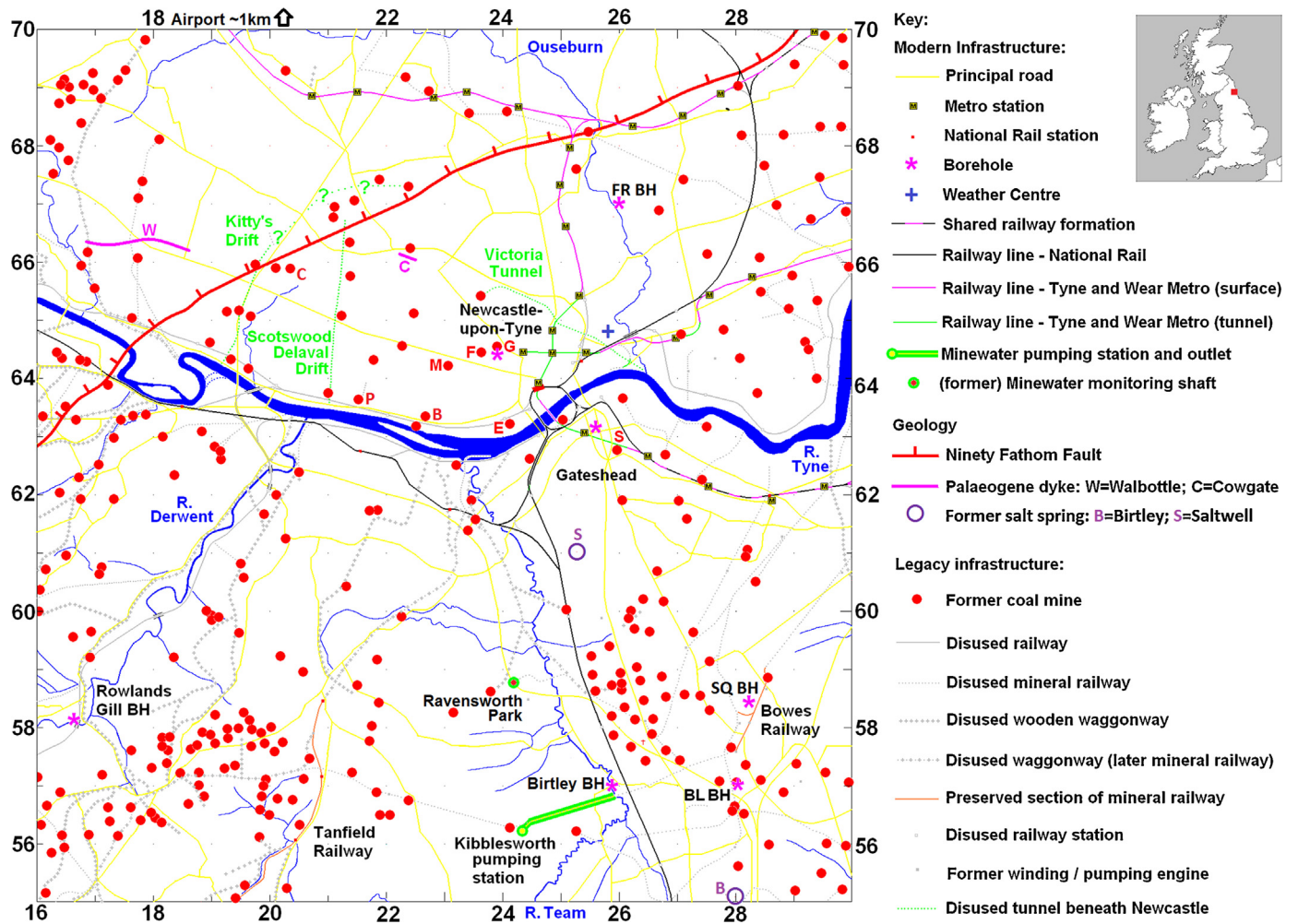


**Fig. 3.** Map of part of Tyneside showing data relevant to the present study. Based on Waggonways (2009), including information from Cook and Hoole (1975), Bennett et al. (1990), and references discussed in the text, with geological information from Mills and Holliday (1998). Location of Kitty's Drift is from Lee (1944); location of the Victoria Tunnel is from the plan dated circa 1900 housed in Newcastle Library ([www.newcastle.gov.uk/tlt](http://www.newcastle.gov.uk/tlt); accession number 013840); location of Scotswood Delaval Drift exit (at NZ 2105 6357) is from Curtis (2012); Scotswood Delaval Drift and Kitty's Drift are also located, in general terms, by Galloway (1898, p. 161 and p. 268), and on the sketch map by Akenhead (1807). Letters denote coal mines, mentioned in the main text or online supplement in connection with disambiguation of key localities (site co-ordinates being provided in supplementary Table S1) or for other reasons. Thus, G denotes the early to mid 19th century Gallowgate or High Elswick pit, later renamed as Elswick North pit, which closed in 1940 and adjoined the Science Central borehole; the shaft log for this pit is depicted in Fig. 11(b). The others are: B, Benwell Colliery, known from the late 19th century until closure in the 1930s as Elswick South pit; E, the early 19th century Engine or Wortley pit, known in the early 19th century as Elswick Colliery according to Mackenzie (1825); F, the mid 19th century Fenham or North Elswick pit; M, the mid 19th century Mill pit, labelled as 'Elswick Colliery' on the local map dating from 1858; and P, the early 19th century Paradise Colliery, also known as Beaumont Colliery and Benwell Colliery (West Pit), which is conflated with Benwell Colliery (i.e., Elswick South pit; B) in some records. C denotes the Caroline Pit of Montagu Main Colliery; BL BH, FR BH and SQ BH denote the Bassett's Lookout, Freeman Road, and Springwell Quarry boreholes. Locations of former salt springs, at Birtley (circa NZ 2799 5510) and Saltwell, Gateshead (NZ 2527 6102), are from Younger et al. (2015).

dure and give the solution to Eq. (1) subject to this surface boundary condition as:

$$T = T_0 + \Delta T_s \exp(-z/D) \cos(\omega t - z/D) \quad (2)$$

(e.g., Turcotte and Schubert, 1982; Eq. 4–89, p. 157). Here,  $\omega$  is the angular frequency of the seasonal oscillation,

$$\tau = \frac{2\pi}{\omega}, \quad (3)$$

is its period (1 year),

$$D = \sqrt{\left(\frac{2\kappa}{\omega}\right)} \quad (4)$$

is the skin depth of the temperature perturbation (i.e., the depth range over which its amplitude decreases by a factor of  $1/e$ ), and  $t$  is time, measured from the midsummer temperature maximum.

Unconsolidated ground may be aerated (i.e., in thermal contact with the atmosphere) to a depth  $z_a$ ; if so, Eq. (2) may still be used with  $z$  measured from zero at  $z_a$ , with the temperature at depths up to  $z_a$  given by the surface boundary condition

$$T = T_0 + \Delta T_s \cos(\omega t). \quad (5)$$

We thus explicitly model the effect at shallow depths of seasonal variations in surface temperature, rather than attempting to smooth the data to remove this effect, as some workers (e.g., Bense and Kooi, 2004) have done, or excluding shallow depths from the modelling, as others (e.g., Huang et al., 2000) have done.

The theory for approximating past changes in GST as a succession of step changes has been published many times (e.g., Birch, 1948; Carslaw and Jaeger, 1959; Westaway and Younger, 2013). The present-day temperature perturbation  $\delta T$  at depth  $z$  resulting

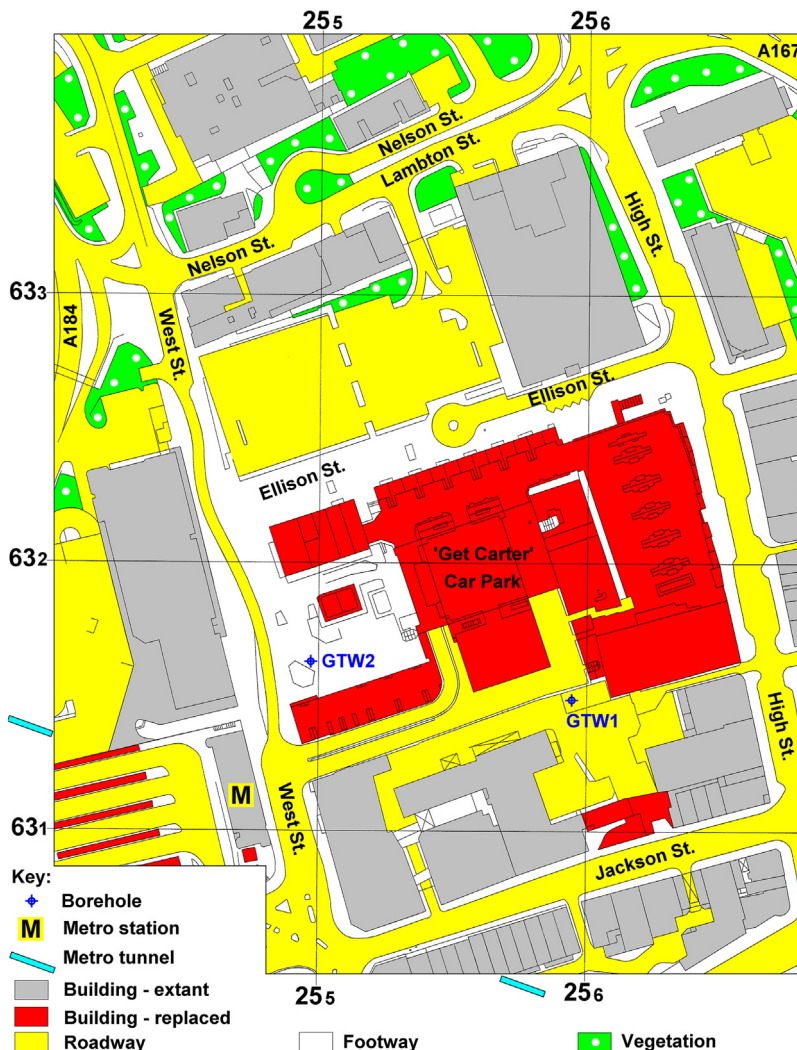


**Fig. 4.** Map of part of Gateshead town centre showing boreholes GTW1 and GTW2 (for both of which David Banks kindly provided precise location details) in relation to their surroundings. The map depicts the locality as it was circa 2000, subsequent changes being labelled using distinct ornament to support discussion in the main text and online supplement.

from a difference  $\Delta T$ , relative to the present-day GST, which ended at time  $t$  before the present and had duration  $\varepsilon \times t$ , is thus given by

$$\delta T(z, t) = \Delta T \left[ \operatorname{erf} \left( \frac{z}{2\sqrt{\kappa t}} \right) - \operatorname{erf} \left( \frac{z}{2\sqrt{(\kappa t(1 + \varepsilon))}} \right) \right]. \quad (6)$$

In the limit of  $\varepsilon \ll 1$ , the last term in Eq. (6) can be approximated using a first-order Taylor expansion about time  $t$ ; after the resulting equation is simplified, one obtains

$$\delta T(z, t) = \frac{\varepsilon \Delta T z}{2\sqrt{\pi \kappa t}} \exp \left( \frac{-z^2}{4\kappa t} \right). \quad (7)$$

Eq. (7) can be differentiated to obtain  $\partial \delta T / \partial z$ :

$$\frac{\partial \delta T(z, t)}{\partial z} = \frac{\varepsilon \Delta T}{2\sqrt{\pi \kappa t}} \left[ 1 - \frac{2z^2}{4\kappa t} \right] \exp \left( \frac{-z^2}{4\kappa t} \right). \quad (8)$$

Setting this derivative to zero gives the depth  $z_m$  where the temperature perturbation is greatest, as

$$z_m = \sqrt{(2\kappa t)}. \quad (9)$$

The maximum temperature perturbation, at depth  $z_m$ , is thus  $\delta T_m$ , where

$$\delta T_m = \frac{\varepsilon \Delta T}{\sqrt{(2\pi e)}}. \quad (10)$$

Eq. (10) can be rearranged to give

$$\varepsilon = \frac{\delta T_m}{\Delta T} \sqrt{(2\pi e)}, \quad (11)$$

thus providing a measure of the 'resolving power' of the method as regards palaeoclimate variations. For example, if one suspects that a temperature anomaly of, say,  $\Delta T = -10^\circ\text{C}$  relative to the present climate (such as might well have existed in the study region during parts of the Late Pleistocene, say, circa 20 ka; cf. [Westaway and Younger, 2013](#)), and one is trying to assess whether this might account for a mismatch between observed and predicted temperature profiles of  $\sim 0.1^\circ\text{C}$ , then from Eq. (11)  $\delta$  will be  $\sim 0.04$ . As a result, the minimum duration of the palaeoclimate variation that might be resolvable would be  $\sim 0.04 \times 20$  ka or  $\sim 800$  years. The durations adopted in the present study for the time steps of the palaeoclimate histories will be specified with this resolution limit in mind, to avoid any potential issues over possible overinterpretation of the underlying data.

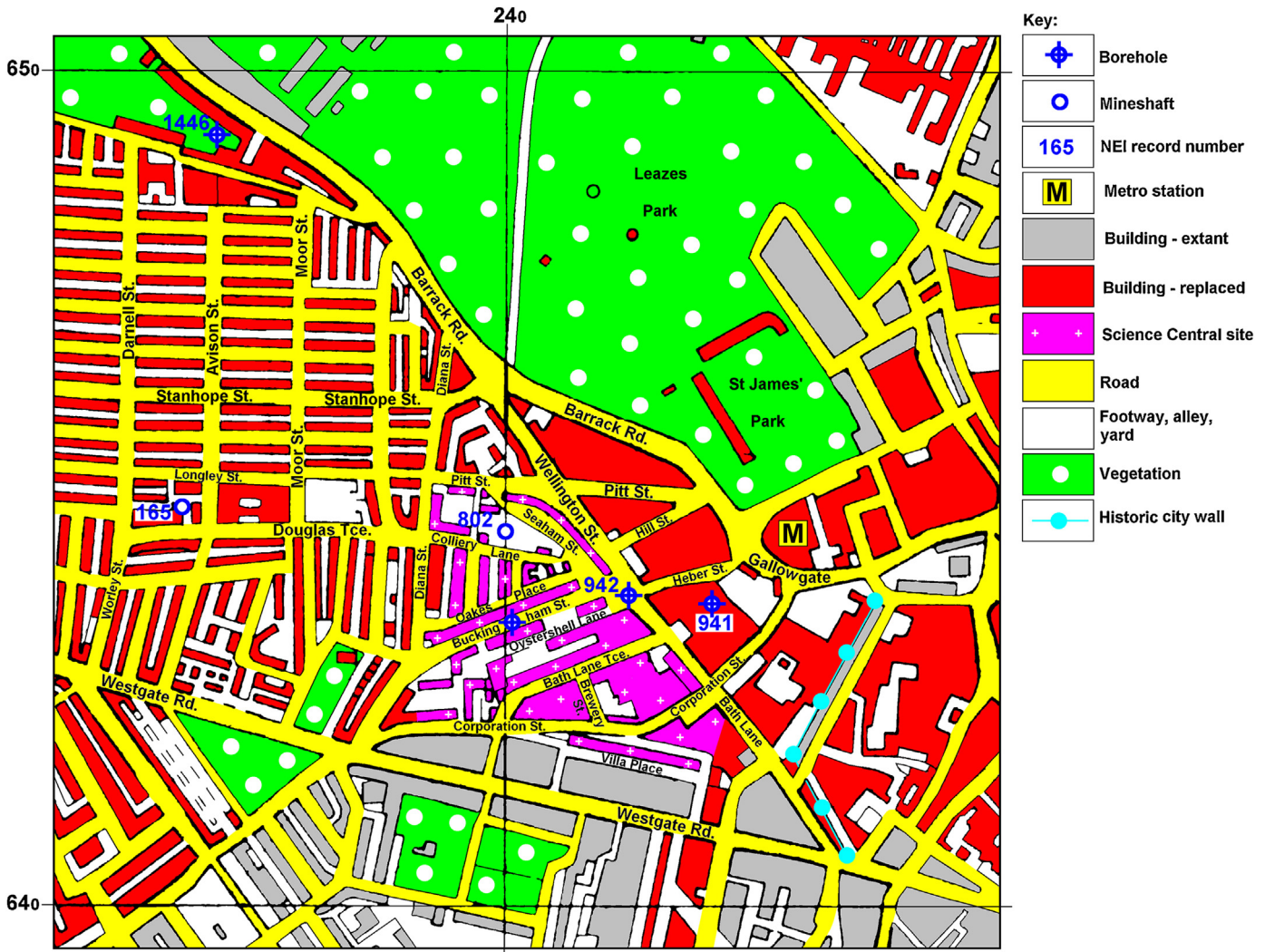


**Fig. 5.** Map of the western edge of Newcastle city centre showing the Science Central borehole in relation to its surroundings. The map depicts the locality as it was circa 1950, subsequent changes, including delineation of the Science Central site, being labelled using distinct ornament to support discussion in the text. The 'NEI numbers' are assigned to borehole and mineshaft records documented by the North of England Institute of Mining & Mechanical Engineers (NEIMME) in their sequence of reports dating from the late 19th and early 20th centuries, which are archived at the Durham Mining Museum and in the Special Collections Section of Newcastle University Robinson Library.

Eq. (8) can be differentiated a second time to obtain the rate of variation with depth of the perturbation to the geothermal gradient ( $\partial^2\delta T/\partial z^2$ ); this can itself be differentiated to find  $\partial^3\delta T/\partial z^3$ , which can be set to zero to determine the depths  $z_s$  and  $z_t$  at which the downward leading edge and downward trailing edge of the temperature perturbation 'strike' (i.e., the depths at which  $\partial^2\delta T/\partial z^2$  is a maximum and a minimum). After many algebraic steps, one obtains:

$$z_s = \sqrt{(6 + \sqrt{24})} \sqrt{(\kappa t)}. \quad (12)$$

and

$$z_t = \sqrt{(6 - \sqrt{24})} \sqrt{(\kappa t)}. \quad (13)$$

Eqs. (9), (12) and (13) are accurate for  $\delta \ll 1$  and so can serve as approximations for temperature perturbations with duration a significant proportion of their age (Fig. 6).

We note in passing that the practical difficulty regarding accurate evaluation of  $\text{erf}(x)$  for the general case of solving Eq. (6), which arises because the Taylor series for this function typically converges slowly, requiring the summation of many terms, led Westaway and Younger (2013) to adopt a computation scheme that

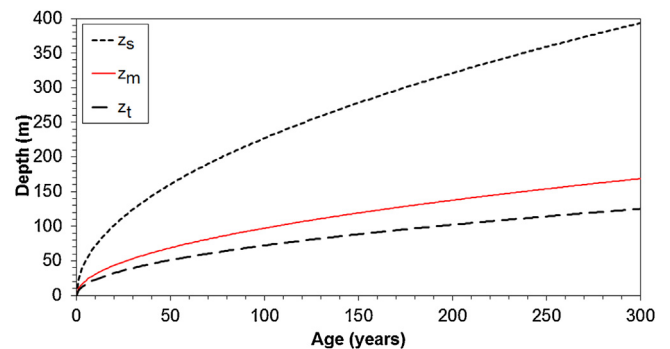


**Fig. 6.** Graphs illustrating the form of Eqs. (9), (12) and (13) for the predicted depth of the subsurface temperature perturbations that result from downward conduction of GST perturbations of a given age, calculated for  $\kappa = 1.5 \text{ mm}^2 \text{ s}^{-1}$ . Thus, for example, for a GST perturbation 100 years ago, the onset ( $z_s$ ) is predicted from Eq. (12) at 227 m, the maximum effect ( $z_m$ ) is predicted from Eq. (9) at 97 m, and the decline ( $z_t$ ) is predicted from Eq. (13) at 72 m depth.

solved for  $\partial\delta T/\partial z$  then numerically integrated the result to obtain  $\delta T$ . However, as discussed by Schöpf and Supancic (2014), the Bürmann series for  $\text{erf}(x)$  converges much more rapidly than its Taylor

series, making efficient accurate computation of this function much more straightforward; this approach can therefore be used with programming languages (such as PHP) that currently lack inbuilt facilities for calculating this function. Nonetheless, for determining conductive temperature profiles affected by GST perturbations we have reused the code from [Westaway and Younger \(2013\)](#), notwithstanding the more efficient alternative computational procedure now feasible.

Vertical heat transport by groundwater flow will be modelled using solutions to the standard one-dimensional differential equation for steady state vertical heat flow and fluid flow in a homogenous, isotropic, saturated, porous medium:

$$\frac{\partial^2 T}{\partial z^2} = \frac{\rho c v}{k} \frac{\partial T}{\partial z}, \quad (14)$$

where  $\rho$  and  $c$  are the density and specific heat capacity of the fluid and  $k$  is the overall thermal conductivity of the rock/fluid medium. If this vertical flow is assumed to be at a uniform rate  $v$  across a vertical distance  $L$ , with fixed-temperature boundary conditions  $T = T_U$  at  $z = 0$  and  $T = T_L$  at  $z = L$ , then the solution to Eq. (14) is

$$T = T_0 + (T_L - T_0) \frac{\exp(Pe_z(z/L)) - 1}{\exp(Pe_z) - 1} \quad (15)$$

([Bredehoeft and Papadopoulos, 1965](#)) where  $Pe_z$ , the Péclet number for the vertical heat transport, the ratio of heat transport by advection (i.e., by the fluid flow) to that by conduction, is defined as

$$Pe_z \equiv \frac{\rho c v L}{k}. \quad (16)$$

Such solutions are similar in form to those for heat transport as a result of heat conduction combined with vertical motion of the rock column due to erosion or sedimentation (e.g., [Westaway, 2002, 2007](#)). In both classes of solution, upward advection results in convex-upward temperature profiles whereas downward advection results in concave-upward temperature profiles (see, also, e.g., [Taniguchi et al., 1999a](#)).

The aforementioned theory was extended by [Mansure and Reiter \(1979\)](#), then by [Lu and Ge \(1996\)](#), who presented a corresponding two-dimensional analysis incorporating both horizontal heat flow and fluid flow and vertical heat flow and fluid flow. Their solution makes the assumption that the vertical components predominate, i.e., that  $|\delta| \ll 1$  where

$$\Delta \equiv \frac{\Delta T_x L \alpha}{(T_L - T_0) H Pe_z} = \frac{u \Delta T_x}{v(T_L - T_0)}, \quad (17)$$

$\alpha$  being a dimensionless parameter defined as

$$\alpha \equiv \frac{\rho c u H}{k}, \quad (18)$$

where  $H$ ,  $u$  and  $\Delta T_x$  are the horizontal extent (in the direction of flow) and horizontal velocity of the flow and the horizontal temperature difference across it. In such a situation, and with  $|\delta| \ll 1$ , temperature varies with depth thus:

$$\frac{T - T_0}{T_L - T_0} - \frac{z}{L} = (1 + \delta) \left( \frac{\exp(Pe_z(z/L)) - 1}{\exp(Pe_z) - 1} - \frac{z}{L} \right). \quad (19)$$

As [Lu and Ge \(1996\)](#) have discussed, Eq. (19) has the property that the geothermal gradient can be negative if  $\delta > 0$ ; this can occur for example with the vertical component of flow downward, provided the horizontal component is in the direction towards which temperature is increasing.

Others have previously devised analytical solutions for the effect of changing surface temperature on subsurface temperature, considering the non-steady-state effects of heat transported both by conduction and by vertical groundwater flow in the subsurface,

notably the works by [Taniguchi et al. \(1999a,b\)](#): both for a linear increase in surface temperature ([Taniguchi et al., 1999a](#)) and for a step change ([Taniguchi et al., 1999b](#)). However, these solutions are not applicable to our study localities: first, because the surface temperature variation has been more complex than was assumed for each of these analyses; and, second, because these analyses do not consider effects of horizontal groundwater flow. As will be shown below (Sections 5 and 6), a key factor governing the subsurface thermal regime in our study locality is the presence of vigorous horizontal groundwater flow through flooded mineworkings where the rock has been ‘permeabilised’ as a result of past mining activity. This horizontal flow effectively imposes subsurface thermal and flow boundary conditions that decouple the subsurface thermal and flow regimes above and below this ‘permeabilised’ layer, necessitating the use of a different approach to the analysis.

We quantify the flux  $q$  (the discharge per unit cross-sectional area) for subhorizontal flow through flooded, abandoned mineworkings using Darcy's Law, as is standard:

$$q = \frac{-k_p \rho g \Delta h}{\eta H} = \frac{K \Delta h}{H} \quad (20)$$

where  $\rho$ ,  $\eta$  and  $k_p$  are the density, viscosity and permeability of the groundwater,  $g$  is the acceleration due to gravity,  $\Delta h$  is the hydraulic head driving the flow and  $H$  again denotes the horizontal extent of this flow (in the direction of flow). The second version of this equation is expressed using hydraulic conductivity  $K$ , which relates to permeability, thus:

$$K \equiv \frac{\rho g k_p}{\eta}. \quad (21)$$

The hydraulic transmissivity  $\Psi$  for horizontal flow through a single layer of thickness  $L$  may also be expressed in terms of its hydraulic conductivity as

$$\Psi \equiv K L. \quad (22)$$

The heat transported per second,  $P$ , by groundwater flow can be calculated as

$$P = Q p c \Delta T, \quad (23)$$

where  $Q$  is the volume flow rate and  $\Delta T$  the temperature difference between the groundwater and the ambient ‘background’.

Finally, notwithstanding the grouping of terms that defines the parameter  $\alpha$  in, it has become customary (e.g., [van der Kamp and Bachu, 1989; Anderson, 2005](#)) to define the Péclet number for horizontal heat transport (or ‘basin Péclet number’)  $Pe^*$  as

$$Pe^* \equiv \frac{\rho c u L^2}{k H}, \quad (24)$$

from which it follows that

$$\alpha \equiv \frac{H^2}{L^2} \quad (25)$$

### 3. Geological setting and regional context

Except for surficial Quaternary deposits and small outcrops of Palaeogene basaltic dykes, the entire area of Fig. 3 is occupied by Upper Carboniferous sediments, known historically as the ‘Coal Measures Series’ and in modern nomenclature as the Pennine Coal Measures Group (PCMG). The succession consists of complex cyclic alternations (‘cyclothsems’) of diverse lithologies, mainly sandstones, mudstones, and coals. The underlying Carboniferous successions, which lack significant coal seams but include beds of marine limestone, were known historically as the ‘Millstone Grit Series’ and ‘Carboniferous Limestone Series’. However, revision of the nomenclature in recent decades (e.g., [Chadwick et al., 1995](#);

([Mills and Holliday, 1998](#)) resulted in the redefinition of the erstwhile upper 'Millstone Grit Series' as the lower part of the PCMG, aligning the base of the PCMG with the Namurian-Westphalian boundary (marked by the *Subcrenatum* Marine Band, known locally as the Quarterburn Marine Band), with its lower (i.e., Namurian) part renamed as the 'Stainmore Group' and the upper part of the underlying 'Carboniferous Limestone Series' as the Alston Group. Although retaining the base of the PCMG at the base Westphalian, subsequent works have made further revision, as summarized by [Waters et al. \(2014\)](#). Thus, the upper part, dominated by coarse fluvial sand, of the erstwhile 'Stainmore Group' has been renamed once again as the 'Millstone Grit Group' and the remainder, dominated by marine mudstone, as the Stainmore Formation; the Alston Group has been renamed as the Alston Formation; and the Yoredale Group, comprising the Stainmore and Alston formations, has been newly designated. The PCMG is itself locally subdivided into the Pennine Lower Coal Measures Formation (PLCMF) and Pennine Middle Coal Measures Formation (PMCMF), the former spanning the Westphalian A stage (known in Britain as the Langsettian) and the latter the Westphalian B and C stages (the Duckmantian and Bolsovian). The boundary between the PLCMF and PMCMF is defined at the Harvey Marine Band, known internationally as the *Vanderbeckei* Marine Band, which typically occurs ~10 m above the Harvey coal seam. These successions indicate cyclic alternations in depositional environments (marine, deltaic, fluvial channel, floodplain, etc.), reflecting adjustments of depositional systems to sea-level variations caused by contemporaneous glaciation (e.g., [Wanless and Shepard, 1936](#); [Heckel, 1986](#); [Gibling and Bird, 1994](#)).

The stratigraphy of the PCMG in the study area, like elsewhere in northeast England, has been subject to considerable confusion, some coal seam names having been used historically in an inconsistent manner between adjacent localities (e.g., [Mills and Holliday, 1998](#)). There is also some uncertainty in local records (including those held by the DMM) regarding the local history of mining, not least due to the proliferation of similar mine names. Incorrect location details are also reported in some 19th century NEIMME records, as can be verified using contemporaneous maps (see the online supplement). In recent decades BGS has attempted to systematize the local stratigraphy; [Jones et al. \(1995\)](#) and [Mills and Holliday \(1998\)](#) thus illustrate how modern and historical coal seam names are interrelated. These issues impact upon our study primarily because we have set out to use historical mineshaft records to establish the shallow stratigraphy (and its thermal properties) sampled by modern boreholes. As is discussed in the online supplement, it was not always straightforward to establish which documentation relates to the correct mineshafts.

The Durham/Northumberland coalfield can be subdivided into two main parts, the historical, inland, 'exposed' coalfield, where the PCMG crops out, and the 'concealed' coalfield nearer the North Sea coast, where it is overlain by Permian rocks, where mining did not begin until the mid-19th century (e.g., [Jones et al., 1995](#); [Fig. 1](#)). As a result of the gentle eastward dip of the PCMG (e.g., [Mills and Holliday, 1998](#)) the mineworkings deepened eastward, some approaching depths of 600 m beneath the North Sea.

The first geothermal measurements in this region, by [Bald \(1819\)](#), made in the deepest coal mines of that era, reaching depths of ~300 m (Jarrow, at NZ 333 655; Percy Main, at NZ 337 670; and Killingworth, at NZ 286 707), demonstrated a geothermal gradient (in modern units) of ~40 °C km<sup>-1</sup>. This high value is attributed in part to the relatively low thermal conductivity of the PCMG (see below) and in part to the presence beneath much of the region of the Devonian Weardale Granite, which is known from gravity studies (e.g., [Bott, 1967](#); [Chadwick et al., 1995](#); [Kimbell et al., 2010](#)) and drilling ([Dunham et al., 1965](#); [Manning et al., 2007](#)) but does not occur at outcrop. The gravity anomalies indicate that this granite extends to mid-crustal depths (e.g., [Kimbell et al., 2010](#)); it is

highly radiogenic (e.g., [Downing and Gray, 1986](#); [Manning et al., 2007](#)) and thus contributes significantly to the heat flow in the shallow crust. Heat flow measurements include 115 mW m<sup>-2</sup> in the Eastgate borehole ([Manning et al., 2007](#)), near the centre of the intrusion, and 99 mW m<sup>-2</sup> in the Rowlands Gill borehole (e.g., [Rollin, 1995](#)), near its northern limit (at NZ 1664 5815; [Fig. 3](#)). Especially for the latter borehole, which reached no deeper than 237 m, these measurements require significant upward revision to correct for the warming at the end of the Pleistocene glaciation to give representative heat flow at depth (cf. [Westaway and Younger, 2013](#); see below). The northern limit of this granite batholith is delineated by the Ninety Fathom Fault, which strikes WSW across the northern part of [Fig. 3](#), passing ~3.5 km NNW of Newcastle city centre. This is a normal fault that was active mainly during the Early Carboniferous, with downthrow to the NNW (e.g., [Chadwick et al., 1995](#); [Mills and Holliday, 1998](#); [De Paola et al., 2005](#)); it separates the Alston Block to the south from the Northumberland Trough to the north and is so named because it offsets coal seams by ~90 fathoms or ~160 m. The southern margin of the Weardale Granite, ~40 km farther south, is likewise delineated by a south-dipping normal fault, the Butterknowle Fault (e.g., [Fraser and Gawthorpe, 1990](#); [Collier, 1991](#); [Chadwick et al., 1995](#)), which extends eastward to the North Sea coast and determines the southern limit of the concealed coalfield in [Fig. 1](#). [Bott et al. \(1972\)](#) first noticed that high heat flow persists farther south of this margin of the granite than is explicable by heat conduction, and proposed that significant upwelling of thermal groundwater (heated by the granite) is occurring, facilitated by the presence of the Butterknowle Fault. The possibility of a similar effect in the vicinity of the Ninety Fathom Fault, potentially explaining the aforementioned local high heat flow measurements and providing a significant source of geothermal energy for Newcastle, motivated the drilling of the Science Central borehole ([Younger, 2013](#)).

To establish the local effects of human activity (coal mining, urban development, etc.) on the subsurface thermal state, borehole data unaffected by these processes are required. We take these from the aforementioned Rowlands Gill borehole (see below). The thermal properties of the Carboniferous sediments are also required; we have therefore compiled representative values ([Table 2](#); see, also, below). Comparison of subsurface and atmospheric temperature variations also requires knowledge of the latter. We use the air temperature dataset from the meteorological observatory in Durham (NZ 267 415; 102 m O.D.); dating back to 1880, this is one of the longest records of climate change in the UK ([Fig. 7](#)).

### 3.1. Rowlands Gill borehole

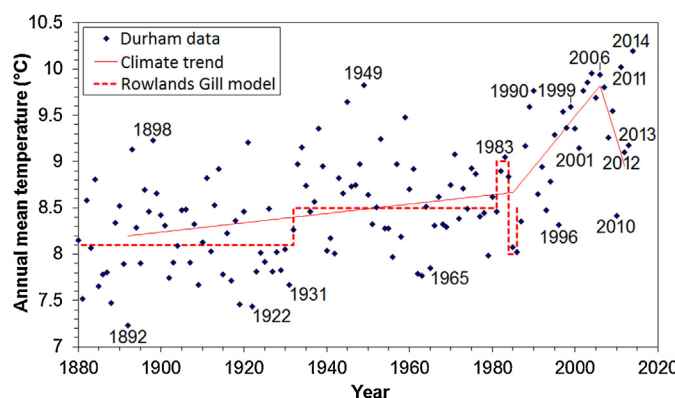
The Rowlands Gill borehole was drilled and logged by BGS in 1986 to measure the heat flow above the NE part of the Weardale Granite. From the Derwent valley floor, at 43.1 m O.D., it reached a depth of 242.9 m, penetrating 26.7 m of Pleistocene till, sand and gravel, then the basal 30.4 m of the PLCMF and the uppermost 185.8 m of the underlying Stainmore Formation ([Mills and Holliday, 1998](#), pp. 120–121, provide a lithological log). Heat flow of 99 mW m<sup>-2</sup> was reported by [Rollin \(1995\)](#), measured in the latter deposit between 132 and 237 m depths. The temperature and thermal conductivity dataset for this borehole, summarized by [Rollin \(1995\)](#) but previously unpublished, was kindly provided by the BGS.

The Rowlands Gill temperature log can be modelled as a record of conductive heat flow in response to past variation in GST ([Fig. 8](#)). The assumed GST history (depicted in [Fig. 8\(a\)](#)) is similar to that adopted for northern England by [Westaway and Younger \(2013\)](#), although more detail has been provided on variations during the Holocene and in particular during historical time. As already discussed, this GST history is approximated as a series of step functions, along with a representation of the seasonal variation

**Table 2**

Thermal properties of Carboniferous lithologies.

Property	Lithology	Sandstone	Mudstone	Coal	Limestone
$k(\text{W m}^{-1} \text{C}^{-1})$	4.9 <sup>a</sup>	1.4 <sup>b</sup>	0.4 <sup>c</sup>	2.85 <sup>a</sup>	2.09 <sup>d</sup>
$k(\text{W m}^{-1} \text{C}^{-1})$	4.02 <sup>d</sup>	1.73 <sup>d</sup>	—	2.500 <sup>f</sup>	2.500 <sup>f</sup>
$\rho(\text{kg m}^{-3})$	2460 <sup>e</sup>	2500 <sup>f</sup>	1310 <sup>g</sup>	1000 <sup>h</sup>	1000 <sup>h</sup>
$c(\text{J kg}^{-1} \text{C}^{-1})$	930 <sup>h</sup>	770 <sup>h</sup>	1300 <sup>i</sup>	—	1.1 <sup>h</sup>
$\kappa(\text{mm}^2 \text{s}^{-1})$	1.3 <sup>h</sup>	0.8 <sup>h</sup>	—	0.23 <sup>j</sup>	1.14 <sup>j</sup>
$\kappa(\text{mm}^2 \text{s}^{-1})$	2.14 <sup>j</sup>	0.73 <sup>j</sup>	—	—	—

Symbols denote:  $k$ , thermal conductivity;  $\rho$ , density;  $c$ , specific heat capacity at constant pressure; and  $\kappa$ , thermal diffusivity.<sup>a</sup> from England et al. (1980).<sup>b</sup> from Bullard and Niblett (1951).<sup>c</sup> estimated from Herrin and Deming (1996), as discussed in the text.<sup>d</sup> nominal value used by BGS for analysis of the Rowlands Gill borehole.<sup>e</sup> value for Woodkirk Sandstone, a form of Carboniferous sandstone from northern England (from <http://www.woodkirkstone.co.uk/docs/WoodkirkStone.pdf>), used as a building stone.<sup>f</sup> from [http://geology.about.com/cs/rock\\_types/a/aarocksgrav.htm](http://geology.about.com/cs/rock_types/a/aarocksgrav.htm); nominal value ( $\pm 100 \text{ kg m}^{-3}$ ).<sup>g</sup> Akenhead (1807, p. 144) reported that the density of samples of Tyneside coal varies (in modern units) between 1250 and 1370  $\text{kg m}^{-3}$ , or  $1310 \pm 60 \text{ kg m}^{-3}$ .<sup>h</sup> from Robertson (1988).<sup>i</sup> representative value ( $\pm 100 \text{ J kg}^{-1} \text{C}^{-1}$ ) for Upper Carboniferous coal from Silesia, SW Poland (Leśniak et al., 2013).<sup>j</sup> calculated as  $k/(c\rho)$  according to definition, using values of  $k$  from the first row of the table.

**Fig. 7.** Record of annual mean temperature for Durham meteorological observatory (102 m O.D.; NZ 267 415), for 1880–2014. We obtained the monthly records from this station, from <http://www.metoffice.gov.uk/climate/uk/stationdata/durhamdata.txt> (accessed 1 July 2015), and used these to calculate the annual mean values that are displayed. Dashed line illustrates the variation, approximated as a series of step changes, fitted by eye, to inform discussion of the Rowlands Gill borehole dataset (Fig. 8). Thin solid line indicates overall local temperature trends, for comparison with Fig. 2; temperature in this locality thus peaked in 2005–2006 before falling for several years then rising until 2014, the warmest year since local records began.

in surface temperature, to facilitate modelling. All these temperature perturbations are calculated for a thermal diffusivity,  $\kappa$ , of  $1.1 \text{ mm}^2 \text{s}^{-1}$ , a value which will be justified by analysis to be presented below. The sum of these perturbations is depicted in Fig. 8(c), superimposed onto a uniform steady-state temperature profiles.

The Durham climate history implies significant GST fluctuations in the early- to mid-1980s (Fig. 7). The annual mean surface air temperature in 1981 was comparable to representative values for several decades beforehand. However, the air temperature was  $\sim 0.5^\circ\text{C}$  higher in 1982–1984 than in 1981; it then decreased for 1985–1986 to values  $\sim 0.5^\circ\text{C}$  lower than for 1981. The effects of these changes, again approximated as step functions, are indicated in Fig. 8(b), the temperature during each interval of time being inferred to be  $0.5^\circ\text{C}$  higher at Rowlands Gill than at Durham, an appropriate difference given the different heights ( $\sim 60 \text{ m}$  lower O.D.) and locations of the sites. Thus, for example, the ‘steady’ surface air temperature up to 1981 is inferred to have been  $9.1^\circ\text{C}$  at Rowlands Gill (Fig. 8(c)) rather than the  $\sim 8.6^\circ\text{C}$  evident at Durham (Fig. 7). The decrease in surface air temperature for 1985–1986 is omitted from the modelling in Fig. 8(c), because the vertical extent of the resulting perturbation to subsurface temperature overlaps

with that of the seasonal effect that has already been included (the calculation of the seasonal effect being formally valid only if superimposed onto a temperature profile that is not time-dependent).

Despite the extensive history of coal mining in the uplands flanking the Derwent valley (Fig. 3), the valley floor in the Rowlands Gill area (in the basal part of the PLCMF) lies beneath the mined succession of coal seams. Some of the mines depicted in this vicinity in Fig. 3 were, indeed, drift mines, extending horizontally into the valley sides rather than downward into underlying strata. One therefore does not expect significant anthropogenic disturbance to the subsurface in this locality, other than the effects of atmospheric temperature change; the modelling in Fig. 8(c) indeed indicates that no such disturbance is evident.

### 3.2. Thermal properties

The presence of the different lithologies, with distinct thermal properties, is well known, from studies of similar cyclic Carboniferous successions elsewhere in the region (e.g., Bott et al., 1972; England et al., 1980), to complicate the analysis of geothermal data. Furthermore, relatively few measurements have been made of the thermal properties of these Carboniferous lithologies, in contrast with younger rocks in Britain that have been much more extensively studied from this point of view (e.g., Bloomer, 1981; Midttømme et al., 1998) because knowledge of such properties bears upon thermal history analysis for petroliferous Mesozoic/Cenozoic sedimentary basins. Thus, Bullard and Niblett (1951) reported that (in modern units) thermal conductivity,  $k$ , is  $0.24$ ,  $1.36$  and  $2.77 \text{ W m}^{-1} \text{C}^{-1}$ , respectively, for Carboniferous coal, mudstone and sandstone. Bott et al. (1972) reported a mean  $k = 4.0 \text{ W m}^{-1} \text{C}^{-1}$  for 24 samples of Carboniferous sandstone from the Woodland borehole in County Durham, whereas England et al. (1980) reported a mean  $k = 4.9 \pm 0.3 \text{ W m}^{-1} \text{C}^{-1}$  for 9 samples of Carboniferous sandstone from the Rookhope borehole, also in County Durham. However, due to poor core recovery, neither of these teams analyzed any mudstone samples; furthermore, their estimates of  $k$  for sandstone are much higher than the corresponding estimates by Bullard and Niblett (1951). Likewise, the Bullard and Niblett (1951) determination for coal seems rather low; more recent analysis suggests values of  $\sim 0.3 \text{ W m}^{-1} \text{C}^{-1}$  for bituminous coal and  $\sim 0.5 \text{ W m}^{-1} \text{C}^{-1}$  for anthracite (Herrin and Deming, 1996). Tyneside coals are close to the transition between these categories (e.g., Jones et al., 1995; Mills and Holliday, 1998), so a value of  $\sim 0.4 \text{ W m}^{-1} \text{C}^{-1}$  can be estimated. Whatever the thermal prop-

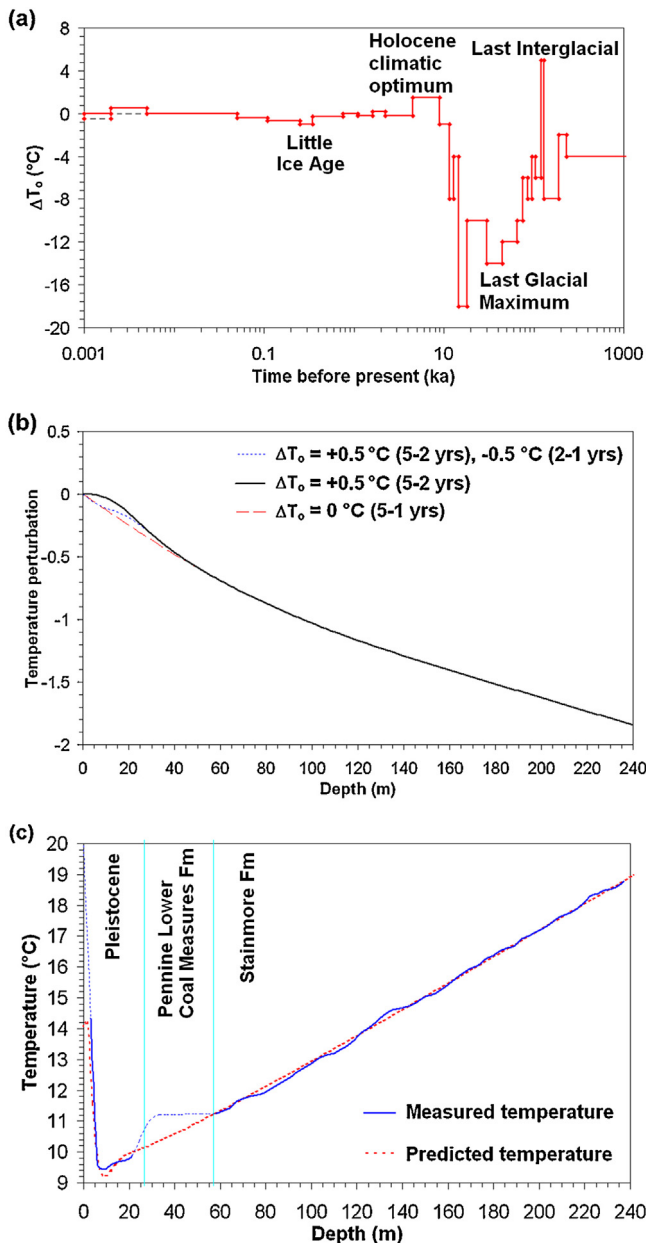


**Fig. 8.** Modelling of the temperature profile measured in the Rowlands Gill borehole (Fig. 3). (a) Assumed variation in surface temperature, represented as a series of step functions and plotted using a logarithmic timescale that records time before the borehole was logged in 1986. Alternative representations of the fluctuations in GST in the early- to mid-1980s are shown. (b) Predicted subsurface perturbations resulting from the different assumed GST histories in (a). (c) Match between observed and predicted temperature profiles calculated for GST varying as the bold lines in (a) and (b), superimposed onto the effect of seasonal temperature fluctuations. Faint ornament denotes the part of the data series that cannot be represented in terms of any plausible GST history (e.g., with identical temperature measurements at successive depths) and is, thus, regarded as ‘duff’. All temperature perturbations are calculated for  $\kappa = 1.1 \text{ mm}^2 \text{ s}^{-1}$ ; the seasonal effect in (c) has  $\Delta T_s = 5^\circ\text{C}$ ,  $z_a = 2 \text{ m}$ , and phase appropriate for midsummer. The steady-state temperature profile superimposed in (c) extrapolates to  $9.1^\circ\text{C}$  with a gradient of  $48.5^\circ\text{C km}^{-1}$ .

erties of the individual lithologies (Table 2), because the heat flow is subperpendicular to the subhorizontal bedding, a representative value of  $k$  (and, thus,  $\kappa$ ) in these sequences should be determined as the harmonic mean, taking account of the percentage of each lithology present (e.g., Bott et al., 1972).

The BGS analysis of the Rowlands Gill borehole dataset assigned each bed a nominal thermal conductivity based on

its lithology (the values they used included  $1.73 \text{ W m}^{-1} \text{ }^\circ\text{C}^{-1}$  for mudstone,  $1.84 \text{ W m}^{-1} \text{ }^\circ\text{C}^{-1}$  for siltstone,  $2.09 \text{ W m}^{-1} \text{ }^\circ\text{C}^{-1}$  for limestone,  $2.92 \text{ W m}^{-1} \text{ }^\circ\text{C}^{-1}$  for conglomerate [i.e., clasts of sandstone in a siltstone matrix] and laminated sandstone/siltstone, and  $4.02 \text{ W m}^{-1} \text{ }^\circ\text{C}^{-1}$  for sandstone), then evaluating the thermal conductivity as the harmonic mean, taking account of the thicknesses of the various beds. Using their data, the depth range from 132 m to 237 m (used for their heat flow measurement; representing the Stainmore Formation) had a total thermal resistance of  $42.8^\circ\text{C W}^{-1}$  and a harmonic mean  $k$  of  $2.46 \text{ W m}^{-1} \text{ }^\circ\text{C}^{-1}$ . The temperature rise over this interval,  $4.35^\circ\text{C}$ , thus yields a heat flow estimate of  $102 \text{ mW m}^{-2}$ . It is not clear why this value differs from the  $99 \text{ mW m}^{-2}$  value reported by Rollin (1995). One possibility is that allowance has been made for the thermal resistance of thin coal seams, reported by Mills and Holliday (1998), which have not been incorporated into the above analysis. Such seams add up to 0.27 m thickness over this 105 m interval, or  $\sim 0.3\%$  of it; if they are assumed to have a very low thermal conductivity (say,  $0.24 \text{ W m}^{-1} \text{ }^\circ\text{C}^{-1}$ ; see above) then the overall harmonic mean thermal conductivity would decrease to  $\sim 2.39 \text{ W m}^{-1} \text{ }^\circ\text{C}^{-1}$  and the estimated heat flow would adjust to  $99 \text{ mW m}^{-2}$ .

An equivalent analysis for the whole  $\sim 179$  m thickness of the Stainmore Formation that was logged for temperature (between 58 m and 237 m depths) is also possible; using the BGS data this succession has a total thermal resistance of  $71.9^\circ\text{C W}^{-1}$  and a harmonic mean thermal conductivity of  $2.49 \text{ W m}^{-1} \text{ }^\circ\text{C}^{-1}$ . The  $7.57^\circ\text{C}$  temperature rise thus yields a heat flow estimate of  $105 \text{ mW m}^{-2}$ . From Mills and Holliday (1998), a total of 0.51 m of coal is also present, again  $\sim 0.3\%$ ; assuming a thermal conductivity of  $0.4 \text{ W m}^{-1} \text{ }^\circ\text{C}^{-1}$  for this layer would reduce the harmonic mean  $k$  to  $2.45 \text{ W m}^{-1} \text{ }^\circ\text{C}^{-1}$  and the resulting heat flow to  $104 \text{ mW m}^{-2}$ . For comparison, the steady-state temperature profile in Fig. 8(c), with a geothermal gradient of  $48.5^\circ\text{C km}^{-1}$  would give, for  $k = 2.45 \text{ W m}^{-1} \text{ }^\circ\text{C}^{-1}$ , a heat flow of  $119 \text{ mW m}^{-2}$ , this value exceeding the other estimates because it is corrected for palaeoclimate. Strictly speaking, any heat flow measurement from a valley floor site like Rowlands Gill should also be corrected for topography; this will reduce the estimated heat flow somewhat (Westaway and Younger, 2013), but such analysis is beyond the scope of the present study.

Because we shall infer thermal conductivity and diffusivity in Newcastle and Gateshead using old mine records (see below), we wish to establish what information could have been obtained from the Rowlands Gill borehole if it had been logged as crudely as these older records. The BGS logging within the Stainmore Formation can be approximated as 29.7% siltstone and mudstone, 23.3% sandstone, 10.3% limestone, and 36.7% other lithologies, mostly interbedded sandstone and siltstone. Using the BGS values for thermal conductivity, from Table 2, together with a nominal  $3 \text{ W m}^{-1} \text{ }^\circ\text{C}^{-1}$  for the ‘other’ category, gives a harmonic mean of  $2.49 \text{ W m}^{-1} \text{ }^\circ\text{C}^{-1}$ , whereas using the data in the first row of Table 2 would give  $2.39 \text{ W m}^{-1} \text{ }^\circ\text{C}^{-1}$ . As discussed above, both these values would be reduced slightly if the small proportion of coal were also factored in. Likewise, using the data in the final row of Table 2, together with a nominal  $1.2 \text{ mm}^2 \text{ s}^{-1}$  for the ‘other’ category would give a harmonic mean thermal diffusivity of  $\sim 1.1 \text{ mm}^2 \text{ s}^{-1}$ ; this reasoning thus provides the basis for the adoption of this value in the calculations underpinning Fig. 8(c). This test suggests that the relative crudeness of the nineteenth century mineshaft logs is unlikely to significantly hinder our present analysis.

### 3.3. Historical mine pumping data

As will become clear, our ability to model the temperature profiles in the Gateshead and Newcastle boreholes depends on knowledge of groundwater flow regimes as well as conductive heat

**Table 3**  
Kibblesworth pumping station data.

Date	T (°C)	z (m O.D.)	Q (l s <sup>-1</sup> )
1987	16.0	-85.4	297
1997	15.8	~ -70	297
14 August 2003	16.5	-22.9	167
28 September 2003	14.6	-25.4	311
7 October 2003	13.7	-25.3	293
11 November 2003	14.1	-26.2	324
28 November 2003	13.5	-26.2	325
3 December 2003	14.7	-26.5	327
26 January 2004	11.1	-27.2	328
30 April 2004	15.0	-24.7	328

Kibblesworth pumping station pumps water from the Glamis shaft of the former Kibblesworth coal mine (at NZ 24358 56232; surface level 73.5 m O.D.), which closed in 1974, into a pipeline buried along the formation of the former Bowes Railway, which heads eastward into the Team Valley (Fig. 3). Temperature T and flow rate Q data for 1987 are from Harrison et al. (1989); the data for 1997 are from Younger (1998). At these times the water was discharged into the River Team (circa NZ 259 568), the temperature being measured at the outfall. The surface level of the groundwater, z, for 1997 is estimated from the earliest records in Fig. 9, which begin in 1999; it may have been the same as when measured by Harrison et al. (1989). The temperature measurements made in 2003–2004 were provided by Karen Johnson in 2013 and were made by her during the development of the Lamesley water treatment project (to treat minewater from Kibblesworth as well as sewage; see Welsh, 2005, or Johnson and Younger, 2006; for details) at the point where the flow now debouches into the water-treatment wetland, ~50 m from its former outfall. The January 2004 temperature measurement was probably perturbed due to contemporaneous cold weather. Values of Q and z for 2003–2004 are from the dataset in Fig. 9, interpolated to the dates when T was measured.

flux. We therefore now summarize relevant details regarding the groundwater flow and water table variations in the study region. The first systematic inventory of the local mining-related hydrogeology, by Harrison et al. (1989), documented the situation extant in 1986 (Fig. 1). At this stage, all collieries in the inland, exposed, part of the coalfield had closed (the last, Sacriston, NW of Durham, at NZ 234 478, closed in November 1985; Jones et al., 1995) but a network of pumping stations and monitoring shafts had been established to maintain the water table at a low level. Large-scale coal production was still under way in the concealed, coastal part of the coalfield; given the gentle eastward dip of the PCMG, the main reason for the inland dewatering at this time was to prevent groundwater from flowing through worked coal seams and flooding these active mineworkings (e.g., Younger, 1993). Harrison et al. (1989) thus reported that, at this time: the largest pumped discharge was from Horden colliery (NZ 442 416), amounting to 1700 m<sup>3</sup> h<sup>-1</sup> or ~15 million tonnes per year; the deepest levels pumped dry were 570 m below O.D. at Wearmouth colliery (NZ 391 581) and 555 m below O.D. at Vane Tempest colliery (NZ 426 503); and the warmest discharge, at 16.4 °C, was from Chartershaugh pumping station (NZ 309 536). Harrison et al. (1989) indeed noted the potential value of the heat thus produced, estimating the resource from the ~9300 m<sup>3</sup> h<sup>-1</sup> or ~82 million tonnes of water pumped per year, much of it at ≥15 °C, as ~50 MW. At this stage there was no water table monitoring directly beneath the urban areas of Newcastle or Gateshead. However, in the monitoring shaft at Dinnington (NZ 232 728; ~8 km north of central Newcastle) the water table was 55.5 m below O.D., whereas at Ravensworth Park (NZ 241 589; ~4 km SW of central Gateshead; Fig. 3) it was 75.3 m below O.D., and at the adjacent Kibblesworth pumping station (NZ 246 565; Fig. 3; Table 3) it was 85.4 m below O.D. As mining, and associated pumping, in this urban area had ended decades earlier (with the aforementioned closure of 'the Monty' in November 1959), we infer that the water table beneath central Newcastle and Gateshead had already risen by the 1980s to near O.D., at which height it was constrained by the presence of the tidal River Tyne and by the subsurface drainage provided by ancient adits, such as the 17th century Scotswood Delaval Drift (e.g., Younger, 2004).

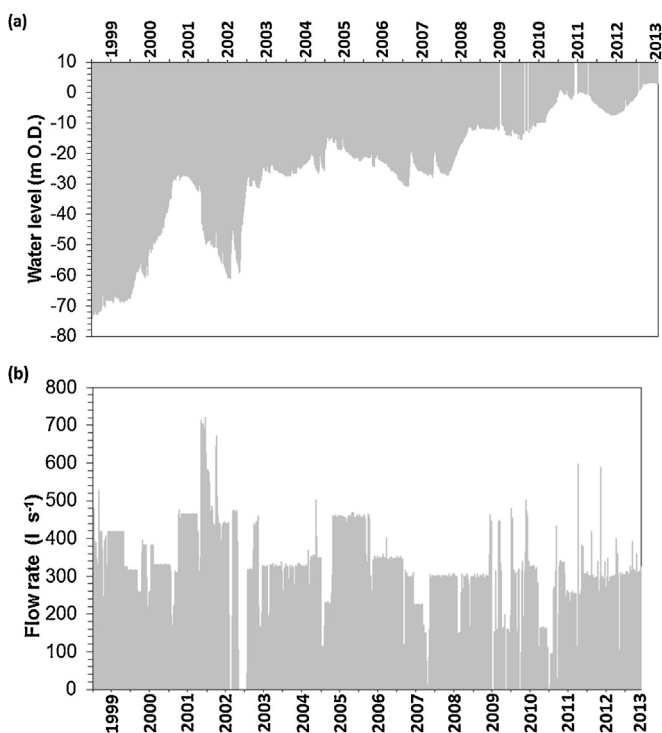


**Fig. 9.** Water level (a) and flow rate (b) data (from the UK Coal Authority) for the Kibblesworth pumping station.

the 18th century Kitty's Drift (e.g., Younger, 2004) and the 19th century Victoria Tunnel (Fig. 3), which all have outlets near O.D. Before large-scale mine pumping began and such drainage adits were constructed the water table within this dewatered area was typically much higher; for example salt-water springs were known historically in Gateshead (Younger et al., 2015; Fig. 3).

The last colliery in the concealed, coastal part of the Durham coalfield, Wearmouth, closed on 24 November 1993; henceforth, only Ellington colliery in Northumberland (NZ 283 917) remained operational, surviving until January 2005. From 1 March 1994, pumping of the former coastal mineworkings in the Durham coalfield was discontinued (Younger, 1995) and water levels began to rise rapidly. Concerns at this time about the pollution that would result if the water table were to regain its 'natural' level throughout the Durham coalfield (e.g., Younger, 1993, 1995, 1998; Younger and Sherwood, 1993; Banks et al., 1996) led to the decision to retain nine of the pumping stations in the inland area, including Kibblesworth (Fig. 9 and Table 3), on a permanent basis (e.g., Younger and Harbourne, 1995; Younger, 1997; Younger and Adams, 1999; Fig. 1), and to construct new pumping stations in the coastal area (at the former Dawdon, Horden, and Bates collieries; Fig. 1; see the online supplement for more details). Bioremediation technologies were also developed to treat these pumped discharges before release into the environment (e.g., Welsh, 2005; Younger and Henderson, 2014).

Since 1994, groundwater monitoring in this region has intensified, using a network of new Coal Authority and Environment Agency boreholes; their dataset for 1994–2004 was compiled by Yu (2006) and summarized by Yu et al. (2006). The geometry of coalfield dewatering by the inland mine pumping network was also investigated by Younger (2006), as depicted in Fig. 1. This illustration is based on a diagram which envisaged the northeast boundary of the region dewatered by this pumping network as running south-eastward from Newcastle and Gateshead. However, subsequent analysis by Younger et al. (2015) of the dataset (collected in 2004) from the Bassett's Lookout Borehole (named as the 'Birtley Fish-

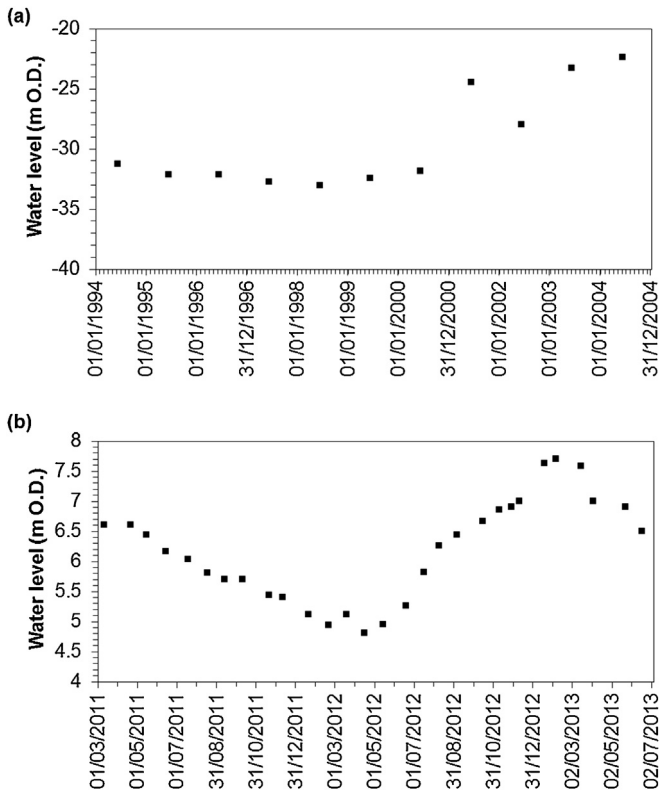


**Fig. 10.** Borehole records demonstrating relative stability of the water table in the vicinity of Newcastle and Gateshead (see Fig. 3 for locations). (a) The Environment Agency Birtley Borehole (BGS inventory code NZ25NE175; NZ 2587 5698); data from Figs. 7–10(b) of Yu (2006). (b) The Coal Authority Freeman Road Borehole, northeast of Newcastle city centre (NZ 25917 67373). This measured water level fluctuated during 2011–2013 within a range of ~3 m, with no overall trend, about a mean value of ~6 m O.D.

ponds' borehole by BGS, reported by them at NZ 28034 56980, with inventory code NZ25NE400) at Birtley, south of Gateshead, requires taking a 'bite' out of the region formerly thought to be thus dewatered (schematically indicated by the different shading in Fig. 1). The reasoning behind this deduction is explained in detail by Younger et al. (2015). In summary, although this borehole is within 4 km of the Kibblesworth mineshaft (Fig. 3), when measured on 30 November 2004 its water level was ~59 m below O.D., compared with ~25 m below O.D. at Kibblesworth (Fig. 9(a)); the groundwater at Bassett's Lookout could therefore not have been draining towards Kibblesworth. At this time, according to Bateson and Lawrence (2012), the water level was ~175 m below O.D. at Boldon Colliery (closed June 1982; NZ 347 623) and ~155 m below O.D. at Westoe Colliery (closed May 1993; NZ 347 623), respectively ~9 and ~11 km NE of Bassett's Lookout. The subsurface drainage from Bassett's Lookout was evidently in this direction (i.e., north-eastward) at the time. Conversely, Yu (2006) and Yu et al. (2006) reported that the water table was much higher (~97 m O.D. in 2001 and ~125 m O.D. in 2004) at Springwell Quarry borehole (NZ 283 584; ~1 km NNE of Bassett's Lookout; Fig. 3). However, by analogy with observations at Bassett's Lookout, this would seem to be a localized perched water table, not the main water table (cf. Younger et al., 2015). Apart from this apparent misinterpretation of a 'groundwater mound' beneath the Springwell area, the illustrations in Fig. 3 of Yu et al. (2006) depict the groundwater changes in this region as annual time steps during 1995–2004. Thus, when (due to a reduced rate of pumping) the water table at Kibblesworth rose from ~70 m to ~30 m below O.D. between 2000 and 2003 (Fig. 9(a)), the water level in the Birtley monitoring borehole, ~2 km away, only rose from ~32 m to ~22 m below O.D. (Fig. 10(a)).

Subsequent further relaxation of pumping at Kibblesworth during 2008–2010 led to a rise in the local water level to circa O.D. (Fig. 9(a)). This adjustment was followed by minor changes in the subsurface drainage in Newcastle, notably the resumption of flow from Scotswood Delaval Drift (Curtis, 2012), which had previously been dry (Younger, 2004). The groundwater level beneath Newcastle has subsequently remained close to O.D., with no apparent trend (Fig. 10(b)).

#### 4. The Trinity Square boreholes, Gateshead

The Trinity Square boreholes in Gateshead, discussed by Banks et al. (2009a,b), were drilled to depths of 55 m (GTW1) and 80 m (GTW2) at the co-ordinates depicted in Fig. 4 and documented in detail in the online supplement, these sites being ~450 m (GTW1) and ~350 m (GTW2) west of the former North Pit of Shipcote Colliery (Fig. 3). We have therefore set out to utilize this mineshaft log (Fig. 11(a)) as a proxy for the thermal properties of the stratigraphic column sampled by these boreholes. The land surface is ~53 m O.D. near the boreholes and ~48 m O.D. around the former mineshaft, the bedding locally dipping eastward at ~1.5° (Mills and Holliday, 1998). Each feature depicted in this mineshaft log is thus expected to be shallower by ~9 m relative to O.D. and by ~4 m relative to the land surface in borehole GTW1, and ~12 m relative to O.D. and by ~7 m relative to the land surface in borehole GTW2. For example, the Main coal seam (in modern terminology; known historically as the Yard seam), at 60 m depth at Shipcote Colliery (Fig. 11(a)), is thus expected at ~56 m depth and ~3 m below O.D. in borehole GTW1 and at ~53 m depth and circa O.D. in borehole GTW2.

The Shipcote mineshaft log spans 119 m of PCMG sediments, reported as ~41.2% sandstone, ~50.8% mudstone, and ~8.0% coal (Fig. 11(a)). Using the data in the second and last rows of Table 2, harmonic means for the thermal conductivity and diffusivity of  $1.68 \text{ W m}^{-1} \text{ }^{\circ}\text{C}^{-1}$  and  $0.90 \text{ mm}^2 \text{ s}^{-1}$  can be estimated from these proportions. For comparison, Banks et al. (2009a) carried out a thermal response test in borehole GTW2 (Fig. 4), which yielded much higher values,  $3.2 \pm 0.2 \text{ W m}^{-1} \text{ }^{\circ}\text{C}^{-1}$  and  $1.5 \text{ mm}^2 \text{ s}^{-1}$ , the volumetric heat capacity ( $\rho \times c$ ) also being estimated as  $\sim 2.1 \text{ MJ m}^{-3} \text{ }^{\circ}\text{C}^{-1}$ . If the higher potential value for  $k$  for sandstone in the first row of Table 2 were used instead, the harmonic mean  $k$  would only increase to  $1.73 \text{ W m}^{-1} \text{ }^{\circ}\text{C}^{-1}$ ; choice of the appropriate thermal conductivity of this lithology is evidently not the cause of the mismatch between our present results and theirs. Conversely, if only the part of the Shipcote stratigraphic column (Fig. 11(a)) shallower than 80 m were to be used in the analysis, the proportion of mudstone would be even higher (~58.9%) and that of sandstone correspondingly lower (~33.1%), so the harmonic mean properties thus determined would be even lower (~ $1.61 \text{ W m}^{-1} \text{ }^{\circ}\text{C}^{-1}$  and  $0.84 \text{ mm}^2 \text{ s}^{-1}$ , respectively). The Banks et al. (2009a) thermal response test involved injecting hot water into the borehole and monitoring the diffusion of heat into its surroundings. It was thus measuring mainly horizontal heat transport, subparallel to the bedding. For assessment of this, the relevant thermal properties should therefore be the arithmetic mean values, rather than the harmonic mean values appropriate for vertical heat transport through horizontal bedding. Recalculation on this basis gives thermal conductivities of  $\sim 2.57 \text{ W m}^{-1} \text{ }^{\circ}\text{C}^{-1}$  for the whole Shipcote stratigraphic column (Fig. 11(a)) and  $\sim 2.38 \text{ W m}^{-1} \text{ }^{\circ}\text{C}^{-1}$  for its part shallower than 80 m. Although higher than the alternatives, these values are still well below that determined by Banks et al. (2009a). Evidently, either Banks et al. (2009a) overestimated the thermal properties, or this 19th century mineshaft log significantly underestimates these properties, presumably due to underestimation of the proportion of sandstone present.

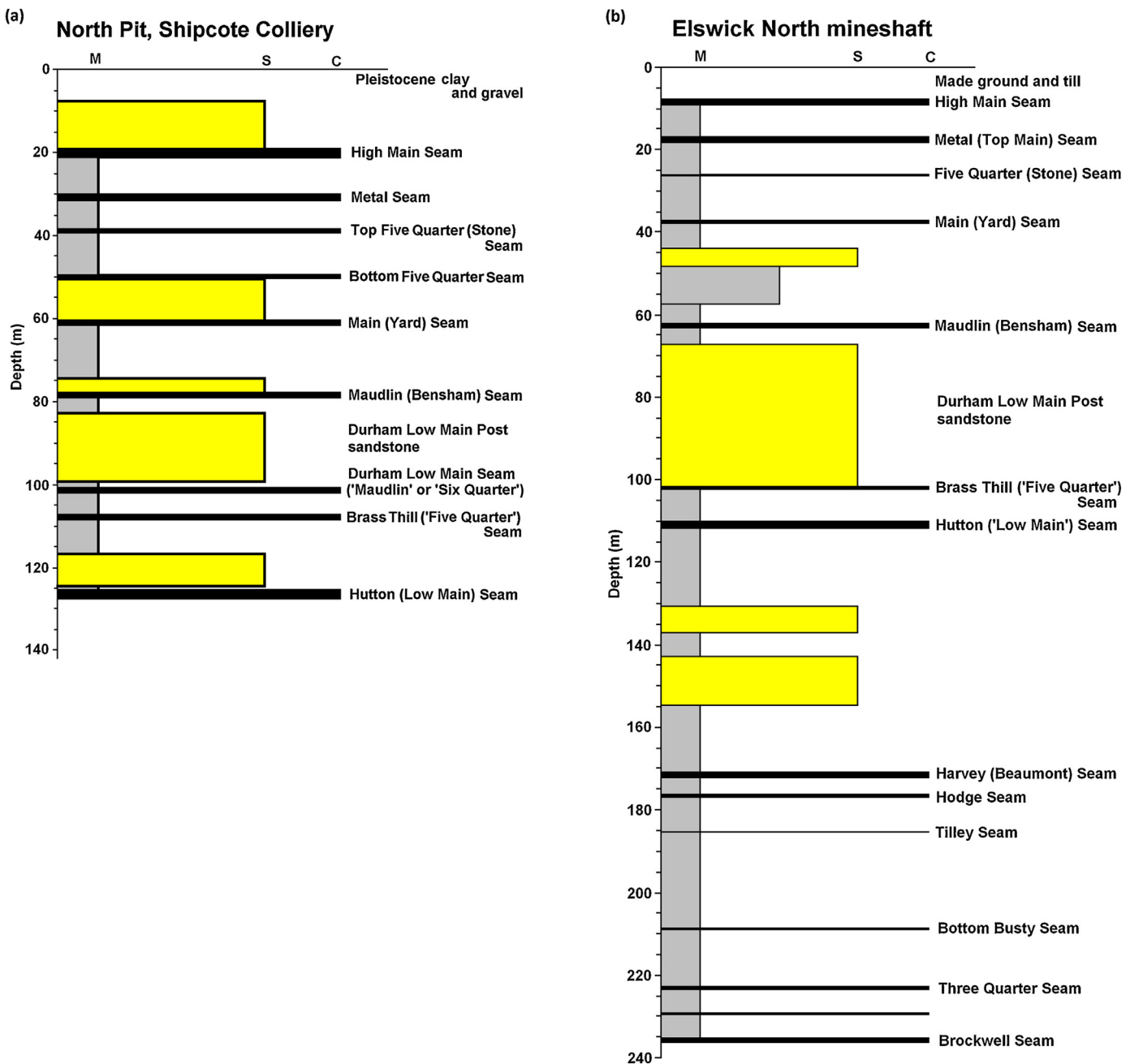


**Fig. 11.** Simplified stratigraphic columns for the North Pit shaft, Shipcote Colliery (a), beneath surface height ~48 m O.D., and Elswick North mineshaft (b), beneath surface height ~72 m O.D. Part (a) is compiled using shaft log 1800 of NEIMME (1894, p. 130). Part (b) is based on shaft log 802 of NEIMME (1881, pp. 299–300), which corresponds to BGS record NZ26SW130B and reportedly reflects the configuration of this mineshaft from 1844, when sunk to 179 m, supplemented by data from BGS record NZ26SW130A from the 1938 resurvey, by which time the mineshaft had been deepened to 237 m. Features are named using both modern and historical stratigraphic terms, the former from Mills and Holliday (1998), with lithology indicated (M = mudstone; S = sandstone; and C = coal). More detailed documentation is provided in the online supplement. These stratigraphic columns have been used to determine percentage compositions, as discussed in the text.

Borehole GTW1 intersected flooded mineworkings at 52 m depth (Banks et al., 2009a). From earlier discussion of the dip of the local bedding, these can be assigned to the Main coal seam (Fig. 11(a)); moreover, they indicate a water table near O.D., as is expected (see above). This observation means that the deeper part of borehole GTW2 is likewise below the water table, raising the possibility that its temperature profile is perturbed by effects of groundwater flow, possibly in accordance with Eqs. (15) or (19). We shall revisit this point later (see the Discussion section); in the meantime we will tentatively regard this borehole record as a conductive temperature profile.

Taking the above considerations into account, our first attempt at modelling the temperature dataset for borehole GTW2 assumes it to be a conductive temperature profile in rock with  $\kappa = 1.5 \text{ mm}^2 \text{ s}^{-1}$ , after Banks et al. (2009a). Subject to these assumptions, the GST history depicted in Fig. 12(a) can fit the subsurface temperature measurements (Fig. 12(b)). This modelling has not considered effects of changes to GST earlier than the 19th century, on the basis that such changes will not be resolvable in such a shallow borehole (cf. Fig. 6). We note, however, that the combination of the steady-state geothermal gradient of  $38^\circ\text{C km}^{-1}$ , inferred from this modelling, with the Banks et al. (2009a)  $k = 3.2 \text{ W m}^{-1} \text{ }^\circ\text{C}^{-1}$ , would imply a rather high steady-

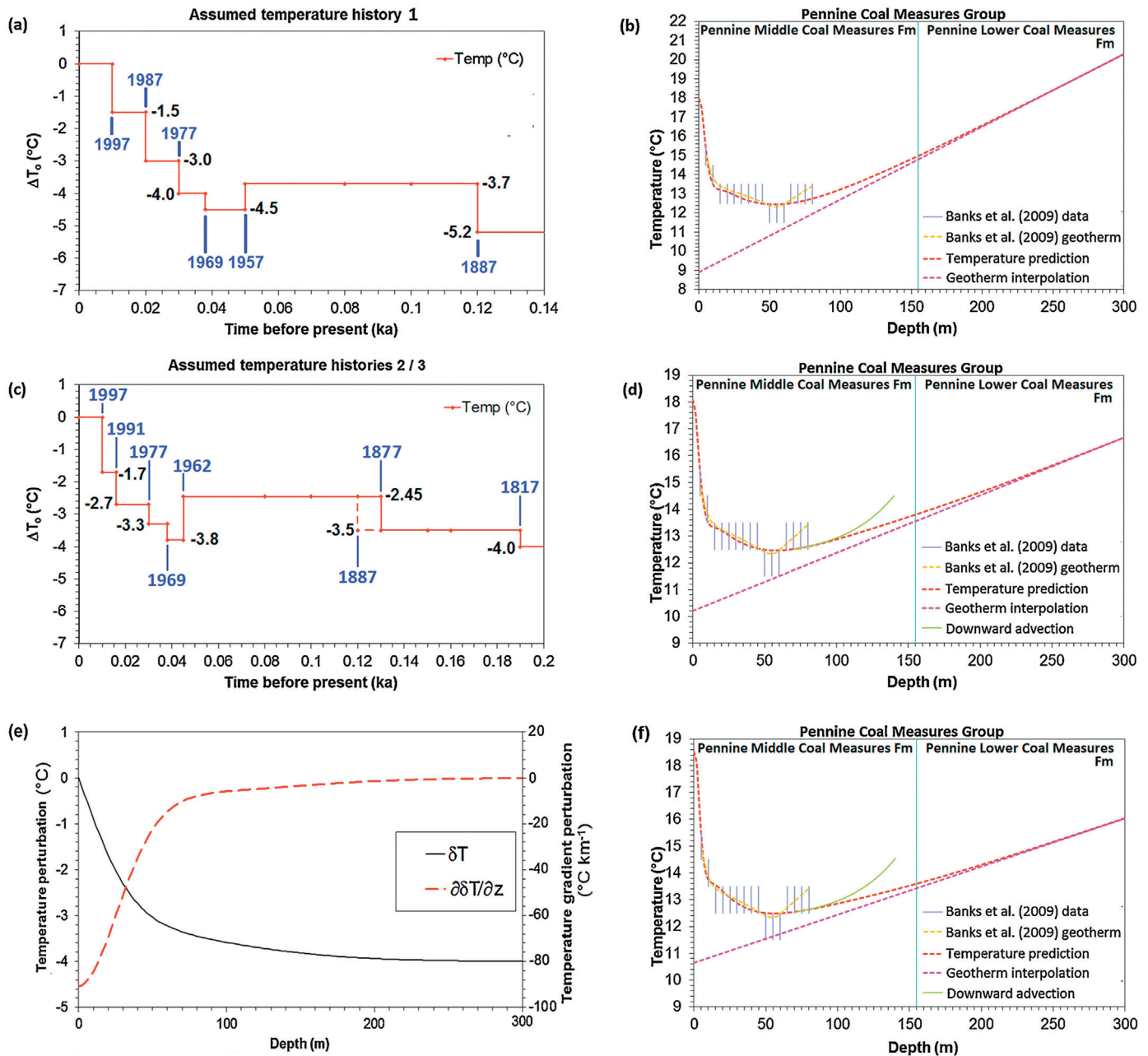


**Fig. 12.** (a) Initial assumed history of variation in annual mean GST, relative to measurement in 2007, for Trinity Square borehole GTW2. (b) Comparison of temperature measurements in borehole GTW2 (from Banks et al., 2009a) with predictions for  $\kappa = 1.5 \text{ mm}^2 \text{ s}^{-1}$ , using the thermal history in (a). The measurements, to the nearest  $1^{\circ}\text{C}$ , are represented with uncertainty  $\pm 0.5^{\circ}\text{C}$  about the nominal value. The seasonal temperature effect is modelled using Eqs. (2) to (5), assuming phase  $t = 1$  month (after the summer peak) (broadly consistent with measurement in late June 2007, as noted by Banks et al., 2009a),  $z_a = 1.2 \text{ m}$ , and annual mean present-day GST,  $T_0$ ,  $14.1^{\circ}\text{C}$  with  $\Delta T_s$ ,  $4.5^{\circ}\text{C}$ . The steady-state temperature profile extrapolates to  $8.9^{\circ}\text{C}$  with a gradient of  $38^{\circ}\text{C km}^{-1}$ , although the latter value over-predicts the likely conductive heat flow. (c) Alternative assumed histories of GST variation: dashed line, consistent with (d); solid line, with (f). (d) Comparison of the same measurements with predictions for the temperature history (dashed line) in (c), assuming the same  $\kappa$ ,  $z_a$  and seasonal heating effect as in (a), with a lower steady-state geothermal gradient,  $21.5^{\circ}\text{C km}^{-1}$ , which extrapolates to  $10.2^{\circ}\text{C}$ . Solid line denotes alternative modelling, assuming downflow of groundwater with  $P_{e2} = 2$  (cf. Eq. (15)) between boundaries at 12.5 and  $14.5^{\circ}\text{C}$  at 70 and 140 m depths. (e) Subsurface perturbation consistent with the GST variation (solid line) in (c). (f) Comparison of the same measurements with predictions for the temperature history (solid line) in (c), assuming the same seasonal heating effect as in (a) and (c), except for  $T_0 = 14.63^{\circ}\text{C}$ ,  $z_a = 1.5 \text{ m}$ ,  $\kappa = 1.0 \text{ mm}^2 \text{ s}^{-1}$ , and steady-state geothermal gradient  $18^{\circ}\text{C km}^{-1}$ , extrapolating to  $10.63^{\circ}\text{C}$ . Solid line denotes alternative modelling, again assuming downflow of groundwater with  $P_{e2} = 2$  (cf. Eq. (15)) between boundaries at 12.536 and  $14.536^{\circ}\text{C}$  at 70 and 140 m depths. See text for discussion.

state heat flow of  $122 \text{ mW m}^{-2}$ . Westaway and Younger (2013) estimated that for a  $\sim 80 \text{ m}$  deep borehole in this region, in rock with  $k = 3 \text{ W m}^{-1} \text{ }^{\circ}\text{C}^{-1}$  and  $\kappa = 1 \text{ mm}^2 \text{ s}^{-1}$ , earlier palaeoclimate changes will necessitate upward correction to heat flow by  $\sim 18 \text{ mW m}^{-2}$ . This would raise the estimated steady-state heat flow to  $\sim 140 \text{ mW m}^{-2}$ ; using the adopted thermal properties for this borehole rather than these nominal values would have a similar effect. This seems much too high for the region, notwithstanding

the proximity of the Weardale Granite (cf. Fig. 3), raising the possibility that the true values of  $k$  and  $\kappa$  are lower than has been assumed for this initial attempt at modelling.

Nonetheless, as it stands, this modelling indicates that the local GST increased by  $1^{\circ}\text{C}$  in 1887. A GST increase with this timing is broadly consistent with the start of operation of engineering works in the vicinity during the latter part of the 19th century, for example the very large Close Works a few hundred metres east of the site,

which began production, initially of railway locomotives, during 1871–1874 (see the online supplement for more details). Energy-intensive industrial processes such as this, at this and other works, including smaller factories on the Trinity Square site itself, may well have resulted in significant heat flow into the subsurface (cf. Westaway et al., 2015). The GST anomaly is also inferred from this modelling to have decreased by  $0.5^{\circ}\text{C}$  in 1957, an effect that we associate with demolition of most of the buildings that had hitherto covered the site, prior to redevelopment. We attribute the subsequent dramatic rise in local GST indicated in Fig. 12(b) to heat losses arising from the subsequent redevelopment of the site in the late 1960s.

As Banks et al. (2009a) discussed, one possible contributory factor to this dramatic heating effect following this redevelopment was downward heat flow from the shopping centre built at this time alongside the 'Get Carter' car park (Fig. 4). Another is likely to be the 'Tyne and Wear Metro' light railway line, which began operation in 1981 and passes through tunnels beneath the site (Fig. 4) (see the online supplement); underground railways elsewhere are known to cause significant heating of their surroundings, primarily due to heat generated by trains braking (e.g., Ampofo et al., 2004). As Fig. 4 indicates, westbound trains will brake beneath the Trinity Square site when stopping at the adjacent 'Gateshead Interchange' station. In the shallow subsurface, borehole GTW1 (not illustrated) yielded temperatures up to  $2^{\circ}\text{C}$  higher than GTW2 (Banks et al., 2009a); it may thus be significant that it is closer to this section of railway tunnel (Fig. 4). Nonetheless, whatever the precise cause of the thermal anomalies, the significant differences between these two adjacent borehole temperature records indicates that very local heat sources have had a major effect.

## 5. Science Central borehole, Newcastle upon Tyne

The Science Central borehole was drilled in 2011 on the western edge of Newcastle city centre to a depth of 1821 m, making it the deepest borehole on Tyneside (Younger, 2013). It was logged for temperature in August 2012 (Fig. 13(a)), with measurements at 0.1 m intervals to  $0.001^{\circ}\text{C}$  precision, with a nominal accuracy of  $\pm 0.4^{\circ}\text{C}$ , using a platinum resistance thermometer. Temperature was measured to 1772 m depth, the highest measurement being  $\sim 73.4^{\circ}\text{C}$ . Relative to a GST of  $\sim 9.4^{\circ}\text{C}$  (cf. Fig. 7), this indicates a mean geothermal gradient of  $\sim 36.1^{\circ}\text{C km}^{-1}$ , consistent with a heat flow of  $\sim 90 \text{ mW m}^{-2}$  if the typical thermal conductivity is  $2.5 \text{ W m}^{-1}\text{C}^{-1}$  or  $\sim 108 \text{ mW m}^{-2}$  if it is  $3.0 \text{ W m}^{-1}\text{C}^{-1}$ . A preliminary account having already been published (Younger, 2013), this borehole dataset will be documented in full elsewhere; for now we investigate its shallow part (Fig. 13(a)). Due to concentration on risks associated with boring into abandoned mineworkings (see below) the shallow ( $<240$  m depth) stratigraphy was not logged; we therefore use the adjacent mineshaft record for the former Elswick North Colliery (labelled 802 in Fig. 5) as a stratigraphic proxy (Fig. 11(b)). This mine, at a surface level of  $\sim 72$  m, was opened in 1825 with its shaft sunk to  $\sim 109$  m depth to reach the Hutton (or Low Main) coal seam; it was deepened in 1844 to 172 m to reach the Harvey (Beaumont) and Hodge seams. After a period of closure it reopened under new ownership in 1881 and was deepened to 237 m to reach the Brockwell seam (Fig. 11(b)), before final closure in 1940 (see the online supplement for more detail).

The uppermost 172 m of this mineshaft log is  $\sim 48.5\%$  mudstone,  $\sim 45.7\%$  sandstone,  $\sim 3.4\%$  coal and  $\sim 2.4\%$  lithologies that are undetermined from the available descriptions, which were written in miners' dialect (see the online supplement, including supplementary Table S4). The 127 m succession reported in the adjacent Gallowgate 'Spring Gardens' borehole (see supplementary Table S3 and Fig. S06(a); labelled 942 in Fig. 5) is  $\sim 48.7\%$  mudstone,  $\sim 46.3\%$

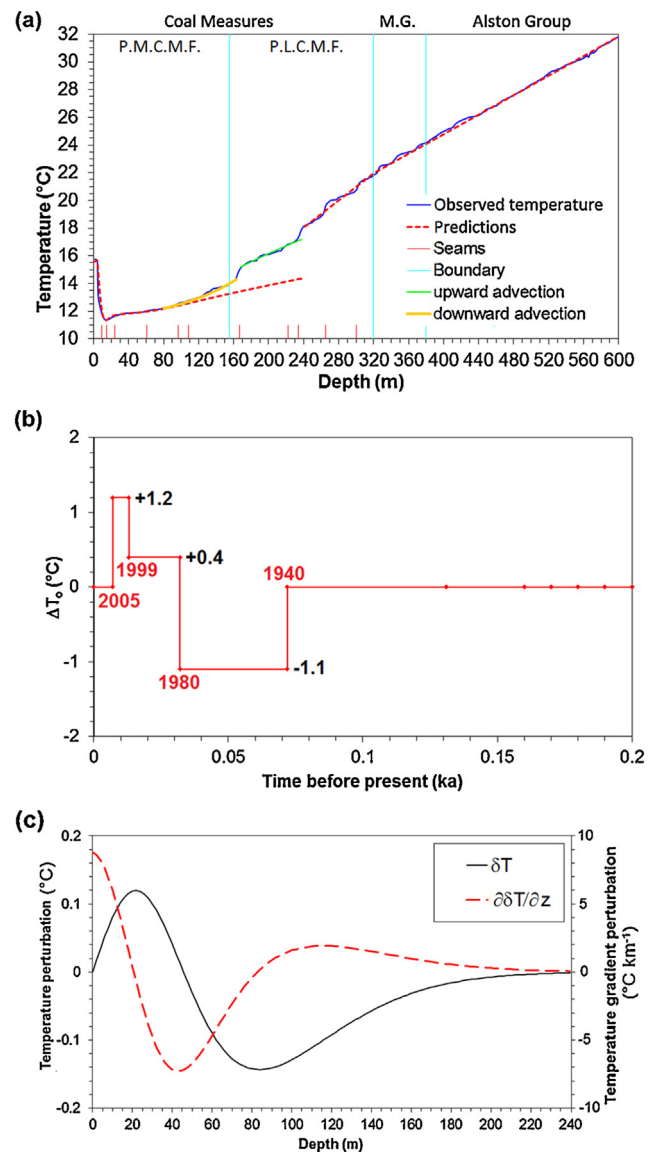


**Fig. 13.** (a) Observed and modelled temperature measurements in the upper 600 m of the Science Central borehole. The measurements were made on 15 August 2012, roughly a month after the borehole had been reworked to clear blockages and ten months after drilling, and are modelled here. First, the seasonal temperature effect is modelled using Eqs. (2) to (5), with  $T_0 = 11.3^{\circ}\text{C}$ ,  $\Delta T_s = 4.5^{\circ}\text{C}$ ,  $z_a = 4.2$  m,  $t = 0.6$  of a month (after the summer peak), and  $\kappa = 1.2 \text{ mm}^2 \text{ s}^{-1}$ . Second, the shallow conductive temperature profile also assumes  $\kappa = 1.2 \text{ mm}^2 \text{ s}^{-1}$ , with the GST history in (b), which gives the subsurface perturbation in (c), superimposed onto a uniform profile with  $T_0 = 11.3^{\circ}\text{C}$  and a gradient of  $13^{\circ}\text{C km}^{-1}$ . Third, the downflow between 80 and 163 m depths is modelled using Eq. (15) with  $P_{e_z} = 1$ ,  $L = 83$  m,  $T_U = 12.2^{\circ}\text{C}$  at depth 80 m and  $T_L = 14.3^{\circ}\text{C}$ . Fourth, the upflow between 238 and 165 m is likewise modelled using Eq. (15) with  $P_{e_z} = -0.2$ ,  $L = 70$  m,  $T_U = 15.2^{\circ}\text{C}$  at depth 168 m and  $T_L = 17.2^{\circ}\text{C}$ . Finally, the conductive temperature profile at  $\geq 240$  m depth is modelled with a uniform gradient, which extrapolates to the Earth's surface at  $8.7^{\circ}\text{C}$ , with a gradient of  $49^{\circ}\text{C km}^{-1}$  in the PCM and  $35.2^{\circ}\text{C km}^{-1}$  in the underlying Millstone Grit Group (M.G.) and Alston Group. (b) Assumed GST history. (c) Perturbations to the subsurface temperature and geothermal gradient consistent with (b). Only the part of these solutions for depths of  $<80$  m is used in (a).

sandstone,  $\sim 4.3\%$  coal and  $\sim 0.7\%$  undetermined lithologies. A representative section for this locality can thus be estimated as 50% mudstone, 47% sandstone, and 3% coal. The succession, therefore, appears somewhat more arenaceous overall than that beneath central Gateshead, largely due to the greater thickness of the Durham Low Main Post sandstone member (compare Fig. 11(a) and (b)). However, the most recent mineshaft log (documented in 1938, shortly before the mine closed; see the online supplement), like-

wise utilizes miners' dialect but is not particularly detailed, listing much of the succession as 'post and metal' (i.e., interbedded sandstone and mudstone), with no details of their proportions, thus raising the possibility that the above estimates of overall percentage composition are subject to considerable uncertainty.

Using the data in the first and last rows of Table 2, the harmonic mean  $k$  and  $\kappa$  can be determined as  $1.89 \text{ W m}^{-1} \text{ }^{\circ}\text{C}^{-1}$  and  $1.01 \text{ mm}^2 \text{ s}^{-1}$ . Using, instead, the BGS data values from Table 2, the harmonic mean  $k$  would be  $2.09 \text{ W m}^{-1} \text{ }^{\circ}\text{C}^{-1}$ . These harmonic mean calculations are most sensitive to the properties of mudstone, which are also arguably the least well constrained of the parameters involved. They are not particularly sensitive to the properties of sandstone or coal; this is due to the relatively high, and relatively tightly constrained, thermal conductivity of sandstone, the uncertainty in which has little impact on the calculations, and to the small proportion of the stratigraphic column represented by coal. For example, if  $\kappa$  for sandstone is reduced from  $2.14 \text{ mm}^2 \text{ s}^{-1}$  (Table 2) to  $1.65 \text{ mm}^2 \text{ s}^{-1}$  (the latter value recommended by Busby et al., 2009; for sandstone in Britain, in general), keeping all other parameters constant, the harmonic mean  $\kappa$  would only adjust to  $0.95 \text{ mm}^2 \text{ s}^{-1}$ . However, the vertical extent of the seasonal temperature pulse (Fig. 13(a)) suggests a rather higher  $\kappa$ ; we have modelled this as  $1.2 \text{ mm}^2 \text{ s}^{-1}$ .

As Younger (2013) has described, drilling of the shallowest part of the Science Central borehole, from the surface level of  $\sim 71 \text{ m O.D.}$  to  $\sim 240 \text{ m}$  depth, required great care, given the risk of breaching into old mineworkings and, thus, loss of drilling fluid. The Brockwell coal seam, at  $\sim 240 \text{ m}$  depth, is the deepest that has been mined locally; however, mining of this and the shallower seams utilized the 'bord and pillar' method, for which pillars of coal were left unmined to support the overburden (e.g., Donnelly, 2006). As a result, the possibility of encountering subsurface voids within or above previously mined coal seams was anticipated. To mitigate this possibility the borehole was located adjacent to the former Elswick North mineshaft, within what was thought to be a 'shaft pillar', a column of unmined coal left in situ to stabilize the mineshaft. From abundant local evidence, such as the data in Figs. 9(a) and 10(b), the uppermost  $\sim 70\text{--}80 \text{ m}$  of the rock column was expected to be, and indeed proved to be, above the water table (see the online supplement). The drilling fluid thus had much higher pressure at each depth than any groundwater present; hence the risk of loss of drilling fluid. Major fluid loss indeed occurred when the drilling hit a void at  $161 \text{ m}$  depth; this was  $\sim 10 \text{ m}$  above the extensively-mined Harvey (or Beaumont) coal seam (Fig. 11(b)) and so (as discussed by Younger, 2013; see, also, Mills and Holliday, 1998) was evidently a 'migrated void', created by the collapse of overburden into workings in this seam. The ease with which drilling fluid escaped from the borehole indicates that groundwater can flow freely at this level, due to voids created by past mining in surrounding areas (see below).

The measured Science Central temperature profile (Fig. 13(a)) exhibits considerable complexity. First, between the depth range affected by the seasonal temperature pulse and  $\sim 80 \text{ m}$ , the record from above the water table has a very low geothermal gradient. Second, below the water table, between  $\sim 80 \text{ m}$  and the  $\sim 160 \text{ m}$  'migrated void', the temperature profile is 'concave upward'. In accordance with theory (cf. Eq. (15)) we interpret this primarily as an effect of downward groundwater flow. Third, between depths of  $\sim 160 \text{ m}$  and  $\sim 240 \text{ m}$ , to the base of the former mineworkings, the temperature profile appears 'convex upward', although more subtly perturbed than at shallower depth. Again in accordance with theory (cf. Eq. (15)) we interpret this as an effect of upward groundwater flow, albeit less vigorous flow than that at shallower depths. Thus, no horizontal components of groundwater flow are assumed over each of these intervals; conversely, vigorous horizontal flow, through 'permeabilised' former mineworkings, is

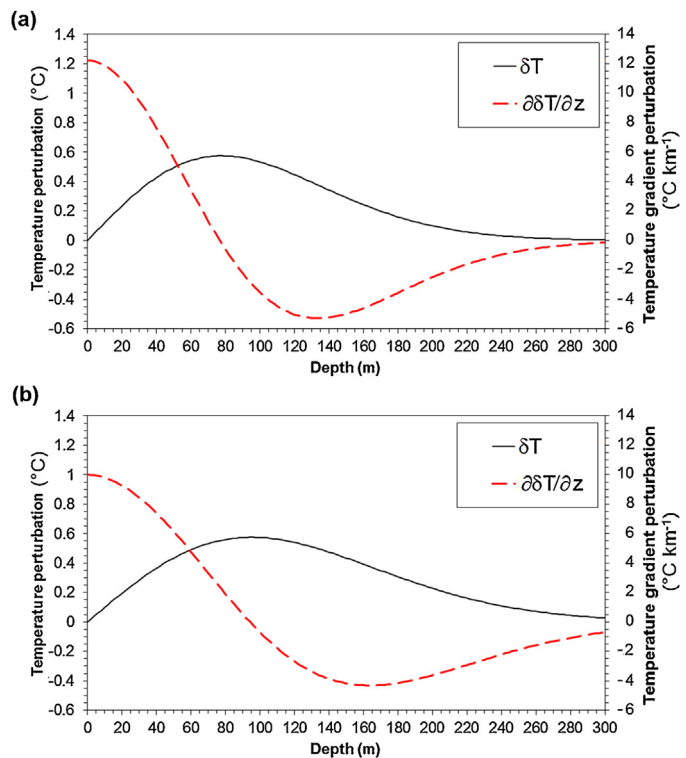


**Fig. 14.** The perturbations to temperature and geothermal gradient predicted following a surface temperature increase of  $4 \text{ }^{\circ}\text{C}$ , which lasted between 131 and 72 years before the present day, representing the span of time between 1881 and 1940 in relation to temperature measurements made in 2012. (a) For  $\kappa = 1.0 \text{ mm}^2 \text{ s}^{-1}$ . (b) For  $\kappa = 1.5 \text{ mm}^2 \text{ s}^{-1}$ .

assumed to be occurring over a narrow depth range circa 160 m, removing the groundwater that has converged on this depth from above and below from the section. Similar behaviour, of groundwater flow converging towards a permeable level in flooded mine workings, has previously been recognized by measurement of vertical flow velocities (e.g., Johnson and Younger, 2002), rather than from the associated temperature perturbations. Fourth, at multiple depths there are relatively abrupt 'steps' in temperature, involving relatively high geothermal gradients each for circa a metre. These depths coincide with coal seams (Fig. 13(a)), indicating that the 'steps' are caused by the low thermal conductivity of the coal (cf. Table 2). Finally, the mean geothermal gradient decreases somewhat, from  $\sim 49 \text{ }^{\circ}\text{C km}^{-1}$  in the deepest part of the PLCMF to  $\sim 35 \text{ }^{\circ}\text{C km}^{-1}$  over 400–600 m depth, within the underlying Alston Group. In principle, this variation might be due to a downward increase in  $k$ ; the Alston Group rocks are richer in limestone and contain less coal and mudstone than the PLCMF (Mills and Holliday, 1998), so higher  $k$  might well be expected. However, an alternative potential explanation is that this variation might be caused (at least in part) by the operation of the coal mine; ventilation or pumping might well have cooled the rock column in the vicinity of the former workings (cf. Rodríguez and Díaz, 2009).

The Brockwell coal seam, the deepest mined (Fig. 11(b)), was worked at Elswick North Colliery between 1881 and 1940 (see online supplement), spanning between 131 and 72 years before the 2012 temperature measurement in the Science Central Borehole. To assess the potential thermal effect of working this mine, Fig. 14 illustrates the form of any resulting temperature perturbation, subject to the assumption that this seam can be treated as the surface boundary of the underlying rock mass, for different potential values of  $\kappa$ . For this particular analysis, 'depth' depicted in this Figure thus represents depth below the Brockwell seam. The purpose of this calculation is to see if the slightly 'humped' part of the

temperature profile circa 330 m depth (Fig. 13(a)), or ~90 m below the Brockwell seam, where the measured temperature is ~0.5 °C warmer than the straight-line trend between ~240 m and ~600 m depths, can plausibly be explained as a consequence of the mining history. However, since this temperature is above the straight-line trend, this assumption requires the mining to have caused a warming effect, whose magnitude has to be ~2 °C to give a ~0.5 °C temperature perturbation at the expected depth (Fig. 14). With  $\kappa = 1.0 \text{ mm}^2 \text{ s}^{-1}$ , the maximum temperature perturbation is thus predicted 78 m below the model boundary (Fig. 14(a)), at 315 m depth for the real Earth, whereas with  $\kappa = 1.5 \text{ mm}^2 \text{ s}^{-1}$  it is predicted 95 m below this model boundary (Fig. 14(b)), at 332 m depth. In principle, the history of mining is, therefore, capable of reproducing this aspect of the observed temperature profile. However, we do not see why mining would cause a temperature increase (as noted above, we indeed consider it more likely to have caused a cooling effect, if it had any measurable direct effect). We therefore discount this potential explanation; we thus instead regard the 'kink' in the Science Central temperature profile at ~320–330 m depth as a consequence of higher thermal conductivity of the Millstone Grit and Alston Group rocks, at depths of >320 m, compared with the PCMG (Fig. 13(a)).

As already noted, the parts of the Science Central dataset between ~80 and ~240 m depths cannot be interpreted in terms of any plausible conductive temperature profile and are modelled instead as consequences of vertical groundwater flow (Eqs. (12) to (15)). The record between ~160 and ~240 m is thus modelled in terms of upward groundwater flow with a Péclet number of 0.2, and that between ~80 and ~160 m depths in terms of downward groundwater flow with a Péclet number of 1.0. Given the other parameter values that contribute to determining Péclet number (i.e. density and specific heat capacity of the groundwater,  $1000 \text{ kg m}^{-3}$  and  $4186 \text{ J kg}^{-1} \text{ °C}^{-1}$ , and thermal conductivity of the rock/fluid medium, estimated as  $2.5 \text{ W m}^{-1} \text{ °C}^{-1}$ ; Eq. (16)), these Péclet numbers indicate a downward groundwater velocity (Darcy velocity) towards ~160 m depth of  $\sim 7.2 \times 10^{-9} \text{ m s}^{-1}$  (or  $\sim 230 \text{ mm yr}^{-1}$ ) and an upward velocity towards the same depth of  $\sim 1.7 \times 10^{-9} \text{ m s}^{-1}$  (or  $\sim 54 \text{ mm yr}^{-1}$ ). Beneath the depth range affected by seasonal temperature perturbations, the shallow part of the temperature profile (above the water table) is modelled as a consequence of conductive heat flow in response to changes in GST, as indicated in Fig. 13(b). For the purposes of this analysis, the 'present day' conditions (Fig. 13(b)) represent the span of the time when the Science Central site was disused and/or had been cleared before redevelopment, the preceding temperature peak marking 1999–2005 when the vicinity of this borehole was occupied by a large beer-bottling plant (see the online supplement for more details). The earlier phases spanning 1940–1980 and 1980–1999 represent the GST of the inner-city environment that existed before this bottling plant was built, the temperature step in 1980 providing a representation of global warming (cf. Fig. 6) and UHI development during this span of time. The surface heating effect thus envisaged since 1980 resulted, in 2012, in a maximum positive temperature perturbation at a depth of 22 m, whereas the cooling effect envisaged during 1940–1980 resulted in the largest-magnitude negative temperature perturbation at 84 m (Fig. 13(c)). We note in passing that the operational life of this bottling plant, 1999–2005, when we infer that heat from the plant operation raised the GST near this borehole, roughly coincided with the air temperature maximum indicated in Fig. 6; the latter effect became significant in 1997, peaking in 2004–2006 ~0.7 °C warmer than it had been beforehand, before tailing off. We infer from this that the surface heating effect at Science Central, which is necessary to explain the shallow part of the temperature profile, in reality represents the combined effect of both processes (i.e., local surface warming and climatic warming), thus being a consequence of a more complicated temperature varia-

tion than is depicted in Fig. 13(b). Nonetheless, since the magnitude of the effect required to match the temperature profile (Fig. 13(b)) exceeds the contemporaneous atmospheric warming, the bottling plant evidently had a significant effect.

The resulting modelling prediction of the time-dependent conductive heat flow anomaly that existed in 2012 extended into the depth range affected by downward groundwater flow, which is itself being modelled as a consequence of constant-temperature boundary conditions. Although the modelling envisages the geothermal gradient as 'dovetailing' between these different depth ranges, strictly speaking these two sets of assumptions are inconsistent with one another. Furthermore, the groundwater flow regime could not itself have remained in a steady-state, like at present, since 1940, because (from earlier discussion) during part of this time span the water table beneath Science Central must have been much lower than at present. As already noted, until 1994 there was no monitoring of the water table beneath this urban area. Nonetheless, the Brockwell seam must have been pumped dry while the Elswick North Colliery was operating, placing the local water table at ~240 m depth or ~160 m below O.D. until 1940. In the absence of direct evidence, we envisage that once this colliery closed and its pumping ceased, the local water table was probably influenced by the pumping in the aforementioned nearby Montagu Main Colliery, which maintained the water table ~90 m below O.D. (see the online supplement). Following the 1959 closure of this latter mine, we envisage that the water table beneath Science Central gradually rose to circa O.D., as the present-day groundwater flow regime envisaged in Fig. 13(a) progressively came into being. Our modelling makes no attempt to capture this complex transient behaviour; nonetheless, due to the changing groundwater flow regime it evidently makes no sense to try to extend the conductive modelling depicted in Fig. 13(b), (c) back in time before 1940.

The modelling solution in Fig. 13(a) is thus for a thermal steady state at depths >80 m but non-steady-state at shallower depths. However, from Fig. 13(c), the temperature at 80 m depth is envisaged as having varied as a result of surface perturbations by no more than 0.14 °C, making these perturbations of little consequence for temperature at this or greater depths; this aspect nonetheless represents an approximation in our modelling. Furthermore, at the transitions envisaged between conductive and convective heat transport at depths of ~80 and ~240 m depths the geothermal gradients have been matched, implying the same heat flow above and below these transitions, consistent with the assumption of a steady state; if, on the other hand, the temperature gradient were to vary abruptly across these boundaries it would imply heat gains or losses at these points in the model, which would require temperature changes and so would not be consistent with a thermal steady state.

Notwithstanding this rather ad hoc set of underlying assumptions, the modelling results for the Science Central dataset (Fig. 13(b)) have the following physical interpretation. The uppermost part of the stratigraphic column, beneath the zone of seasonal temperature variations, is above the water table and, thus, characterized by a conductive temperature profile, albeit with a relatively low geothermal gradient, estimated as  $13 \text{ °C km}^{-1}$ , and associated low heat flow, estimated (for  $k = 2.5 \text{ W m}^{-1} \text{ °C}^{-1}$ ) as only  $\sim 32.5 \text{ mW m}^{-2}$ . Beneath the water table there is a zone of downward groundwater flow, which terminates at ~160 m depth at a migrated void overlying former workings in the Harvey coal seam. Deeper still, down to the ~240 m depth of the deepest mineworkings in the area, in the Brockwell coal seam, is a zone of upward groundwater flow, terminating at the same ~160 m-deep migrated-void level. The upward groundwater flow between ~240 and ~160 m depths is entraining a large proportion of the conductive heat flow originating from greater depths; we infer that this heat flux enters the void at ~160 m and flows subhorizontally

along it. Furthermore, the conductive temperature profile in the shallow subsurface is warmer ( $\sim 12^\circ\text{C}$ ) than would be expected from the regional climate, indicating that this part of the stratigraphic column has experienced warming as a result of past urban development. We infer that the geothermal gradient across this depth range is low in part because so much of the upward heat flow from the Earth's interior has been removed by the aforementioned upward groundwater flow, and in part because the anthropogenic surface warming has acted to try to reverse the natural upward geothermal gradient. At greater depths, down to the  $\sim 600\text{ m}$  limit analyzed in the present study, conductive heat flow resumes, with a much higher geothermal gradient. This is estimated in the basal part of the PCMG as  $49^\circ\text{C km}^{-1}$  (Fig. 13(a)), corresponding (again for  $k = 2.5\text{ W m}^{-1} \text{ }^\circ\text{C}^{-1}$ ) to a heat flow of  $\sim 122.5\text{ mW m}^{-2}$ . Conversely, if  $k = 2.0\text{ W m}^{-1} \text{ }^\circ\text{C}^{-1}$  (as is possible; see above), these heat flow estimates would adjust to  $26\text{ mW m}^{-2}$  at shallow depths and  $98\text{ mW m}^{-2}$  at  $\sim 320\text{ m}$  depth. The associated  $35.2^\circ\text{C km}^{-1}$  geothermal gradient estimated in Fig. 13(a) in the Millstone Grit and older rocks implies a thermal conductivity 39% higher than in the PCMG, thus indicating  $2.78$  or  $3.48\text{ W m}^{-1} \text{ }^\circ\text{C}^{-1}$  for the two PCMG thermal conductivity values considered above. Correction of this deeper part of the temperature profile for palaeoclimate will increase the geothermal gradient by  $\sim 6^\circ\text{C km}^{-1}$  (Westaway and Younger, 2013), raising the estimated heat flow to  $\sim 115$  or  $\sim 143\text{ mW m}^{-2}$  for the latter two thermal conductivity values. The second of these estimates is so high that we discount it, given the regional context, in favour of the former estimate and the associated thermal conductivity values.

It follows from the above reasoning that the water that is flowing downwards in the uppermost zone beneath the water table (between  $\sim 160$  and  $\sim 240\text{ m}$  depths) has been heated by the surface warming. The horizontal flow network at  $\sim 160\text{ m}$  depth thus dissipates heat arising in part from heat flow from the Earth's interior and in part from the warming of the Earth's surface and shallow subsurface. As already noted, the Kibblesworth pumping station, for dewatering the surrounding region of the disused coalfield, is located  $\sim 9\text{ km}$  south of Newcastle (Figs. 3, 9; Table 3). The area between Newcastle city centre and Kibblesworth has long been recognized as a hydraulically interconnected 'minewater pond' (e.g., Sherwood and Younger, 1994). We therefore suggest that the subsurface flow network now identified at  $\sim 160\text{ m}$  depth beneath Science Central leads southward to this pumping station, which is thus returning to the Earth's surface waters that have been heated, beneath Newcastle city centre and elsewhere, by both surface warming and heat from the Earth's interior. The fact that the temperature at the depth beneath Science Central, where this inferred horizontal flow of groundwater is concentrated, is  $\sim 15^\circ\text{C}$  (Fig. 13(a)), indistinguishable from the typical temperature of the Kibblesworth minewater discharge (Table 3), bolsters confidence in this interpretation (see also below).

## 6. Discussion

In the light of the above analysis of the Science Central dataset, which establishes that much of the expected conductive heat flow from the Earth's interior is 'captured' by groundwater flow through flooded former mineworkings, we have revisited the Trinity Square, Gateshead, dataset, to look for evidence of the same effect. As Fig. 12(c),(d) shows, in addition to the aforementioned modelling solution (Fig. 12(a),(b)) the same set of temperature measurements can also be fitted assuming a much lower steady-state heat flow ( $68.8\text{ mW m}^{-2}$ , if the same thermal conductivity of  $3.2\text{ W m}^{-1} \text{ }^\circ\text{C}^{-1}$  as before is assumed, compared with  $122\text{ mW m}^{-2}$ ), with a slightly different surface thermal history (Fig. 12(c),(d)). This associated revised GST history involves a longer duration of heating, but a smaller temperature rise,  $4^\circ\text{C}$  (Fig. 12(c)) compared with  $5.2^\circ\text{C}$

(Fig. 12(a)), although the resulting inferred pre-surface-warming steady-state GST of  $\sim 10.2^\circ\text{C}$  in Fig. 12(c) seems rather high (cf. Figs. 2 and 7). Furthermore, as already noted, part of this dataset was collected from below the water table, raising the possibility (Banks et al., 2009a) that the observed temperature profile might be perturbed by groundwater flow. The concave-upward part of this temperature profile deeper than the temperature minimum at  $\sim 55\text{ m}$  depth might, indeed, reflect downward groundwater flow rather than being purely a conductive effect. An alternative temperature profile, consistent with this assumption, has thus been added to Fig. 12(d). The assumption of a Péclet number of 2 for its calculation (using Eq. (15)) indeed enables the gradient of this advective temperature profile to 'dovetail' with that of the conductive temperature profile at shallower depth. Using Eq. (16), this Péclet number can be resolved as before into physical quantities; with  $\rho = 1000\text{ kg m}^{-3}$ ,  $c = 4186\text{ J kg}^{-1} \text{ }^\circ\text{C}^{-1}$ ,  $k = 2.5\text{ W m}^{-1} \text{ }^\circ\text{C}^{-1}$ , and  $L = 70\text{ m}$ , a downward flow velocity of  $\sim 1.7 \times 10^{-8}\text{ m s}^{-1}$  or  $\sim 540\text{ mm yr}^{-1}$  is indicated.

Fig. 12(e) and (f) illustrate a third alternative GST history and modelling solution for Trinity Square, Gateshead, subject to the assumption that  $k$  and  $\kappa$  are low, consistent with the mineshaft log in Fig. 11(a) but inconsistent with the Banks et al. (2009a) thermal response test. Thus,  $\kappa$  has been reduced to  $1\text{ mm}^2 \text{ s}^{-1}$ , the GST history in Fig. 12(c) has been adjusted slightly, with the principal surface heating time-step a decade earlier to compensate for the slower thermal diffusion and to replicate the observed pattern of subsurface temperature anomalies at the correct depth. The predicted seasonally-averaged GST of  $14.63^\circ\text{C}$  for 2007 implies, given the GST history assumed in Fig. 12(e), a pre-industrial-revolution GST of  $10.63^\circ\text{C}$ , again rather high. The steady-state conductive geothermal gradient for this solution is  $18^\circ\text{C km}^{-1}$ , which for  $k = 2\text{ W m}^{-1} \text{ }^\circ\text{C}^{-1}$  means a heat flow of  $36\text{ mW m}^{-2}$ . Like at Science Central, we infer as part of this solution that much of the upward heat flux from the Earth's interior beneath this part of Gateshead is intercepted by groundwater flow and transported elsewhere; however, the limited depth of the dataset means that this effect cannot be modelled directly.

Strictly speaking, the modelling depicted in Fig. 12(d) and (f) (like that for Science Central, already discussed) is not formally correct, because Eq. (15), which has been used in the calculations, assumes that the downflow is in a thermal steady-state, whereas the conductive modelling indicates that the temperature at its upper boundary has slowly increased over time, and so is not in a steady-state, therefore the downflow cannot itself be in a thermal steady-state. The presence of this downflow in both solutions means, in turn, that information on the surface thermal history prior to the past few decades (which might otherwise be recorded at depths of  $>70\text{ m}$ ) has been lost. It is therefore not meaningful to extrapolate a notional steady-state conductive temperature profile, representing the unperturbed temperature profile prior to the onset of GST changes, to the land surface; as a result, the predictions of the initial GST of  $10.2^\circ\text{C}$  for Fig. 12(c) or  $10.63^\circ\text{C}$  for Fig. 12(e), previously noted as too high, cease to have any significance and are therefore no longer a problem for the modelling. Notwithstanding, once again, the ad hoc set of underlying assumptions, the modelling results for Gateshead borehole GTW2 (Fig. 12(d)) can be interpreted analogously to those for Science Central (Fig. 13(b)); beneath both localities, groundwater flow is transporting away heat originating both from the Earth's interior and from the surface warming.

The present analysis thus demonstrates that the conductive heat flow at depths overlying flooded mineworkings in the study region has been dramatically modified by the existence of these workings and is thus unrepresentative of the heat flux from the Earth's interior. Other subsurface temperature measurements for determination of heat flow in this coalfield region are thus called into question. For example, temperature measurements made in 1872

in a borehole at South Hetton Colliery (NZ 382 452), between the worked Hutton seam at 355 m depth and 529 m depth were analyzed by Anderson (1945) and by Bott et al. (1972), who determined a heat flow of  $58 \text{ mW m}^{-2}$ . However, mines farther west in the exposed part of the coalfield were already, by 1872, working stratigraphically lower coal seams (for example, Coxhoe Colliery, at NZ 327 366, had by 1872 been working the Harvey seam for several decades, according to the DMM records – see <http://www.dmm.org.uk/colliery/c008.htm>). Contemporaneous pumping in this and other collieries may well have affected the temperature at South Hetton at the depths of measurement.

The present study also indicates the extent of interaction in the study region between atmospheric and subsurface UHIs and of downward transport of heat generated by surface energy use into the deeper subsurface. It is hoped that such a demonstration will inform future modelling studies of atmospheric UHIs, which will improve upon the limited manner in which such studies have represented energy transfer into the subsurface hitherto (cf. Porson et al., 2010a,b); in our view such studies should consider seasonal and longer-timescale surface heating effects and the interactions between these effects and changing patterns of subsurface groundwater flow (i.e., most of the processes analyzed in the present study), rather than only considering diurnal effects as has been the case hitherto. The dramatic perturbations that have occurred to the conductive temperature profiles, in the urban localities that we have investigated, indicate that smaller-magnitude – albeit, still substantial – perturbations can be expected as a consequence of more modest anthropogenic changes. We are therefore sceptical of the previous claims that palaeoclimate can be inferred from inventory studies of raw geothermal records (e.g., Huang et al., 2000; Beltrami et al., 2002; Hopcroft et al., 2007). We recommend that such results are checked carefully for potential confounding factors, such as changes in land use, which might account for some or all of the aforementioned counterintuitive results; in the meantime, derived parameters, such as the figure of 3% of the energy content of global warming that is taken up by subsurface warming (e.g., Beltrami et al., 2002; Rhein et al., 2013), should be treated with caution.

As already noted, many workers (e.g., Leoni, 1985; Harrison et al., 1989; Banks et al., 2003; Heitfeld et al., 2006; Watzlaw and Ackman, 2006; Michel, 2009a,b; Hall et al., 2011; Ramos and Falcone, 2013; Coldewey et al., 2014) have recognized that water in flooded mineworkings forms a potentially valuable heat source, although the limited information currently available on hydraulic transport properties in British Coal Measures rocks that have been ‘permeabilised’ (cf. Younger et al., 2015) by coal mining impacts on one’s ability to undertake quantitative assessments (e.g., Gillespie et al., 2013). For example, the lack of basic data inhibited Gillespie et al. (2013) from quantifying the groundwater flow regime beneath the former Scottish coalfield as part of their assessment of the local geothermal energy resource (see below). We therefore now set out to quantify, at least to first order, these properties for our own study region. The typical flow rate  $Q$  for the pumping at Kibblesworth is indeed substantial (Fig. 9(b)); for example Welsh (2005) estimated  $\sim 3401 \text{ s}^{-1}$  (cf. Table 3). More recently, Younger and Henderson (2014) determined a mean value of  $276 \pm 85 \text{ l s}^{-1}$  ( $\pm 1\sigma$ ) from 1422 measurements; this is equivalent to  $276 \pm 51 \text{ s}^{-1}$  ( $\pm 2\sigma$ ). An appropriate rounded value is thus  $\sim 300 \text{ l s}^{-1}$  or  $\sim 0.3 \text{ m}^3 \text{ s}^{-1}$  (cf. Fig. 9). The typical temperature of this discharge is  $\sim 15^\circ\text{C}$  (Table 3); taking the annual mean GST as  $\sim 9^\circ\text{C}$  (cf. Fig. 7), the excess temperature of the discharge  $\Delta T$ , seasonally averaged, is  $\sim 6^\circ\text{C}$ . The thermal power output can thus be estimated using Eq. (23); with the aforementioned values for  $\rho$  and  $c$ , this gives  $\sim 0.3 \text{ m}^3 \text{ s}^{-1} \times 1000 \text{ kg m}^{-3} \times 4186 \text{ J kg}^{-1} \text{ }^\circ\text{C}^{-1} \times 6^\circ\text{C}$  or  $\sim 7.5 \text{ MW}$ . Looked at another way, the notional value of the heat energy in this discharge can be determined as the cost of providing

heat at this rate, say, by burning natural gas. At a standard UK retail price for natural gas of  $\sim 4 \text{ p kWh}^{-1}$  or  $\sim 1.1 \text{ p MJ}^{-1}$ ,  $\sim 7.5 \text{ MW}$  of heat output would equate to  $\sim 240 \text{ TJ yr}^{-1}$ , with a notional annual value of  $\sim \text{£}2,600,000$ . However, the lack of any heat load in the vicinity currently prevents this value from being realized.

Other instances of similar-magnitude anthropogenic flows of thermal water from the subsurface are also evident. Notable examples occur in the Carboniferous limestone uplands of the Peak District ( $\sim 200 \text{ km}$  south of Tyneside). Many thermal springs are known here, several having been engineered as health spas. According to Brassington (2007), the largest thermal power output occurs at Saint Anne's Well, Buxton (at SK 057 735), which has a typical flow rate of  $635 \text{ l min}^{-1}$  (equivalent to  $\sim 0.011 \text{ m}^3 \text{ s}^{-1}$ ) at a typical temperature of  $27.5^\circ\text{C}$ . Taking the annual mean GST as  $\sim 8^\circ\text{C}$ , the associated thermal output is  $\sim 0.8 \text{ MW}$ . Significant flows of heat also occur in outflows from drainage adits (known locally as ‘soughs’) for former lead mines in this area; Gunn et al. (2006) reported that the largest of these is from Meerbrook Sough near Wirksworth (at SK 327 552). The discharge from this adit has been estimated, for example, by James (1997) as  $\sim 75 \text{ Ml day}^{-1}$  or by Shepley (2007) as  $\sim 60 \text{ Ml day}^{-1}$ ; these values equate to  $\sim 0.69\text{--}0.87 \text{ m}^3 \text{ s}^{-1}$ . Gunn et al. (2006) reported the temperature of these waters as  $17.0^\circ\text{C}$ ,  $\sim 8.6^\circ\text{C}$  warmer than ‘cold’ groundwater in the area. On the other hand, Shepley (2007) stated that the discharge temperature varies seasonally between  $\sim 13$  and  $\sim 15^\circ\text{C}$ , with an annual mean of  $\sim 14^\circ\text{C}$  and, thus, a typical temperature anomaly of  $\sim 5.6^\circ\text{C}$ . Banks et al. (1996) reported the flow rate as varying between  $0.74$  and  $1.0 \text{ m}^3 \text{ s}^{-1}$  and the water temperature as  $15.3^\circ\text{C}$ , indicating a typical temperature anomaly of  $\sim 6.9^\circ\text{C}$ . Taking these uncertainties into account, the typical heat flux from this adit can be estimated as  $\sim 20 \text{ MW}$  (Gunn et al., 2006). Most of this discharge is used as a local water supply (e.g., James, 1997; Shepley, 2007), no attempt being currently made to utilize its heat content.

The hydrology of the groundwater circulation associated with these Peak District thermal waters has also been investigated (e.g., Gunn et al., 2006; Brassington, 2007; Shepley, 2007); although details differ between interpretations (cf. Bottrell et al., 2008; Brassington, 2008) it is evident that the discharges represent mixing of meteoric water with thermal groundwater that has circulated to depths of many hundreds of metres. The circulation systems envisaged are laterally extensive, over distances of tens of kilometres. Shepley (2007) estimated that Meerbrook Sough has itself drawn down the water table over a  $\sim 40 \text{ km}^2$  area ( $\sim 10 \text{ km}$  west-east  $\times \sim 4 \text{ km}$  north-south), although James (1997) reported that its construction in the 18th-19th centuries reduced the surface flow in rivers up to  $\sim 15 \text{ km}$  away, suggesting even more extensive effects. An indication of its extent can be obtained by comparing its  $\sim 20 \text{ MW}$  heat output with the local heat flow, estimated as  $\sim 60\text{--}70 \text{ mW m}^{-2}$  by Busby et al. (2011). Taking the upper bound to this range, the ratio of these values indicates that this heat output is equivalent to the geothermal heat supply over an area of  $\sim 20 \text{ MW}/70 \text{ mW m}^{-2}$  or almost  $300 \text{ km}^2$ , far greater than the  $\sim 40 \text{ km}^2$  catchment area estimated by Shepley (2007). However, it is unclear to us where the reported  $\sim 60\text{--}70 \text{ mW m}^{-2}$  heat flow originates, as compilations of such data (e.g., Downing and Gray, 1986; Rollin, 1995) do not report any local heat flow measurements in this range. Indeed, the only geothermal measurement reported in the Peak District is for the Eyam borehole (BGS inventory code SK27NW15; at SK 2096 7603,  $\sim 25 \text{ km}$  NNW of Meerbrook Sough). This borehole reaches a depth of 1851 m, being in Carboniferous limestone to 1803 m before entering Lower Palaeozoic ‘basement’ (Dunham, 1973), but for some reason only its uppermost 612 m has been logged for temperature (Burley et al., 1984; Downing and Gray, 1986), a very low heat flow of only  $17 \text{ mW m}^{-2}$  being indicated, with an inverted temperature profile for part of this vertical extent. This unusual dataset has been interpreted in terms of

downward flow of groundwater (e.g., Holliday, 1986; Gunn et al., 2006), the negative geothermal gradient being consistent with an additional horizontal component of heat flow (cf. Eq. (19)). It is evident that another potential contributory factor that may influence this low heat flow is that (by analogy with the Science Central borehole; cf. Fig. 13) a proportion of the expected much higher upward heat flow has been entrained horizontally, at depths below those in which temperature has been measured, and has traversed substantial distances within the permeable bedrock, potentially contributing to the heat output in Meerbrook Sough. Meerbrook Sough and other mine drainage adits may thus have the effect of ‘suppressing’ conductive heat flow beneath a substantial area of the Peak District, in a manner analogous to the effect of mine pumping in northeast England.

Although many authors have noted that karstified Carboniferous limestone, such as that in the Peak District, has high permeability (or high hydraulic conductivity or transmissivity), few published quantitative estimates exist. Worthington and Ford (2009) reported that its transmissivity is highly variable, with a mean value of  $22 \text{ m}^2 \text{ day}^{-1}$  and an upper bound of  $8800 \text{ m}^2 \text{ day}^{-1}$ ; these values equate to  $2.5 \times 10^{-4}$  and  $0.10 \text{ m}^2 \text{ s}^{-1}$ . Lewis et al. (2006) reported similar variability in its hydraulic conductivity, spanning  $0.1\text{--}1000 \text{ m day}^{-1}$  ( $\sim 10^{-6}$  to  $\sim 10^{-2} \text{ m s}^{-1}$ ). We therefore make first-order estimates of the hydraulic transport properties for the subsurface catchment drained by Meerbrook Sough. From Shepley (2007), we note that the water depth is  $\sim 30 \text{ m}$  at the inlet to this adit and  $\sim 130 \text{ m}$  at the distal limit of the catchment,  $\sim 10 \text{ km}$  to the west; we thus infer a hydraulic head of  $\sim 100 \text{ m}$ . Shepley (2007) also estimated the horizontal extent of this flow (perpendicular to the flow direction) as  $\sim 4 \text{ km}$  north–south. If we also assume that the vertical extent of this flow is  $\sim 100 \text{ m}$ , then the values of many hydrological transport properties can be calculated (Table 4), including values for hydraulic conductivity and transmissivity that fall within the ranges estimated previously.

It was previously tentatively inferred that the components of upward and downward groundwater flow inferred from the Science Central temperature profile (Fig. 13(a)) combine to flow southward through a ‘minewater pond’, comprising an interconnected network of ‘migrated voids’ to form part of the discharge at Kibblesworth,  $\sim 9 \text{ km}$  to the south. We now present first-order calculations to test this hypothesis. Based on Fig. 1 we infer that maybe one third of the Kibblesworth discharge, or  $\sim 0.1 \text{ m}^3 \text{ s}^{-1}$ , originates from the north, within a zone that is  $\sim 5 \text{ km}$  wide east–west. If this flow is concentrated within ‘migrated voids’ that are typically  $\sim 10 \text{ m}$  high, given the aforementioned evidence from Science Central, then the horizontal flux  $q$  through this part of the subsurface flow network can be estimated as  $\sim 0.1 \text{ m}^3 \text{ s}^{-1}/(\sim 5000 \text{ m} \times \sim 10 \text{ m})$  or  $\sim 2 \times 10^{-6} \text{ m s}^{-1}$ . To balance this horizontal flux of groundwater, an equivalent flux must enter this flow network from above and below. If this inflow is assumed to be spatially uniform across the horizontal extent of the network, with dimensions  $\sim 9 \text{ km}$  north–south and  $\sim 5 \text{ km}$  east–west, and to also be equal from above and from below, the associated (Darcy) flow velocity can be estimated as  $\sim 0.1 \text{ m}^3 \text{ s}^{-1}/(2 \times \sim 5000 \text{ m} \times \sim 9000 \text{ m})$  or  $\sim 10^{-9} \text{ m s}^{-1}$ . This is in rough agreement with the flow velocities inferred from the Science Central thermal modelling, which were  $\sim 2 \times 10^{-9} \text{ m s}^{-1}$  upward and  $\sim 7 \times 10^{-9} \text{ m s}^{-1}$  downward (Fig. 13(a)), and from the Gateshead modelling in Fig. 12(f),  $\sim 17 \times 10^{-9} \text{ m s}^{-1}$  downward. Likewise, if one third of the heat transported in the Kibblesworth discharge, or  $\sim 2.5 \text{ MW}$ , originates from this southward component of subsurface flow, and enters this flow by upward heat transport at a uniform rate, then the associated heat flow is  $\sim 2.5 \text{ MW}/(\sim 5000 \text{ m} \times \sim 9000 \text{ m})$  or  $\sim 60 \text{ mW m}^{-2}$ . The Science Central thermal modelling (Fig. 13) indicates that heat is lost from vertical conduction into the horizontal groundwater flow at a rate that will equal the difference in the conductive tempera-

ture gradient above and below this horizontal groundwater flow, which is  $\sim 49^\circ \text{C km}^{-1}$  minus  $\sim 13^\circ \text{C km}^{-1}$  or  $\sim 36^\circ \text{C km}^{-1}$ , multiplied by the estimated thermal conductivity of the sediments, of  $\sim 2 \text{ W m}^{-1} \text{ }^\circ\text{C}^{-1}$ , or  $\sim 70 \text{ mW m}^{-2}$ , again indicating approximate agreement.

One may thus make first-order estimates for the hydraulic transport properties of this horizontal flow network. To do so, we take the upper bound for the hydraulic head as the  $\sim 80 \text{ m}$  difference between the depth of the ‘migrated void’ network ( $\sim 160 \text{ m}$ ) and the depth of the water table ( $\sim 80 \text{ m}$ ) at Science Central, which gives a lower bound for permeability,  $\sim 3 \times 10^{-11} \text{ m}^2$ , and for other transport properties (Table 4). For comparison, coarse sandstone might have a permeability of  $\sim 3 \times 10^{-12} \text{ m}^2$  (e.g., Bloch, 1991); we have thus calculated very high values, which evidently reflect flow through substantial voids. As another comparison, by modelling the flooding of other former mineworkings, Whitworth (2002) determined permeability values (for a hydrostatic pressure gradient) in the range  $\sim 0.2 \times 10^{-7} \text{ m s}^{-1}$  to  $\sim 10^{-7} \text{ m s}^{-1}$ . These convert to  $\sim 0.002\text{--}0.01 \text{ darcies}$  or  $\sim 0.2 \times 10^{-14} \text{ to } 10^{-14} \text{ m}^2$ , far below our estimate. However, these were for collieries where longwall mining had been in operation, where after each panel of coal was cut the overburden was allowed to collapse throughout the area of the panel, and thus eliminate much of the void space present (cf. Younger and Adams, 1999). In contrast, as already noted, the historical mining in the inland part of the Northeast England coalfield was largely by the ‘bord and pillar’ method, with pillars of coal left in situ to support the overburden; the potential for this mining method to leave subsurface voids that can act as conduits for groundwater flow is evidently far greater than for longwall mining. Furthermore, as Whitworth (2002) pointed out, coal mining in recent decades has been regulated so coal within  $45 \text{ m}$  of any flooded former mineworkings must be left in situ. In contrast, it was not until 1850, by which time much of the mining in the inland part of this coalfield (Fig. 1) had already taken place, that a legal requirement was established for mine owners to provide public records of mine plans (Donnelly et al., 1998), so there must have been many instances where coal was mined much closer to existing workings. All these factors can be expected to enhance the overall ‘permeabilisation’ of early mineworkings relative to their more modern counterparts. Our estimates of permeability and hydraulic conductivity for the subsurface flow network through this abandoned coalfield are indeed comparable to our estimates in karstified Carboniferous Limestone (see above).

The existence beneath this part of Britain of a flow network with such a high transmissivity has potential significance for future ‘geo-engineering’ of the urban environment regarding sustainable energy use; users who wish to dissipate excess energy, for example when cooling large buildings, might utilize such a flow network as a heat sink; other users, for example requiring heat supply, might draw upon this subsurface thermal resource. In other cities, subsurface aquifers are already used for this purpose; an example is the Chalk beneath London, although its transmissivity is relatively low ( $\sim 100 \text{ m}^2 \text{ day}^{-1}$ ; e.g., Birks et al., 2013). Pleistocene river gravels have also been used as a heat sink in London; they have somewhat higher transmissivity ( $\sim 550 \text{ m}^2 \text{ day}^{-1}$ ; Birks et al., 2013), but because they are freely connected hydraulically to London’s river, the Thames, they cannot be used for heat storage as might be feasible for old mine workings in Carboniferous sediments. The heat thus released therefore enters this river and so ultimately contributes to making the North Sea slightly warmer than it would otherwise be. As already noted, in Tyneside, the downward component of groundwater flow into the flooded mineworkings from shallower depths also removes from the shallow subsurface some of the subsurface heating effect (both from global warming and from local energy use) that would otherwise contribute to the buildup of a subsurface UHI and might indeed

**Table 4**

Summary of results for the dynamics of horizontal flow.

	L(km)	H(km)	D(km)	$\delta h(m)$	L/H	$Q(m^3 s^{-1})$	$q(mm s^{-1})$	$K(mm s^{-1})$	$\Psi(m^2 s^{-1})$	$k_p(m^2)$	$Pe^*$	$a$
Meerbrook Sough	100	10	4	100	0.01	0.8	2.0	0.2	0.02	$2 \times 10^{-11}$	14	140000
Gateshead (Kibblesworth) minewater pond	10	9	5	80	0.001	0.1	2.0	0.2	0.002	$3 \times 10^{-11}$	0.16	130000
Bath-Bristol area	ND	ND	ND	ND	0.029	ND	ND	ND	ND	ND	1.8	2100

L, H and D denote the estimated vertical extent and horizontal extents of the flow, parallel and perpendicular to the flow direction,  $\delta h$  denotes the hydraulic head, and Q denotes the discharge (all estimated in the main text). The Darcy flow velocity q is calculated  $q \equiv Q/(L \times D)$ . The hydraulic conductivity K is calculated from q, H and L using Eq. (20), from which the transmissivity  $\Psi$  is calculated using Eq. (22). The permeability  $k_p$  is then calculated using Eq. (21) assuming  $\rho = 1000 \text{ kg m}^{-3}$  (density of water),  $g = 9.81 \text{ m s}^{-2}$  (acceleration due to gravity), and  $\eta = 1.15 \text{ mPa s}$  (viscosity of water at  $\sim 15^\circ\text{C}$ ),  $Pe^*$  (the 'Basin Pécelt number') is calculated using Eq. (24) for the same value of  $\rho$ , with  $c = 4186 \text{ J kg}^{-1} \text{ }^\circ\text{C}^{-1}$  (specific heat capacity of water) and  $k = 0.6 \text{ W m}^{-1} \text{ }^\circ\text{C}^{-1}$  (thermal conductivity of water), with the dimensionless parameter a calculated using Eq. (25). Results for flow through the Carboniferous limestone in the Bath-Bristol area of SW England, for comparison, are from Anderson (2005); ND denotes 'not determined'.

feed back into a local atmospheric UHI. This process, recognized neither in previous studies of subsurface UHIs (e.g., Menberg et al., 2013a,b), nor in investigations of atmospheric UHIs over cities (e.g., Bohnenstengel et al., 2011, 2014), nor in previous discussions of ATES (e.g., Andersson, 2007), evidently has a UHI mitigation effect and might in future be engineered to enhance this effect to improve living conditions in urban environments.

We note in passing that two small-scale applications of minewater for heating, using heat pumps, have been operating for more than a decade in central Scotland (e.g., Banks et al., 2003, 2009b). At Shettleston in eastern Glasgow (NS 644 637), water at  $\sim 12^\circ\text{C}$  has been drawn since 1999 from old mine workings at  $\sim 100 \text{ m}$  depth, and at Lumphinnans, near Cowdenbeath, Fife (NT 171 928), water at  $14.5^\circ\text{C}$  has been drawn since 2000 from workings at  $172.5 \text{ m}$  depth; in both cases, the maximum heat output is stated as 65 kW. Much larger-scale projects have also been envisaged to exploit the thermal energy in minewater elsewhere in the former Scottish coalfield (e.g., PB Power, 2004; ÓDochartaigh, 2009; Gillespie et al., 2013). These reports have indeed claimed that huge energy resources are present, but not all the limited calculations presented are transparently supported by data. For example, PB Power (2004) estimated that the then current time-averaged rate of minewater pumping from the disused Monktonhall Colliery (NT 323 703; in the SE outskirts of Edinburgh) of  $311 \text{ s}^{-1}$  produced 1.85 MW of heat. Given the other parameter values, the form of Eq. (23) means that this heat output would require a water temperature  $\sim 14^\circ\text{C}$  above ambient; but the same report estimated the minewater discharge temperature as  $\sim 15^\circ\text{C}$ , making it only  $\sim 6^\circ\text{C}$  above ambient, whereas Minewater Project (2008) reported it as  $\sim 13^\circ\text{C}$  or only  $\sim 4^\circ\text{C}$  above ambient. PB Power (2004) also estimated that this site might produce 9.45 MW of heat, which from the above calculation would mean increasing the pumping rate to  $1581 \text{ s}^{-1}$ , and also discussed the possibility of a pumping rate of  $2501 \text{ s}^{-1}$  which for the same temperature difference would yield  $\sim 15 \text{ MW}$  of heat, these pumping rates being considered feasible on the basis of pumping rates that had been required for dewatering this and neighbouring mines when the coalfield was active. Furthermore, PB Power (2004) estimated that a network of interconnected flooded mineworkings spanning an area of  $\sim 50 \text{ km}^2$  is locally present, from which heat could be drawn at this rate. However, given the local heat flow of  $\sim 60 \text{ mW m}^{-2}$  (e.g., Busby et al., 2011), 9.45 or 15 MW are equivalent to the heat flux through  $\sim 160$  or  $\sim 250 \text{ km}^2$  of land area, not  $\sim 50 \text{ km}^2$  as had been suggested. Gillespie et al. (2013) gave the impression that drawing heat from minewater is a 'one-off' energy supply, rather than an energy source that can be managed sustainably, since it is effectively 'capturing' a proportion of the heat flux over a large region in a manner that would otherwise be difficult to accomplish; however, if heat were to be extracted faster than it could be replenished from the Earth's interior, as these calculations imply, then the process would indeed be unsustainable. In addition, Gillespie et al. (2013) argued that this Monktonhall proposal was economically unfavourable due to a lack of local heat load. On the contrary, the land formerly occupied by this colliery is being redeveloped as a new Edinburgh suburb, to be called Shawfair. District

heating of this new suburb, using minewater as the heat source, was proposed (e.g., Banks et al., 2003; PB Power, 2004) and, according to Minewater Project (2008), was a feasible project that was later abandoned because public funding for capital costs was unavailable and because the developer regarded a minewater-powered district heating system as a financial and marketing risk. On the contrary, investigations by one of us (P.Y.) established that when the Monktonhall coal mine closed, a stopping was placed in its shaft at a depth of  $\sim 180 \text{ m}$  ( $\sim 160 \text{ m}$  below O.D.) to restrict groundwater flow up this shaft, and that the  $\sim 311 \text{ s}^{-1}$  time-averaged pumping rate was roughly the maximum that could be drawn through this blockage. The heat yield of this mineshaft could thus not be increased in the manner that PB Power (2004) envisaged; the stopping effectively prevented its reuse for large scale heat supply, so any such project in future will require purpose-drilled extraction and injection boreholes. The UK Coal Authority subsequently discontinued pumping this mineshaft; this coalfield now decants naturally into a sewer near the North Sea coast at Joppa (circa NT 325 733). In the meantime, reopening of a disused railway to serve the new Shawfair suburb has included the injection of thousands of tonnes of grout into subsurface voids in the former mineworkings to stabilize the ground; this work, which has been described as 'mining remediation' (Network Rail, 2013), might instead be regarded as adding to the destruction of part of a significant potential future energy supply. We indeed consider the potential value as a future energy source of subsurface groundwater flow networks through abandoned mineworkings in general, whether in northeast England, central Scotland, or elsewhere in the UK, to be so great that more detailed investigations are warranted; in the meantime these networks should be protected from other adverse developments.

The effect documented in the present study, whereby groundwater flow through old mineworkings can 'capture' a substantial proportion of the geothermal heat flux over substantial areas, warrants comparison with the effect of thermal springs, which others have previously noted (e.g., Forster and Smith, 1989; Manga, 1998; Ferguson and Grasby, 2011). For example, Ferguson and Grasby (2011) reported that the largest springs in North America effectively 'capture' the geothermal heat flux over areas of  $\sim 1000 \text{ km}^2$ ; they are thus much larger than the mineworking-related groundwater circulation systems discussed in the present study. Nonetheless, these systems have the effect of significantly redistributing subsurface heat over substantial areas, concentrating it in some places but depleting it in others. Although the outflows from such systems can in principle be exploited as sources of heat (see above), the downside is that elsewhere in the affected regions the conductive heat flow and associated geothermal gradient in the shallow subsurface can be significantly reduced, as the record from Science Central (Fig. 13(a)) illustrates. Care must therefore be taken to consider such effects when designing projects to extract heat from the subsurface in future.

Finally, our analysis bears upon the magnitude of the direct anthropogenic contribution to the global energy budget, a topic that has hitherto at times entered the domain of 'mavericks'. Thus, for example, Nordell (2003, 2007) has claimed that global warm-

ing is the direct effect of human energy use, with no demonstrable contribution from feedbacks related to increasing concentrations of atmospheric greenhouse gases, whereas Mu and Mu (2013) have argued that coal mining and petroleum extraction have reduced the Earth's thermal resistance, increasing the heat flow from its interior and, thus, raising surface temperatures. From Hartmann et al. (2013, p. 181), the Earth overall has a positive energy balance of  $\sim 0.6 \pm 0.4 \text{ W m}^{-2}$  or  $\sim 9.7 \pm 6.5 \text{ ZJ yr}^{-1}$  (i.e.,  $\sim 9.7 \pm 6.5 \times 10^{21} \text{ J yr}^{-1}$ ), indicating that it is out of steady-state by between  $\sim 3.2$  and  $\sim 16.2 \text{ ZJ yr}^{-1}$ . From Davies and Davies (2010) and Davies (2013), the terrestrial heat flux is  $\sim 44 \text{ TW}$  or  $\sim 1.4 \text{ ZJ yr}^{-1}$ . From IEA (2014, p. 28), global energy consumption in 2012 (the most recent year with data currently available) was 8979 million tonnes of oil equivalent, most of this energy having been converted to heat. Using the standard conversion factor (1 t.o.e.  $\equiv 41.868 \text{ GJ}$ ), this equates to  $\sim 0.38 \text{ ZJ yr}^{-1}$ . The Earth's annual energy gain is thus an order-of-magnitude larger than the human energy use and several times larger than the total geothermal heat flux; in their original form, both the aforementioned claims about the Earth's energy imbalance are therefore demonstrably incorrect. However, Rhein et al. (2013, p. 264) partitioned the Earth's energy gain as  $\sim 93\%$  into the oceans,  $\sim 3\%$  into melting of ice (from glaciers and polar ice sheets),  $\sim 3\%$  into the subsurface, and  $\sim 1\%$  into the atmosphere. The subsurface and atmospheric energy gains can thus be estimated as  $\sim 0.3$  and  $\sim 0.1 \text{ ZJ yr}^{-1}$ , respectively; both are therefore comparable to the heating effect resulting directly from human energy use. Since this direct heating effect from human energy use will be concentrated in the atmosphere and subsurface, rather than in glaciers or the oceans, and in urban areas rather than being evenly distributed globally, it follows that the thermal state of both the atmosphere and the subsurface in urban areas must differ dramatically from what one might predict based simply on considerations of global feedbacks involving greenhouse gases. Our analysis demonstrates that the subsurface thermal state in our case study localities indeed differs dramatically from what might be expected based simply on such considerations; given the global estimations noted above, with hindsight this deduction is unsurprising.

## 7. Conclusions

Using analytical modelling, we have investigated borehole temperature records from sites in the urban centres of Gateshead and Newcastle upon Tyne in northeast England, to ascertain the effects of the historical legacy of coal mining and more recent urban development on subsurface temperatures. These effects are shown to be substantial, albeit with significant variations on a very local scale (Table 5). Significant subsurface UHIs are indeed evident in both urban centres, estimated as  $2.0^\circ\text{C}$  in Newcastle and  $4.5^\circ\text{C}$  in Gateshead, the former value being comparable to the atmospheric UHI of  $1.9^\circ\text{C}$  determined for this conurbation as a whole (Kershaw et al., 2010). We interpret these large-magnitude subsurface UHIs as a consequence of the region's long history of urban and industrial development and associated surface energy use, possibly supplemented in Gateshead by the thermal effect of trains braking in an adjacent shallow railway tunnel. Our analysis of conductive heat flow utilized nineteenth-century mineshaft logs to establish the thermal properties of the stratigraphic column in each locality. We found that these gave reasonable results, probably accurate to within  $\sim 10\%$ ; we thus adopted nominal values, for our modelling, of  $2 \text{ W m}^{-1} \text{ }^\circ\text{C}^{-1}$  for thermal conductivity and  $1 \text{ mm}^2 \text{ s}^{-1}$  for thermal diffusivity. Furthermore, in both Gateshead and Newcastle, a large proportion of the expected conductive heat flow from the Earth's interior becomes entrained by groundwater flow and transported elsewhere, through former mineworkings in which the rocks have been 'permeabilised' by

**Table 5**  
Summary of results for thermal properties.

Parameter and units	Note	Locality	
		Gateshead Trinity Square (2007)	Newcastle Science Central (2012)
$h (\text{m})$	a	53	71
$k (\text{W m}^{-1} \text{ }^\circ\text{C}^{-1})$	b	2.0	2.0
$k (\text{W m}^{-1} \text{ }^\circ\text{C}^{-1})$	c	1.68	1.89
$\kappa (\text{mm}^2 \text{ s}^{-1})$	b	1.0	1.2
$\kappa (\text{mm}^2 \text{ s}^{-1})$	c	0.90	1.01
$T_o (\text{ }^\circ\text{C})$	d	14.63	11.3
$\Delta T_s (\text{ }^\circ\text{C})$	d	4.5	4.5
$T_a (\text{ }^\circ\text{C})$	e	10.14	9.32
$\nabla T_b (\text{ }^\circ\text{C km}^{-1})$	d	ND	49.0
$q_b (\text{mW m}^{-2})$	f	ND	98.0
$\nabla T_u (\text{ }^\circ\text{C km}^{-1})$	d	18	13.0
$q_u (\text{mW m}^{-2})$	f	36	26.0
$\nabla T_d (\text{ }^\circ\text{C km}^{-1})$	d	-90.9	-7.25
$z (\nabla T_d) (\text{m})$	d	0	44
$q_d (\text{mW m}^{-2})$	f	-181.7	-14.5
$\Delta T_l (\text{ }^\circ\text{C})$	g	4.49	1.98
$v_u (\text{mm yr}^{-1})$	h	ND	54
$v_d (\text{mm yr}^{-1})$	h	540	230

ND indicates 'not determined'. Notes:

a Height,  $h$ , of the land surface above O.D.

b Nominal values used in analytical modelling (Figs. 12(f) and 13(a)).

c Values determined from the stratigraphy of adjacent mineshafts.

d Determined by fitting subsurface temperature data with analytical modelling solutions;  $\nabla T_b$ ,  $\nabla T_u$  and  $\nabla T_d$  are, respectively, the geothermal gradient beneath depths where temperatures are perturbed by coal mining, the steady-state upward geothermal gradient estimated in the shallow subsurface, and the maximum downward geothermal gradient associated with the subsurface UHI;  $z (\nabla T_d)$  denotes the depth at which  $\nabla T_d$  occurs.

e Determined by taking the annual mean temperatures from the Durham meteorological observatory (Fig. 7) for the respective years, and adding a correction for differences in land surface height, calculated at  $7 \text{ }^\circ\text{C km}^{-1}$ , with no correction for location.

f Determined from fitting subsurface temperature data with analytical modelling solutions, using nominal values for thermal conductivity;  $q_b$ ,  $q_u$  and  $q_d$  correspond, respectively, to  $\nabla T_b$ ,  $\nabla T_u$  and  $\nabla T_d$ .

g Determined as  $T_o - T_a$ .

h Upward/downward groundwater flow velocities, below/above mineworkings voids.

the region's long history of coal mining. Discharge of groundwater at a nearby mine pumping station, Kibblesworth, transports a heat flux that we estimate as  $\sim 7.5 \text{ MW}$ ; it thus transports the equivalent of roughly two thirds of the geothermal heat flux through a  $>100 \text{ km}^2$  surrounding region. Modelling of the associated groundwater flow regime provides first-order estimates of the hydraulic transport properties of 'permeabilised' Carboniferous Coal Measures rocks, comprising permeability  $\sim 3 \times 10^{-11} \text{ m}^2$  or  $\sim 30$  darcies, hydraulic conductivity  $\sim 2 \times 10^{-4} \text{ m s}^{-1}$ , and transmissivity  $\sim 2 \times 10^{-3} \text{ m}^2 \text{ s}^{-1}$  or  $\sim 200 \text{ m}^2 \text{ day}^{-1}$ ; these are very high values, comparable to those for karstified Carboniferous limestone. These large-magnitude subsurface UHIs create significant downward components of conductive heat flow in the shallow subsurface, which are supplemented by downward heat transport by groundwater movement towards the flow network through the former mineworkings. The warm water in these workings is thus heated in part by heat drawn from the shallow subsurface, in addition to heat flowing from the Earth's interior. Similar conductive heat flow and groundwater flow responses are expected in other urban former coalfield regions of Britain; further analysis of the processes involved may facilitate their use as heat stores and may also contribute to UHI mitigation. In the words of the song, although coal mining in these regions is, indeed, finished, the abandoned, flooded workings may yet have a 'life' as energy sources and/or as temperature regulators for urban environments.

## Conflicts of interest

The authors have no conflicts of interest.

## Acknowledgements

We thank Jon Busby of BGS for the Rowlands Gill temperature and thermal conductivity dataset, which was made available through the BritGeothermal partnership. Ian Watson and Lee Wyatt of the UK Coal Authority kindly provided the Kibblesworth flow rate and water level dataset and the Freeman Road water level dataset; Karen Johnson kindly provided the Kibblesworth water temperature dataset; and David Banks kindly provided unpublished documentation for the Trinity Square, Gateshead, boreholes. The historical map excerpts in the online supplement are reproduced with the permission of the National Library of Scotland. The historical air photographs in the online supplement are reproduced with the permission of Historic England. The staff of the special collections section of the Newcastle University Robinson Library, the Durham Mining Museum, and the municipal archives of Newcastle upon Tyne, Gateshead, and County Durham, are thanked for their assistance. We also thank the two anonymous reviewers for their thoughtful and constructive comments.

## Appendix A. Supplementary data

Supplementary data associated with this article can be found, in the online version, at <http://dx.doi.org/10.1016/j.geothermics.2016.06.009>.

## References

- Akenhead, D., 1807. *The Picture of Newcastle upon Tyne, Containing a Guide to the Town and Neighbourhood, an Account of the Roman Wall and a Description of the Coal Mines*. D. Akenhead & Sons, Newcastle upon Tyne, pp. 191, Reprinted 1969 by E.W. Books, London.
- Amfofo, F., Maidment, G., Missenden, J., 2004. Underground railway environment in the UK. Part 2: Investigation of heat load. *Appl. Therm. Eng.* 24, 633–645.
- Anderson, M.P., 2005. Heat as a ground water tracer. *Ground* 43, 951–968.
- Anderson, W., 1945. On the chloride waters of Great Britain. *Geol. Mag.* 82, 267–274.
- Andersson, O., 2007. Thermal energy storage for sustainable energy consumption. In: Paksoy, H.Ö. (Ed.), *Thermal Energy Storage for Sustainable Consumption*. NATO Science Series, Series II, vol. 234. Springer, Dordrecht, The Netherlands, pp. 155–176.
- Bald, R., 1819. On the temperature of air and water in the coal mines of Great Britain: particularly in those which are of the greatest depth. *Edinburgh Philos. J.* 1, 134–137.
- Banks, D., Gandy, C.J., Younger, P.L., Withers, J., Underwood, C., 2009a. Anthropogenic thermogeological 'anomaly' in Gateshead, Tyne and Wear, UK. *Q. J. Eng. Geol. Hydrogeol.* 42, 307–312.
- Banks, D., Fraga Pumar, A., Watson, I., 2009b. The operational performance of Scottish minewater-based ground source heat pump systems. *Q. J. Eng. Geol. Hydrogeol.* 42, 347–357.
- Banks, D., Skarphagen, H., Wiltshire, R., Jessop, C., 2003. Mine water as a resource: space heating and cooling via use of heat pumps. *Land Contam. Reclam.* 11 (2), 191–198.
- Banks, D., Younger, P.L., Dumpleton, S., 1996. The historical use of mine-drainage and pyrite-oxidation waters in central and eastern England, United Kingdom. *Hydrogeol. J.* 4, 55–68.
- Bateson, L., Lawrence, D., 2012. Case study for the application of Terra firma ground motion services to areas of abandoned mining: Northumberland, UK. BGS Open Report OR12055, 8 pp. Available online: <http://nora.nerc.ac.uk/20061/1/OR12055.pdf> (accessed 5.07.15).
- Beltrami, H., Smerdon, J.E., Pollack, H.N., Huang, Shaopeng, 2002. Continental heat gain in the global climate system. *Geophys. Res. Lett.* 29 (1167), <http://dx.doi.org/10.1029/2001GL014310>, 3 pp.
- Bennett, G., Clavering, E., Rounding, A., 1990. *A Fighting Trade: Rail Transport in Tyne Coal 1600–1800. 2 Volumes. Portcullis (Gateshead Metropolitan Borough Council)*, Gateshead.
- Bense, V.F., Kooi, H., 2004. Temporal and spatial variations of shallow subsurface temperature as a record of lateral variations in groundwater flow. *J. Geophys. Res.* 109 (B04103), <http://dx.doi.org/10.1029/2003JB002782>, 13 pp.
- Birch, F., 1948. The effects of Pleistocene climatic variations upon geothermal gradients. *Am. J. Sci.* 246, 729–760.
- Birks, D., Whittall, S., Savill, I., Younger, P.L., Parkin, G., 2013. Groundwater cooling of a large building using a shallow alluvial aquifer in Central London. *Q. J. Eng. Geol. Hydrogeol.* 46, 189–202.
- Bloch, S., 1991. Empirical prediction of porosity and permeability in sandstones. *Am. Assoc. Pet. Geol. Bul.* 75, 1145–1160.
- Bloomer, J.R., 1981. Thermal conductivities of mudrocks in the United Kingdom. *Q. J. Eng. Geol. Hydrogeol.* 14, 357–362.
- Bohnenstengel, S.I., Evans, S., Clark, P.A., Belcher, S.E., 2011. Simulations of the London urban heat island. *Q. J. R. Meteorol. Soc.* 137, 1625–1640.
- Bohnenstengel, S.I., Hamilton, I., Davies, M., Belcher, S.E., 2014. Impact of anthropogenic heat emissions on London's temperatures. *Q. J. R. Meteorol. Soc.* 140, 687–698.
- Bott, M.H.P., 1967. Geophysical investigations of the northern Pennine basement rocks. *Proc. Yorks. Geol. Soc.* 36, 139–168.
- Bott, M.H.P., Johnson, G.A.L., Mansfield, J., Wheilden, J., 1972. Terrestrial heat flow in north-east England. *Geophys. J. R. Astron. Soc.* 27, 277–288.
- Bottrell, S., Lowe, D., Gunn, J., Worthington, S., Brassington, F.C., 2008. Discussion of 'A proposed conceptual model for the genesis of the Derbyshire thermal springs' by F.C. Brassington. *Q. J. Eng. Geol. Hydrogeol.* 40, 35–46. *Q. J. Eng. Geol. Hydrogeol.* 41, 119–120.
- Brassington, F.C., 2007. A proposed conceptual model for the genesis of the Derbyshire thermal springs. *Q. J. Eng. Geol. Hydrol.* 40, 35–46.
- Brassington, F.C., 2008. Discussion of 'Analysis of flows from a large Carboniferous Limestone drainage adit, Derbyshire England' by M.G. Shepley. *Q. J. Eng. Geol. Hydrogeol.* 40, 123–135. *Q. J. Eng. Geol. Hydrogeol.* 41, 121–122.
- Bredehoeft, J.D., Papadopoulos, I.S., 1965. Rates of vertical groundwater movement estimated from the Earth's thermal profile. *Water Resour. Res.* 1, 325–328.
- Bullard, E.C., Niblett, E.R., 1951. Terrestrial heat flow in England. *Monthly Notes of the Royal Astronomical Society. Geophys. Suppl.* 6, 222–238.
- Burley, A.J., Edmunds, W.M., Gale, I.N., 1984. Catalogue of Geothermal Data for the Land Area of the United Kingdom. Technical Report WJ/GE/84/020. British Geological Survey, Keyworth.
- Busby, J., Kingdon, A., Williams, J., 2011. The measured shallow temperature field in Britain. *Q. J. Eng. Geol. Hydrogeol.* 44, 373–387.
- Busby, J., Lewis, M., Reeves, H., Lawley, R., 2009. Initial geological considerations before installing ground source heat pump systems. *Q. J. Eng. Geol. Hydrogeol.* 42, 295–306.
- Carslaw, H.S., Jaeger, J.C., 1959. *Conduction of Heat in Solids*. Oxford University Press, 509 pp.
- Chadwick, R.A., Holliday, D.W., Holloway, S., Hulbert, A.G., 1995. *The Structure and Evolution of the Northumberland-Solway Basin and Adjacent Areas*. British Geological Survey Subsurface Memoir, HMSO London, 90 pp.
- Chisholm, T.J., Chapman, D.S., 1992. Climate change inferred from analysis of borehole temperatures: an example from western Utah. *J. Geophys. Res.* 97, 14155–14175.
- Coldewey, W.G., Wesche, D., Brandt, A., 2014. Evaluating the geothermal potential of abandoned mine workings: an appropriate approach based on geological and technical conditions. In: Sui, WangHua, Sun, Yajun, Wang, ChangShen (Eds.), *An Interdisciplinary Response to Mine Water Challenges: Proceedings of the 12th International Mine Water Association Congress*, Xuzhou, China, 18–22 August, 2014. China University of Mining and Technology Press, Xuzhou, China, pp. 632–635. Available online: [https://www.imwa.info/docs/imwa\\_2014/IMWA2014.Coldewey.632.pdf](https://www.imwa.info/docs/imwa_2014/IMWA2014.Coldewey.632.pdf) (accessed 15.07.15).
- Collier, R.E.L., 1991. The Lower Carboniferous Stainmore Basin, N. England extensional basin tectonics and sedimentation. *J. Geol. Soc. Lond.* 148, 379–390.
- Cook, R.A., Hoole, K., 1975. *North Eastern Railway Historical Maps. The Railway and Canal Historical Society, Mold*.
- Costantini, V., Martini, C., 2010. The causality between energy consumption and economic growth: a multi-sectoral analysis using non-stationary cointegrated panel data. *Energy Econ.* 32, 591–603.
- Curtis, A., 2012. Scotswood Delaval Drift, Scotswood Road. Available online: <http://www.geograph.org.uk/photo/2838819> (accessed 4.07.15).
- Davies, J.H., 2013. Global map of solid Earth surface heat flow. *Geochem. Geophys. Geosyst.* 14, 4608–4622.
- Davies, J.H., Davies, D.R., 2010. Earth's surface heat flux. *Solid Earth* 1, 5–24.
- Davis, M.G., Harris, R.N., Chapman, D.S., 2010. Repeat temperature measurements in boreholes from northwestern Utah link ground and air temperature changes at the decadal time scale. *J. Geophys. Res.* 115 (B05203), <http://dx.doi.org/10.1029/2009JB006875>, 12 pp.
- De Paola, N., Holdsworth, R.E., McCaffrey, K.J.W., 2005. The influence of lithology and pre-existing structures on reservoir-scale faulting patterns in transtensional rift zones. *J. Geol. Soc. Lond.* 162, 471–480.
- Donnelly, L.J., 2006. Investigation of Geological Hazards and Mining Risks, Gallowgate, Newcastle upon Tyne. From IAEG2006. Engineering geology for tomorrow's cities: The 10th IAEG International Congress, Nottingham, 6–10 September 2006. Paper number 113, 12 pp. The International Association for Engineering Geology and The Geological Society, London. Available online: [http://www.iaeg.info/iaeg2006/papers/iaeg\\_113.pdf](http://www.iaeg.info/iaeg2006/papers/iaeg_113.pdf).
- Donnelly, L.J., Dumpleton, S., Culshaw, M.G., Sheldock, S.L., McCann, D.M., 1998. The legacy of abandoned mining in the urban environment in the UK. In: Forde, M.C. (Ed.), *Polluted and Marginal Land. Proceedings of the 5th International Conference on re-use of Contaminated Land and Landfills*, London, 7–9 July 1998. Engineering Technics Press, Edinburgh, pp. 559–572.
- Downing, R.A., Gray, D.A. (Eds.) 1986. Geothermal Energy – The Potential in the United Kingdom. Her Majesty's Stationery Office, London, 187 pp.

- Dunham, K.C., 1973. A recent deep borehole near Eyam, Derbyshire. *Nat. Phys. Sci.* 241, 84–85.
- Dunham, K.C., Dunham, A.C., Hodge, B.L., Johnson, G.A.L., 1965. Granite beneath Viséan sediments with mineralization at Rookhope North Pennines. *Q. J. Geol. Soc. Lond.* 121, 383–417.
- England, P.C., Oxburgh, E.R., Richardson, S.W., 1980. Heat refraction and heat production in and around granite plutons in north-east England. *Geophys. J. Int.* 62 (2), 439–455.
- Ferguson, G., Grasby, S.E., 2011. Thermal springs and heat flow in North America. *Geofluids* 11, 294–301.
- Ferguson, G., Woodbury, A.D., 2007. Urban heat island in the subsurface. *Geophys. Res. Lett.* 34 (L23713), <http://dx.doi.org/10.1029/2007GL032324>, 4 pp.
- Forster, C., Smith, L., 1989. The influence of groundwater flow on thermal regimes in mountainous terrain: a model study. *J. Geophys. Res.* 94, 9439–9451.
- Fraser, A.J., Gawthorpe, R.L., 1990. Tectonostratigraphic development and hydrocarbon habitat of the Carboniferous in northern England. In: Hardman, R.F.P., Brooks, J. (Eds.), *Tectonic Events Responsible for Britain's Oil and Gas Reserves*. Geological Society, London, Special Publications 55, 49–86.
- Galloway, R.L., 1898. *Annals of Coal Mining and the Coal Trade. Volume 1 (First Series, up to 1835)*. Colliery Guardian Company Ltd, London, pp. 534. Reprinted 1971 by David & Charles, Newton Abbot.
- Gibling, M.R., Bird, D.J., 1994. Late Carboniferous cyclotherms and alluvial paleovalleys in the Sydney Basin, Nova Scotia. *Geol. Soc. Am. Bull.* 106, 105–117.
- Gillespie M.R., Crane E.J., Barron H.F., 2013. Deep geothermal energy potential in Scotland. Study into the potential for deep geothermal energy in Scotland. Scottish Government Project Number: AEC/001/11, Volume 2 of 2. British Geological Survey Commissioned Report, CR/12/131, 129 pp. Available online: <http://www.gov.scot/Resource/0043/00437996.pdf> (accessed 29.06.15).
- Gunn, J., Bottrell, S.H., Lowe, D.J., Worthington, S.R.H., 2006. Deep groundwater flow and geochemical processes in limestone aquifers: evidence from thermal waters in Derbyshire, England, UK. *Hydrogeol. J.* 14, 868–881.
- Hall, A., Scott, J.A., Shang, H., 2011. Geothermal energy recovery from underground mines. *Renew. Sustain. Energy Rev.* 15, 916–924.
- Harrison, R., Scott, W.B., Smith, T., 1989. A note on the distribution, levels and temperatures of minewaters in the Northumberland and Durham coalfield. *Q. J. Eng. Geol.* 22, 355–358.
- Hartmann, D.L., Klein Tank, A.M.G., Rusticucci, M., Alexander, L.V., Brönnimann, S., Charabi, Y., Dentener, F.J., Dlugokencky, E.J., Easterling, D.R., Kaplan, A., Soden, B.J., Thorne, P.W., Wild, M., Zhai, P.M., 2013. Observations: atmosphere and surface. In: Stocker, T.F., Qin, D., Plattner, G.-K., Tignor, M., Allen, S.K., Boschung, J., Nauels, A., Xia, Y., Bex, V., Midgley, P.M. (Eds.), *Climate Change 2013: The Physical Science Basis. Contribution of Working Group I to the Fifth Assessment Report of the Intergovernmental Panel on Climate Change*. Cambridge University Press, Cambridge.
- Heckel, P.H., 1986. Sea-level curve for Pennsylvanian eustatic marine transgressive-regressive depositional cycles along midcontinent outcrop belt, North America. *Geology* 14, 330–334.
- Heitfeld, M., Rosner, P., Schetelig, K., Sahl, H., 2006. Nutzung aufgegebener Tagesschächte des Steinkohlenbergbaus für die Gewinnung von Erdwärmе – Ergebnisse einer Machbarkeitsstudie für das Aachener Revier. *Glückauf* 142, 432–438.
- Herrin, J.M., Deming, D., 1996. Thermal conductivity of U.S. coals. *J. Geophys. Res.* 101, 25381–25386.
- Holliday, D.W., 1986. Devonian and Carboniferous basins. In: Downing, R.A., Gray, D.A. (Eds.), *Geothermal Energy – The Potential in the United Kingdom*. Her Majesty's Stationery Office, London, pp. 84–110.
- Hopcroft, P.O., Gallagher, K., Pain, C.C., 2007. Inference of past climate from borehole temperature data using Bayesian Reversible Jump Markov chain Monte Carlo. *Geophys. J. Int.* 171, 1430–1439.
- Huang Shaopeng, Pollack, H.N., 1997. Late Quaternary temperature changes seen in world-wide continental heat flow measurements. *Geophys. Res. Lett.* 24, 1947–1950.
- Huang Shaopeng, Pollack, H.N., Shen Po-Yu, 2000. Temperature trends over the past five centuries reconstructed from borehole temperatures. *Nature* 403, 756–758.
- Hughes, K., 2006. The impact of urban areas on climate in the UK: a spatial and temporal analysis with an emphasis on temperature and precipitation effects. *Earth Environ.* 2, 54–83.
- IEA, 2014. Key World Energy Statistics. International Energy Agency, Paris, pp. 82. Available online: <http://www.iea.org/publications/freepublications/publication/KeyWorld2014.pdf> (accessed 15.07.15).
- IPCC, 2013. Climate Change 2013: The Physical Science Basis. Contribution of Working Group I to the Fifth Assessment Report of the Intergovernmental Panel on Climate Change [Stocker, T.F., Qin, D., Plattner, G.-K., Tignor, M., Allen, S.K., Boschung, J., Nauels, A., Xia, Y., Bex, V., Midgley, P.M. (Eds.)]. Cambridge University Press, Cambridge.
- James, R., 1997. Mine drainage and water resources. *Bull. Peak Dist. Mines Hist. Soc.* 13 (4), 74–80.
- Johnson, K.L., Younger, P.L., 2002. Hydrogeological and geochemical consequences of the abandonment of Frazer's Grove carbonate hosted Pb/Zn fluorite mine, North Pennines, UK. In: Younger, P.L., Robins, N.S. (Eds.), *Mine Water Hydrogeology and Geochemistry*. Geological Society, London, Special Publications, 198, 347–363.
- Johnson, K.L., Younger, P.L., 2006. The co-treatment of sewage and mine waters in aerobic wetlands. *Eng. Geol.* 85, 53–61.
- Jones, J.M., Magraw, D., O'Mara, P.T., 1995. Carboniferous Westphalian coal measures. In: Johnson, G.A.L. (Ed.), *Robson's Geology of North East England. Transactions of the Natural History Society of Northumbria*, vol. 56, part 5. The Natural History Society of Northumbria, Newcastle upon Tyne, pp. 267–282.
- Kershaw, T., Sanderson, M., Coley, D., Eames, M., 2010. Estimation of the urban heat island for UK climate change projections. *Build. Serv. Eng. Res. Technol.* 31 (3), 251–263.
- Kimbell, G.S., Young, B., Millward, D., Crowley, Q.G., 2010. The North Pennine batholith (Weardale Granite) of northern England: new data on its age and form. *Proc. Yorks. Geol. Soc.* 58, 107–128.
- Lee, C.E., 1944. An ancient underground railway. *The Railway Magazine* 90, 331–334. Available online: <http://www.aditnow.co.uk/documents/Kittys-Drift-Tunnel/Kenton.pdf> (accessed 4.07.15).
- Leśniak, B., Ślipik, Ł., Jakubina, G., 2013. The determination of the specific heat capacity of coal based on literature data. *Chemik* 67, 560–571.
- Leoni, L., 1985. Water filled abandoned mines as a heat source for district heating. *Underground* 9, 23–27.
- Lewis, M.A., Cheney, C.S., ÓDochartaigh, B.É., 2006. *Guide to Permeability Indices. British Geological Survey, Information Products Programme, Open Report CR/06/160N*. British Geological Survey, Keyworth, Nottingham, 29 pp.
- Lu Ning, Ge, Shemin, 1996. Effect of horizontal heat and fluid flow on the vertical temperature distribution in a semiconfining layer. *Water Resour. Res.* 32, 1449–1453.
- Mackenzie, E., 1825. *An Historical, Topographical, and Descriptive View of the County of Northumberland, and of Those Parts of the County of Durham Situated North of the River Tyne, with Berwick Upon Tweed, and Brief Notices of Celebrated Places on the Scottish Border*. Mackenzie and Dent, Berwick-upon-Tweed, 515 pp.
- Manga, M., 1998. Advective heat transport by low-temperature discharge in the Oregon Cascades. *Geology* 26, 799–802.
- Manley, G., 1953. The mean temperature of Central England: 1698 to 1952. *Q. J. R. Meteorol. Soc.* 79, 242–261.
- Manley, G., 1974. Central England Temperatures: monthly means 1659 to 1973. *Q. J. R. Meteorol. Soc.* 100, 389–405.
- Manning, D.A.C., Younger, P.L., Smith, F.W., Jones, J.M., Dufton, D.J., Diskin, S., 2007. A deep geothermal exploration well at Eastgate Weadale, UK: a novel exploration concept for low-enthalpy resources. *J. Geol. Soc. Lond.* 164, 371–382.
- Mansure, A.J., Reiter, M., 1979. A vertical groundwater movement correction for heat flow. *J. Geophys. Res.* 84, 3490–3496.
- Menberg, K., Bayer, P., Zosseder, K., Rumohr, S., Blum, P., 2013a. Subsurface urban heat islands in German cities. *Sci. Total Environ.* 442, 123–133.
- Menberg, K., Blum, P., Schaffitel, A., Bayer, P., 2013b. Long-term evolution of anthropogenic heat fluxes into a subsurface urban heat island. *Environ. Sci. Technol.* 47, 9747–9755.
- Met Office, 2015. Mean central England temperature: annual anomalies, 1772 to 31st Dec 2014. <http://www.metoffice.gov.uk/hadobs/hadct/> (accessed 3.01.15).
- Michel, F.A., 2009a. Utilisation of Abandoned Mine Workings for Thermal Energy Storage in Canada. Stockton College, New Jersey, pp. 8. Available online: [http://intraweb.stockton.edu/eyos/energy\\_studies/content/docs/effstock09/Session\\_11.1-Casestudies\\_Overviews/105.pdf](http://intraweb.stockton.edu/eyos/energy_studies/content/docs/effstock09/Session_11.1-Casestudies_Overviews/105.pdf) (accessed 12.07.15).
- Michel, F.A., 2009b. Development of Thermal Energy Storage Systems in Abandoned Mine Workings. Ground Water Protection Council 2009 Annual Forum, Salt Lake City, Utah, pp. 13–16. Available online: <http://www.gwpc.org/sites/default/files/event-sessions/Michel-Fred.pdf> (accessed 12.07.15).
- Midttømme, K., Roaldset, E., Aagaard, P., 1998. Thermal conductivity of selected claystones and mudstones from England. *Clay Miner.* 33, 131–145.
- Mills, D.A.C., Holliday, D.W., 1998. *Geology of the District Around Newcastle upon Tyne, Gateshead and Consett: Memoir for 1:50 000 Scale Geological Map Sheet 20 (England and Wales)*. The Stationery Office, London, 148 pp.
- Minewater Project, 2008. Mine Water as a Renewable Energy Resource. An Information Guide Based on the Minewater Project and the Experiences at Pilot Locations in Midlothian and Heerlen. The European Union, Brussels, pp. 48. Available online: [http://skrconline.net/content/images/stories/documents/mine\\_water\\_renewable\\_energy\\_guide.pdf](http://skrconline.net/content/images/stories/documents/mine_water_renewable_energy_guide.pdf) (accessed 29.06.15).
- Mu Yao, Mu Xinzhili, 2013. Energy conservation in the Earth's crust and climate change. *J. Air Waste Manag. Assoc.* 63 (2), 150–160.
- NEIMME, 1881. An Account of the strata of Northumberland & Durham as proved by Borings & Sinkings, Volume I: C–E. North of England Institute of Mining & Mechanical Engineers, Newcastle upon Tyne.
- NEIMME, 1894. An Account of the strata of Northumberland & Durham as proved by Borings & Sinkings, Volume V: S–T. North of England Institute of Mining & Mechanical Engineers, Newcastle upon Tyne.
- Network Rail, 2013. Mining remediation works will help bring line one step closer. <http://www.bordersrailway.co.uk/news/2013/april/mining-remediation-works-will-help-bring-line-one-step-closer.aspx> (accessed 29.06.15).
- NOAA, 2013. NOAA Paleoclimatology Borehole Data Sets. Available online: <https://hurricane.ncdc.noaa.gov/pls/paleox/f?p=517:1:0::APP:PROXYDATASETLIST:1> (accessed 7.12.14).
- Nordell, B., 2003. Thermal pollution causes global warming. *Global Planet. Change* 38, 305–312.
- Nordell, B., 2007. Global warming is large-scale thermal energy storage. In: Paksoy, H.Ö. (Ed.), *Thermal Energy Storage for Sustainable Consumption*. NATO Science Series, Series II, vol. 234. Springer, Dordrecht, The Netherlands, pp. 75–86.

- ÓDochartaigh, B.É., 2009. A Scoping Study into Shallow Thermogeological Resources Beneath Glasgow and the Surrounding Area. Clean Coal and Renewables Team Internal Report IR/09/024. British Geological Survey, Keyworth, Nottingham21, Available online: <http://nora.nerc.ac.uk/20952/1/IRO9024.pdf> (accessed 29.06.15).
- Oke, T.R., 1973. City size and the urban heat island. *Atmos. Environ.* 7, 769–779.
- Pandrich, J., 1959. Farewell to the Monty. Available online: <http://www.dmm.org.uk/pitwork/html/song.htm> (accessed 27.06.15).
- Parker, D.E., Horton, E.B., 2005. Uncertainties in the Central England Temperature series since 1878 and some changes to the maximum and minimum series. *Int. J. Climatol.* 25, 1173–1188.
- Parker, D.E., Legg, T.P., Folland, C.K., 1992. A new daily Central England Temperature Series, 1772–1991. *Int. J. Climatol.* 12, 317–342.
- Patton A.M., Farr G.J., Boon D.P., James D.R., Williams B., Newell A.J., 2015a. Shallow groundwater temperatures and the Urban Heat Island effect: the first U.K. city-wide geothermal map to support development of ground source heating systems strategy. *Geophysical Research Abstracts*, 17, EGU2015-3488. Available online: <http://meetingorganizer.copernicus.org/EGU2015/EGU2015-3488.pdf> (accessed 19.05.15).
- Patton, A.M., Farr, G.J., Boon, D.P., James, D.R., Williams, B., Newell, A.J., 2015b. Shallow groundwater temperatures and the Urban Heat Island effect: the first U.K. city-wide geothermal map to support development of ground source heating systems strategy. Available online: <http://nora.nerc.ac.uk/510723/1/EGU Poster.pdf> (accessed 19.05.15).
- PB Power, 2004. Shawfair Minewater Project: Scottish National Minewater Potential Study. Parsons Brinckerhoff, London, pp. 70. Available online: <http://www.gov.scot/Resource/Doc/982/0056515.pdf> (accessed 29.06.15).
- Pollack, H.N., Huang Shaopeng, Shen Po-Yu, 1998. Climate change record in subsurface temperatures: a global perspective. *Science* 282, 279–281.
- Porson, A., Clark, P.A., Harman, I.N., Best, M.J., Belcher, S.E., 2010a. Implementation of a new urban energy budget scheme in MetUM. Part I: Description and idealized simulations. *Q. J. R. Meteorolog. Soc.* 136, 1514–1529.
- Porson, A., Clark, P.A., Harman, I.N., Best, M.J., Belcher, S.E., 2010b. Implementation of a new urban energy budget scheme into MetUM. Part II. Validation against observations and model intercomparison. *Q. J. R. Meteorolog. Soc.* 136, 1530–1542.
- Ramos, E.P., Falcone, G., 2013. Recovery of the geothermal energy stored in abandoned mines. In: Hou, M.Z., Xie, H.P., Were, P. (Eds.), *Clean Energy Systems in the Subsurface: Production, Storage and Conversion*. Proceedings of the 3rd Sino-German Conference on Underground Storage of CO<sub>2</sub> and Energy. Goslar, Germany, 21–23 May 2013. Springer, Berlin, pp. 143–155.
- Reiter, M., 2006. Vadose zone temperature measurements at a site in the northern Albuquerque Basin indicate ground-surface warming due to urbanization. *Environ. Eng. Geosci.* 12, 353–360.
- Rhein, M., Rintoul, S.R., Aoki, S., Campos, E., Chambers, D., Feely, R.A., Gulev, S., Johnson, G.C., Josey, S.A., Kostianoy, A., Mauritzen, C., Roemmich, D., Talley, L.D., Wang, F., 2013. Observations: ocean. In: Stocker, T.F., Qin, D., Plattner, G.-K., Tignor, M., Allen, S.K., Boschung, J., Nauels, A., Xia, Y., Bex, V., Midgley, P.M. (Eds.), *Climate Change 2013: The Physical Science Basis. Contribution of Working Group I to the Fifth Assessment Report of the Intergovernmental Panel on Climate Change*. Cambridge University Press, Cambridge.
- Robertson, E.C., 1988. Thermal properties of rocks. U.S. Geological Survey Open-File Report 88-441, 110 pp.
- Rodríguez, R., Díaz, M., 2009. Analysis of the utilisation of mine galleries as geothermal heat exchangers by means a semi-empirical prediction method. *Renew. Energy* 34, 1716–1725.
- Rollin, K.E., 1995. A simple heat-flow quality function and appraisal of heat-flow measurements and heat-flow estimates from the UK Geothermal Catalogue. *Tectonophysics* 244, 185–196.
- Sakakibara, Y., Matsui, E., 2005. Relation between heat island intensity and city size indices/urban canopy characteristics in settlements of Nagano Basin, Japan. *Geogr. Rev. Jpn.* 78, 812–824.
- Schöpf, H.M., Supancic, P.H., 2014. On Bürmann's Theorem and its application to problems of linear and nonlinear heat transfer and diffusion: expanding a function in powers of its derivative. *Math. J.* 16, 44, Available online: <http://www.mathematica-journal.com/data/uploads/2014/11/Schoepf.pdf>.
- Shepley, M.G., 2007. Analysis of flows from a large Carboniferous Limestone drainage adit, Derbyshire, England. *Q. J. Eng. Geol. Hydrogeol.* 40, 123–135.
- Sherwood, J.M., Younger, P.L., 1994. Modelling groundwater rebound after coalfield closure: an example from County Durham, UK. In: Proceedings of the 5th International Mine Water Congress, Nottingham, 17–24 September 1994, International Mine Water Association, Wendelstein, Germany, pp. 769–777, Available online: [https://www.imwa.info/docs/imwa.1994/IMWA1994-Sherwood\\_769.pdf](https://www.imwa.info/docs/imwa.1994/IMWA1994-Sherwood_769.pdf) (accessed 6.07.15).
- Stewart, I.D., 2011. A systematic review and scientific critique of methodology in modern urban heat island literature. *Int. J. Climatol.* 31, 200–217.
- Taniguchi, M., Shimada, J., Tanaka, T., Kayane, I., Sakura, Y., Shimano, Y., Dapaah-Siakwan, S., Kawashima, S., 1999a. Disturbances of temperature-depth profiles due to surface climate change and subsurface water flow: 1. An effect of linear increase in surface temperature caused by global warming and urbanization in the Tokyo Metropolitan Area, Japan. *Water Resour. Res.* 35, 1507–1517.
- Taniguchi, M., Uemura, T., 2005. Effects of urbanization and groundwater flow on the subsurface temperature in Osaka, Japan. *Phys. Earth Planet. Inter.* 152, 305–313.
- Taniguchi, M., Williamson, D.R., Peck, A.J., 1999b. Disturbances of temperature-depth profiles due to surface climate change and subsurface water flow: 2. An effect of step increase in surface temperature caused by forest clearing in southwest western Australia. *Water Resour. Res.* 35, 1519–1529.
- Turcotte, D.L., Schubert, G., 1982. *Geodynamics: Applications of Continuum Physics to Geological Problems*. Wiley, Chichester, 450 pp.
- van der Kamp, G., Bachu, S., 1989. Use of dimensional analysis in the study of thermal effects of various hydrogeological regimes. In: *Hydrogeological Regimes and Their Subsurface Thermal Effects*, Beck, A.E., Garven, G., Stegmaier, L. (Eds.). *Geophysical Monograph Series*, 47, American Geophysical Union, Washington, D.C., pp. 23–28.
- Waggonways, 2009. Waggonways in North East England. Available online: <https://sites.google.com/site/waggonways/> (accessed 18.06.15).
- Wanless, H.R., Shepard, F.P., 1936. Sea level and climatic changes related to Late Paleozoic cycles. *Geol. Soc. Am. Bull.* 47, 1177–1206.
- Waters, C.N., Millward, D., Thomas, C.W., 2014. The Millstone Grit Group (Pennsylvanian) of the Northumberland–Solway Basin and Alston Block of northern England. *Proc. Yorks. Geol. Soc.* 60, 29–51.
- Watzlaf, G., Ackman, T., 2006. Underground mine water for heating and cooling using geothermal heat pump systems. *Mine Water Environ.* 25, 1–14.
- Welsh, K., 2005. Lamesley Combined Water Treatment Scheme: first wetland to co-treat minewater and final effluent. *Wastewater Treat. Sewerage*, 35–37, Available online: [http://www.waterprojectsonline.com/case\\_studies/2005/IndustrialLamesley20WwTW202005.pdf](http://www.waterprojectsonline.com/case_studies/2005/IndustrialLamesley20WwTW202005.pdf) (accessed 23.06.15).
- Westaway, R., 2002. The Quaternary evolution of the Gulf of Corinth: central Greece: coupling between surface processes and flow in the lower continental crust. *Tectonophysics* 348, 269–318.
- Westaway, R., 2007. Improved modelling of the Quaternary evolution of the Gulf of Corinth, incorporating erosion and sedimentation coupled by lower-crustal flow. *Tectonophysics* 440, 67–84.
- Westaway, R., Scotney, P.M., Younger, P.L., Boyce, A.J., 2015. Subsurface absorption of anthropogenic warming of the land surface: the case of the world's largest brickworks (Stewartby, Bedfordshire, UK). *Sci. Total Environ.* 508, 585–603.
- Westaway, R., Younger, P.L., 2013. Accounting for palaeoclimate and topography: a rigorous approach to correction of the British geothermal dataset. *Geothermics* 48, 31–51.
- Whitworth, K.R., 2002. The monitoring and modelling of mine water recovery in UK coalfields. In: Younger, P.L., Robins, N.S. (eds.), *Mine Water Hydrogeology and Geochemistry*. Geological Society, London, Special Publications, 198, 61–73.
- Worthington, S.R.H., Ford, D.C., 2009. Self-organized permeability in carbonate aquifers. *Ground Water* 47, 326–336.
- Younger, P.L., 1993. Possible environmental impact of the closure of two collieries in County Durham. *Water Environ. J.* 7, 521–531.
- Younger, P.L., 1995. Hydrogeochemistry of minewaters flowing from abandoned coal workings in County Durham. *Q. J. Eng. Geol.* 28, S101–S113.
- Younger, P.L., 1997. The longevity of minewater pollution: a basis for decision making. *Sci. Total Environ.* 194–195, 457–466.
- Younger, P.L., 1998. Coalfield abandonment: geochemical processes and hydrochemical products. In: Nicholson, K. (Ed.), *Energy and the Environment: Geochemistry of Fossil, Nuclear and Renewable Resources*. MacGregor Science, Mount Vernon, Washington, pp. 1–29.
- Younger, P.L., 2004. Making water: the hydrogeological adventures of Britain's early mining engineers. In: Mather, J.D. (Ed.), *200 Years of British Hydrogeology*. Geological Society, London, Special Publications, 225, 121–157.
- Younger, P.L., 2006. Orphaned and abandoned mines: in pursuit of best practice. From: National Orphaned/Abandoned Mines Initiative Workshop, Winnipeg, Canada, 26–27 October 2006. Available online: <http://www.abandoned-mines.org/pdfs/presentations/OrphAban-PursuitofBestPractYounger.pdf> (accessed 23.06.15).
- Younger, P.L., 2013. Deep geothermal: the Newcastle Science Central borehole. *Geotherm. Assoc. Irel. Newsrl.* 21, 9–13.
- Younger, P.L., Adams, R., 1999. Predicting Mine Water Rebound. R&D Technical Report W179. The Environment Agency, Bristol, 108 pp.
- Younger, P.L., Boyce, A.J., Waring, A.J., 2015. Chloride waters of Great Britain revisited: from subsea formation waters to onshore geothermal fluids. *Proc. Geol. Assoc.* 126, 453–465.
- Younger, P.L., Harbourne, K.J., 1995. To pump or not to pump? cost-benefit analysis of future environmental management options for the abandoned Durham Coalfield. *J. Chart. Inst. Water Environ. Manag.* 9, 405–415.
- Younger, P.L., Henderson, R., 2014. Synergistic wetland treatment of sewage and mine water: pollutant removal performance of the first full-scale system. *Water Res.* 55, 74–82.
- Younger, P.L., Sherwood, J.M., 1993. The cost of decommissioning a coalfield: potential environmental problems in County Durham. *Miner. Plan.* 57, 26–29.
- Yu Myong-Hwan, 2006. Geohazards Associated with Rising Groundwater in Urban Areas Affected by Former Coal Mining. Ph.D. Thesis. Birmingham University, 273 pp.
- Yu Myong-Hwan, Jefferson, I., Culshaw, M., 2006. Geohazards caused by rising groundwater in the Durham Coalfield, U.K. From: IAEG2006, Engineering Geology for Tomorrow's Cities. In: The 10th IAEG International Congress, Nottingham, 6–10 September 2006. Paper 367, p. 12, Available online: [http://iaeg2006.geolsoc.org.uk/cd/PAPERS/IAEG\\_367.PDF](http://iaeg2006.geolsoc.org.uk/cd/PAPERS/IAEG_367.PDF) (accessed 4.07.15).